Prog. Quant. Electr. 1992, Vol. 16, pp. 1–71
Printed in Great Britain.

0079-6727/92 $15.00

THEORETICAL METHODS IN QUANTUM OPTICS: S-MATRIX AND KELDYSH TECHNIQUES FOR STRONG-FIELD PROCESSES

H. R. REISS
Department of Physics, The American University, Washington, DC 20016-8058, U.S.A.

CONTENTS

1. INTRODUCTION

1.1. *The Strong-Field Environment*

The physical conditions which define a strong field will be identified in detail below, but it is instructive to begin with the examination of a practical example of a field which is unquestionably strong, and presently achievable. It is now possible to obtain an energy flux of 10^{19} W/cm^2 from a laser operating at a wavelength of about 1 μm. An isolated electron in such a field has an energy of interaction with the field (the 'ponderomotive potential') of approximately 10^6 eV. Since the energy of a single photon of this laser field is about 1 eV, this means that the electron must have interacted with at least 10^6 photons in order simply to exist in the presence of the field. Furthermore, 10^6 eV is roughly 10^5 times the binding energy of an outer shell electron in an atom, so if the electron whose behavior is being examined has just been ionized from an atom, it will regard the atom as a small disturbance in comparison with the laser field. Finally, we remark that the 10^6 eV field-interaction energy of the electron is even in excess of the 511 keV rest energy of an electron, so that the electron is a relativistic particle irrespective of its net translational velocity.

All of the above comparisons bespeak a physical environment quite foreign to the conventional world of low-intensity laser physics. The simultaneous interaction of the electron with 10^6 photons makes it very clear that the lowest-order-dominant concepts of perturbation theory have lost all meaning. One's intuitive guess that it is irrelevant whether the electron is in interaction with 1,000,000 or 1,000,001 or 1,000,100 photons can be shown to be justified. The fact that the interaction of the electron with the laser field is 10^5 times stronger than atomic binding energies means that an electron, once ionized, behaves almost as if the atom is not present. (The properties of the atom, however, remain very important for the electron while still bound—a point of considerable significance.) The relativistic nature of the ionized electron means that relativity enters into atomic physics purely as a function of the intensity of the laser field, and with no a priori considerations of electron velocities comparable to the velocity of light. The electron will inevitably acquire such velocities as a result of its laser-field-induced motion.

The above qualitative features of the strong-field environment have gradually come into focus over the past decade or so. As commonly occurs when a major shift in experimental circumstances forces a corresponding adjustment in conceptual views of the underlying physics, inertial effects in the change of 'paradigm'[1] are not hard to find. The aim of this review is to go directly to strong-field techniques without detours through evolutionary changes in low-intensity methods. The goal is to expound theoretical techniques which are entirely independent of perturbative concepts, incorporate field-dominated electron behavior

in a natural way, and accommodate relativistic techniques in a fashion parallel to the treatment of the non-relativistic problem. All of this can be done from first principles in an efficient manner. In some ways, the strong-field environment has a theoretical structure simpler than the conventional physics of the interaction of atoms and molecules with electromagnetic fields.

For all the recent emphasis on strong-field phenomena, it must be pointed out that many of the most interesting and curious results which are the focus of so much current attention have been known for a long time. As will be recorded below, one of the basic tools of strong-field research, the Volkov or Gordon–Volkov solution, was known in 1926. The shifting of conservation conditions and hence 'peak suppression' was known in 1962; the 'ATI' effect, or loss of dominance of lowest order processes was discussed in 1970; the same year that the effect now known as 'stabilization' was described.

1.2. *Implications of Strong Fields for Quantum Optics*

As the discussion of Section 1.1 strongly implies, many familiar qualitative aspects of quantum optics become radically altered in very strong fields. When the laser field is so strong that the ponderomotive potential of an electron in that field approaches the magnitude of the atomic binding potential, then the fundamental premise of perturbation theory fails. That is, perturbation theory presumes that an atom is only slightly 'perturbed' by an external influence or interaction. When the interaction rivals in magnitude the cohesive energy that is responsible for the identity of the atom, then the concept of a perturbation is inappropriate.

Long-developed intuition and qualitative concepts in quantum optics depend to a considerable degree on insights guided by perturbation theory. With the failure of perturbation theory one must abandon the concept of an nth-order transition as the orderly progression of an atom in n steps from an initial state to a final state while passing through $n-1$ intermediate states. Although in some strong-field theories, it may still be possible to speak of the absorption or emission of exactly n photons, it is generally no longer possible or fruitful to specify the intermediate states. Once-useful concepts like oscillator strengths vanish from the theory. S-matrix methods as described herein invoke reference states in which no field is present. In some of these formalisms, it is then no longer appropriate to speak of Stark-shifted ionization potentials. Energy requirements for ionization are, indeed, altered by the laser, but field-dependent ionization energy requirements appear in a guise different from a Stark-shifted ionization potential.

The loss of perturbation theory as a viable quantum-mechanical calculational procedure corresponds to a qualitative change in the physical nature of an atom. Sufficiently strong laser fields will cause the energy levels of an atom to shift and broaden to such a degree that they overlap to the point of losing any useful identity. It is no longer fruitful to even think in such terms. An example of this alteration to a new way of thinking is the concept of ionization by tunneling. It is useful, in a strong, low frequency laser field, to think of ionization as occurring as a result of the thinning of one side of the atomic potential by the quasi-static electric field of the laser. The electron can then 'leak out' over the top of the depressed atomic potential, or tunnel through the thin upper layer of the modified potential. This mechanism for ionization takes the place of the notion of the absorption of a discrete number of photons by the atom and its passage through a succession of excited states.

A further remark about the failure of perturbation theory is that one must exercise caution in the application of strong-field corrections to the perturbation theory as the field strength increases. Some useful quantitative and qualitative results can be obtained by adding terms to the nominal nth-order term required by lowest order perturbation theory, as long as the field strength does not exceed the radius of convergence of perturbation theory. When that radius is exceeded (which may not be evident in practical application), the calculated results

may appear reasonable, but may have no relationship to the correct answer. An elementary analog is provided by the geometric series

$$1/(1-x) = 1 + x + x^2 + x^3 + \ldots, |x| < 1. \tag{1}$$

Suppose the sum in Eqn. (1) is truncated at some finite order N. Suppose further, for ease of visualization, that x is positive. As long as one is within the radius of convergence, $|x| < 1$, an increase in the value of N will yield an answer from the finite sum which improves in accuracy as N increases. However, when $|x| > 1$, the left-hand side, $1/(1-x)$ turns negative, while the truncated sum continues to exhibit positive values. In a physical problem where the actual radius of convergence is not known (as is generally the case in perturbation theory), the truncated perturbative sum may continue to produce reasonable-looking results when, in fact, the finite sum has ceased to bear any meaningful relationship to the actual value of the physical quantity it nominally represents.

One further remark is in order about the implications of strong fields. Photon occupation numbers are so large that semiclassical theories are indicated. It is not necessary to quantize the laser field.

1.3. *Measures of Intensity*

1.3.1. *Preliminaries.* It is current practice in strong-field physics to point out that qualitative changes in behavior from the low-intensity case are to be expected when the electric field of the laser is of the same order of magnitude as the electric field experienced by an electron situated at one Bohr radius from a Coulomb center of force arising from a single positive nuclear charge. That is, a strong field is one in which the laser's electric field equals the Coulomb electric field experienced by the ground state electron in a simple Bohr model of the hydrogen atom. This is simply stated as the field such that $\mathscr{E} = 1$, where $\mathscr{E}$ is the electric field in atomic units. In SI units, this amounts to 5.14×10^{11} V/m. This is a plausible criterion, and it has the convenient feature that a laser field of 3.51×10^{16} W/cm^2 (3.51×10^{20} W/m^2 in SI units, $I = 1$ in atomic units) will give rise to $\mathscr{E} = 1$, irrespective of the frequency of the laser.

In fact, the definition of a strong field as one which has $\mathscr{E} = 1$ is unsatisfactory, and the reason is that the onset of strong-field behavior is observed to be decidedly frequency dependent. For example, ionization of atoms with an excimer laser of 193 nm at 10^{15} W/cm^2 [2] (or even at 10^{17} W/cm^2) [3] does not have as well developed a strong-field character as multiphoton ionization with a CO_2 laser at 10^{14} W/cm^2.[4-6] The 193 nm experiments with $\mathscr{E} = 0.17$ involve multiphoton orders of ten or less, whereas the CO_2 experiments with $\mathscr{E} = 0.05$ require a minimum photon order, for some ionization channels, of several hundred. Even this type of comparison does not make the point as strongly as possible because the energy of a laser photon at 193 nm is about 50 times the energy of a CO_2 laser photon, which makes for vastly disparate photon orders at threshold. A more direct comparison is to match the intensity conditions at two different wavelengths for cases where the lowest photon multiplicities are about the same. This cannot be done exactly, but the photoionization experiments with the excimer laser might reasonably be compared to negative ion photodetachment experiments with the CO_2 laser.[7,8] In that case, the low-intensity threshold order with the CO_2 laser is seventh order, and an intensity of 2×10^{10} W/cm^2 results in very well developed strong-field behavior. The field strength in atomic units is then only $\mathscr{E} = 0.0008$!

A more satisfactory and universal means of judging strong-field behavior is based on energy comparisons. This is consistent with the fact, to be discussed shortly, that all of the intensity parameters which arise in the strong-field theory can be expressed as ratios of energies.

The special role of energies as opposed to field strengths is not surprising. The Schrödinger equation, for example, is essentially the statement that $H = T + V$, where H is the total Hamiltonian, and T, V are the kinetic and potential energies. In particular, the Schrödinger

equation for an electron in interaction with the electromagnetic field can be written in terms of the electromagnetic potentials, but not directly in terms of the fields. Determined attempts in the 1960s to re-express quantum mechanics directly in terms of fields rather than potentials[9–14] met with failure (although there was an ancillary development of path-integral methods which proved fruitful for other purposes). It has been argued[15] that potentials are more fundamental than fields, despite the contrary traditional view. A case in point is the Aharonov–Bohm effect,[16–18] which occurs[19–23] in regions with electromagnetic potentials, but with no fields present. There is thus strong evidence that energies—including electromagnetic interaction energies—are more basic measures in quantum mechanics than are field strengths.

1.3.2. *Ponderomotive potential.* A central element in strong-field photoionization is the behavior of a free electron in a plane-wave electromagnetic field. This problem has been exactly solved, both classically[24,25] and quantum mechanically.[26,27] The classical equations show the electron to follow a path which, apart from any uniform translation, is a circular motion in a circularly polarized light wave, or a figure-eight motion in a linearly polarized field. The circular motion is about the propagation direction as axis. The figure-eight motion is in the plane defined by the polarization vector and the direction of propagation, with the double lobe of the 8 deployed along the polarization direction.

Of particular interest here is the relativistic energy of the electron's motion. As given by Sarachik and Schappert[25] for the classical case, this is

$$E = mc^2 - e^2A^2/2mc^2, \tag{2}$$

where A^2 is the square of the electromagnetic four-vector potential A^μ according to the inner-product rule

$$A^2 \equiv A^\mu A_\mu = A_\mu A^\mu = (A^0)^2 - \mathbf{A}^2 = \phi^2 - \mathbf{A}^2, \tag{3}$$

with the scalar potential designated either as A^0 or ϕ, and where $\mathbf{A}$ is the three-vector potential. The indices μ range over the values 0, 1, 2, 3. The leading term in Eqn. (2) is the relativistic rest energy of the electron, and the second term is the ponderomotive potential U_p. As Eqn. (3) shows, U_p is a relativistic invariant. That is, it has the same expression in every Lorentz frame of reference.

Although the ponderomotive potential is expressed in terms of the four-vector potential, it is independent of gauge. The general gauge transformation is

$$A^\mu \rightarrow A'^\mu = A^\mu + \partial^\mu \Lambda, \tag{4}$$

where Λ is a scalar function of the space-time four-vector x^μ. It is then possible to show[26] that $A^\mu A_\mu = A'^\mu A'_\mu$ for all 'simple' gauge transformations as well as for transformations between the relativistic length and velocity gauges.[28] It is thus possible to evaluate the ponderomotive potential in any convenient gauge and arrive at a universal result. If the Coulomb gauge is selected, then $A^0 = 0$, and $|\mathbf{A}|^2 = |\mathscr{E}|^2/\omega^2c^2$, where ω is the circular frequency of the electric field vector $\mathscr{E}$. The time-averaged $\mathscr{E}^2$ is $\langle\mathscr{E}^2\rangle = \mathscr{E}^2/2$, where $\mathscr{E}$ is the amplitude of $\mathscr{E}$. Hence, the ponderomotive potential can be written as

$$U_p = e^2\mathscr{E}^2/4m\omega^2, \tag{5}$$

a form frequently used.

1.3.3. *Non-perturbative intensity parameter.* One of the intensity parameters which arises naturally in strong-field theories of atomic ionization[29–31] is

$$z \equiv U_p/\hbar\omega = e^2\mathscr{E}^2/4\hbar m\omega^3, \tag{6}$$

with the last expression in SI units. Alternative expressions in atomic units are

$$z = U_p/\omega = I/4\omega^3 = \mathscr{E}^2/4\omega^3. \tag{7}$$

Yet another form is instructive, given in terms of the density of photons ρ, the wavelength of the radiation λ, and the electron Compton wavelength λ_c,

$$z = \rho\alpha\lambda\!\!\!^{-2}\lambda_c, \tag{8}$$

where α is the fine structure constant and $\lambda\!\!\!^{-} \equiv \lambda/2\pi$. This form is useful since it essentially defines an interaction volume associated with z. In atomic units, this becomes simply

$$z = \rho/\omega^2. \tag{9}$$

There are two reasons why z may be called a 'non-perturbative intensity parameter'. The first comes from the formal consideration that if the non-perturbative theory[31] is expanded in a perturbation series, the expansion parameter is exactly z. The second reason is qualitative. An electron, when released from an atom to become a free particle in the laser field, acquires the ponderomotive energy U_p. If this energy is greater than $\hbar\omega$, that means that many photons must collaborate in order to provide the electron with this field-interaction energy. It is inherently a multiphoton process in which many photons must interact simultaneously with the electron. It is thus fundamentally non-perturbative. Only if $\hbar\omega > U_p$ is it possible to have a single-photon process provide the necessary field interaction energy.

The parameter z occurs prominently in Ref. 31. It occurs also in the work of Keldysh,[29] but he makes no explicit mention of it.

1.3.4. *Bound-state intensity parameter.* It will be seen in Sections 4 and 5 that Keldysh-like theories are useful for practical application to the prediction of ionization yields in very strong laser fields. Such theories are also known as Keldysh–Faisal–Reiss[29–31] or KFR theories. When the large-z limit of a KFR theory is sought, a new intensity parameter automatically appears. This is the 'bound-state intensity parameter' or 'field-dominant intensity parameter' z_1, defined by

$$z_1 \equiv 2U_p/E_B = (e\mathscr{E}/\omega)^2/2mE_B, \tag{10}$$

where E_B is the atomic binding energy, and again the last expression is in SI units. Expressions in atomic units are

$$z_1 = I/2\omega^2 E_B = (\mathscr{E}/\omega)^2/2E_B = 2\rho/\omega E_B. \tag{11}$$

This is the parameter emphasized by Keldysh,[29] although he did not write it in the form of an intensity parameter. Instead, he defined a quantity γ which declines with rising intensity. The connection is $z_1 = 1/\gamma^2$.

The definition in Eqn. (10) provides the most direct physical interpretation of z_1. If $U_p > E_B$, then the energy of interaction of the electron with the field exceeds the binding energy of the electron, and the field can be said to be the dominant influence on the detached electron. That is, $z_1 > 1$ corresponds to the field-dominant or strong-field domain.

An alternative view in terms of more traditional atomic quantities comes from noting that the amplitude of power broadening of atomic levels is of the order of $|e\boldsymbol{\mathscr{E}}\cdot\mathbf{r}| \approx e\mathscr{E}_0 a_0$, where a_0 is the Bohr radius, or, more generically, the size of the bound system. When this is compared with a single photon energy and squared, one has

$$\left(\frac{|e\boldsymbol{\mathscr{E}}\cdot\mathbf{r}|}{\hbar\omega}\right)^2 \approx z_1 \tag{12}$$

when the general connection

$$a_0^2 = \hbar^2/2mE_B \tag{13}$$

is used. Qualitatively, this means that $z_1 > 1$ signifies an intensity at which the power broadening of levels exceeds a single photon energy, and it is no longer reasonable to separately identify levels in the field-interacting atom. They are smeared beyond redemption.

1.3.5. *Free-electron intensity parameter.* The last of the intensity parameters to be discussed is, historically, the first to receive significant notice. The free-electron parameter, z_f, is defined by

$$z_f = 2U_p/mc^2 = (e\mathscr{E}/mc\omega)^2/2, \tag{14}$$

with the last expression in SI units, or in atomic units as

$$z_f = \alpha^2 I/2\omega^2 = (\alpha\mathscr{E}/\omega)^2/2 = 2\alpha^2\rho/\omega, \tag{15}$$

where α is the fine structure constant.

The quantity z_f arose many years ago[32–34] in the context of the quantum-mechanical behavior of a free electron in a strong plane-wave electromagnetic field. The first problem considered was photon–multiphoton pair production,[32] followed by the related crossed-channel processes of photon–multiphoton pair annihilation[33] and strong-field Compton scattering.[33,34] It was found that z_f occurs, and can be viewed as a 'mass-shift' effect,[32–34] where the normal mass of a free electron is modified by the field to an apparent increased mass according to

$$m^2 \to m^2 + \Delta m^2 = m^2(1 + z_f). \tag{16}$$

It is seen from Eqns (2), (5) and (14) that this corresponds exactly to the classical result. It is possible also to show how Eqn. (16) can be obtained by a formal mass renormalization procedure.[35]

The physical meaning of z_f is quite clear. When the interaction energy of the electron with the field (U_p) is greater than the electron's rest energy, then the effects of the field will be relativistic in nature. This conclusion is explicitly borne out by calculations of photoionization done by a completely relativistic method,[36] where the consequences of relativity are found to be measured precisely by the parameter z_f. This same parameter arises in another important way described in the next section.

1.3.6. *Classical free-particle motion.* The classical relativistic equations of motion for a free, charged particle in interaction with a plane-wave electromagnetic field can be solved exactly.[24,25] In the frame of reference in which there is no net motion of the electron over a full period of the field, a linearly polarized laser with electric and magnetic fields given by

$$\mathscr{E} = \mathscr{E}_0 \cos[\omega(t - x/c)]; \quad \mathbf{B} = (c\mathbf{k}/\omega) \times \mathscr{E} \tag{17}$$

causes an electron motion such that

$$\omega y/c = -\zeta^{1/2} \cos[\omega(t - x/c)] \tag{18}$$

$$\omega x/c = -(\zeta/8)\sin[2\omega(t - x/c)], \tag{19}$$

where $\mathbf{k}$ is the propagation vector for the field of circular frequency ω, the electric field is polarized along the y axis, the direction of propagation is x, and the parameter ζ is defined by

$$\zeta \equiv 2z_f/(1 + z_f). \tag{20}$$

The motion given in Eqns (18) and (19) is in the form of the numeral eight, oriented upright along the direction of polarization in a plane defined by the directions of polarization and propagation.

A profoundly important implication of the above results is that the proportions of the electron figure-8 motion are determined entirely by z_f. The amplitude of the motion depends both on z_f and on the frequency ω, but the proportions depend only on the dimensionless intensity parameter z_f. The 'fatness' of the Fig. 8 as compared to its height is given by $\zeta^{1/2}/8$, which approaches the limit $2^{-5/2}$ in the extreme relativistic case, and approaches 0 in the non-relativistic limit. That is, in the non-relativistic case, one obtains the expected linear oscillation of the electron along the direction of the electric field. The amplitude of the motion in the electric field direction, from Eqn. (18) is, in general

$$\alpha_0 = c\zeta^{1/2}/\omega, \tag{21}$$

which gives the non-relativistic limit

$$\alpha_0 \approx e\mathscr{E}/m\omega^2. \tag{22}$$

This last result is easily derived directly. It is now becoming very familiar in strong-field work because it is so intimately involved in the Kramers–Henneberger transformation[37,38] which is the subject of much recent attention in connection with the stabilization phenomenon in atomic processes.[39–49] (Stabilization is a uniquely strong-field effect in which, beyond a certain critical intensity, further increases in intensity cause a decline in transition rate, rather than the 'obvious' increase one would expect.) Stabilization is treated in Section 5.2.

Since the free-particle amplitude of motion in the laser field is now in widespread use, the intensity parameters will be stated in terms of the non-relativistic α_0 as given in Eqn. (22). The expressions are

$$z = m\omega\alpha_0^2/4\hbar, \tag{23}$$

$$z_1 = m(\omega\alpha_0)^2/2E_B, \tag{24}$$

$$z_f = (\omega\alpha_0/c)^2/2. \tag{25}$$

It is really more consistent to express z_f in terms of the relativistic α_0 as given by Eqn. (21), in which case z_f is

$$z_f = (\omega\alpha_0)^2/[2c^2 - (\omega\alpha_0)^2]. \tag{26}$$

1.3.7. *Critical values of the intensity parameters.* It is instructive to examine the laser energy fluxes required to achieve a value of unity for each of the intensity parameters z, z_1, z_f. The word 'laser' is used here in a generic sense, since it is wished to describe not only laser environments, but strong-field microwave environments as well. Four representative wavelengths are considered: 200 nm (typical of an excimer laser); 1 μm (Nd laser); 10 μm (CO_2 laser); and 3 cm (i.e., 10 GHz) representing the microwave case.

The non-perturbative intensity parameter is considered first. The value $z = 1$ is a clear upper limit for the radius of convergence of perturbation theory,[31] since a necessary (but not sufficient) condition for convergence of a series is that successive terms should decline in magnitude. The demand that $z = 1$ means that $I = 4\omega^3$ in atomic units, from Eqn. (7). Table 1 lists the required intensity both in atomic units and in W/cm^2 to achieve a unit value of z.

The most noticeable fact in Table 1 is the relatively modest intensities needed to surpass the perturbative regime. At 1 μm, the 10^{13} W/cm^2 limit is in accord with the ATI (above-threshold ionization) experiments, where, after extended debate, the consensus is that perturbation theory fails at that intensity. Note, however, how small the critical intensity is in atomic units. In other words, the electric field of the laser is significantly smaller than the Coulomb field of the atom at the intensity where perturbation theory fails. This conclusion is even more striking with the CO_2 laser, where both the 3.8×10^{-7} au and the 1.3×10^{10} W/cm^2 numbers are very modest.

TABLE 1. Intensity required to obtain unit value for the non-perturbative intensity parameter, z

Wavelength	Intensity (atomic units) for $z = 1$	Intensity (W/cm^2) for $z = 1$
200 nm	0.047	1.66×10^{15}
1 μm	3.78×10^{-4}	1.33×10^{13}
10 μm	3.78×10^{-7}	1.33×10^{10}
3 cm	1.40×10^{-17}	0.493

Most notable of all is the microwave example. The frequency employed in the example is similar to the 8.2 GHz used by Gallagher[50] in a set of experiments carried out at 3×10^4 W/cm^2, corresponding to $z = 10^5$. Even though the intensity in the Gallagher experiments is only about 10^{-12} in atomic units, the physical behavior observed was extremely non-perturbative. A relatively weak laser, sufficient in energy only to excite a Rydberg state in a beam of sodium atoms, was intersected with the atomic beam in a cavity with intense microwaves. Photoelectrons were observed to emerge with energies of nearly 10 eV, where this considerable kinetic energy could come only from the microwave field. The microwave photons have only 3×10^{-5} eV apiece, so more than 10^5 photons have to act cooperatively to produce the final state. This is consistent with a z value of 10^5, but it is not at all suggested by a microwave intensity of 10^{-12} au, which means an electric field amounting to only 10^{-6} of the atomic Coulomb field at the Bohr radius. This reinforces the remark above that the field is most meaningfully measured by energy ratios, as in the z, z_1 parameters, and not by the electric field strength.

Table 2 is the analog of Table 1, but for the bound-state intensity parameter z_1. Two separate sets of values are given in this table. One is for photoionization from the ground state, where the hydrogenic principal quantum number is $n = 1$; and the other is for an initial Rydberg state, where $n = 20$. This is especially relevant for the microwave frequency, where the field will normally be used only to ionize Rydberg states, and not the ground state.

The results displayed in Table 2 are particularly important because the parameter z_1 is the essential measure of the applicability to atomic ionization of Keldysh-like methods, to be introduced in Section 4. Keldysh-like methods, or the KFR method (or the SFA—strong-field approximation) are the quintessential strong-field techniques, and their applicability demands $z_1 > 1$. (This is true for long-range potentials. For short-range potentials, the requirements are less stringent.[31]) A laser environment with $z_1 > 1$ can properly be termed a strong-field environment, and Table 2 shows (even for the $n = 1$ case) that the intensity in atomic units need not be at all close to the value unity so often assumed to be the hallmark of the strong-field situation.

For completeness, Table 3 is included here, to show when relativistic effects are important. Table 3 gives the intensity at which $z_f = 1$. Relativistic effects, however, are most likely to be in evidence at $z_f \approx 0.1$.[36] This means that relativity is already of significance in present state-of-the-art environments at the shorter wavelengths in Table 3, whereas it may never be of significance for the long wavelength cases.

TABLE 2. Intensity required to obtain unit value for the bound-state intensity parameter z_1

	Intensity (atomic units) for $z_1 = 1$		Intensity (W/cm^2) for $z_1 = 1$	
Wavelength	$n = 1$	$n = 20$	$n = 1$	$n = 20$
200 nm	0.052	1.30×10^{-4}	1.82×10^{15}	4.55×10^{12}
1 μm	2.08×10^{-3}	5.19×10^{-6}	7.29×10^{13}	1.82×10^{11}
10 μm	2.08×10^{-5}	5.19×10^{-8}	7.29×10^{11}	1.82×10^{9}
3 cm	2.31×10^{-12}	5.77×10^{-15}	8.11×10^{4}	2.03×10^{2}

TABLE 3. Intensity required to obtain unit value for the free-particle intensity parameter z_f

Wavelength	Intensity (atomic units) for $z_f = 1$	Intensity (W/cm^2) for $z_f = 1$
200 nm	1950	6.84×10^{19}
1 μm	78	2.74×10^{18}
10 μm	0.78	2.74×10^{16}
3 cm	8.68×10^{-8}	3.04×10^{9}

TABLE 4. Peak values for intensity parameters with laser systems presently available

Wavelength	W/cm^2	z	z_1	z_f
248 nm	10^{19}	11500	8440	0.225
1.054 μm	10^{19}	88200	152000	4.06
10.6 μm	10^{14}	8970	154	0.00411

1.4. *Available Strong-Field Environments*

A brief compendium is supplied here of 'state-of-the-art' laser intensities for some commonly used systems. The principal intent is to demonstrate that z and z_1 parameters are currently attainable that are well into the strong-field domain. With the presumption that relativistic effects will become visible within the region of $0.1 \leqslant z_f \leqslant 1$, it appears that relativistic experiments can be done with existing lasers.

The excimer laser is represented by the example of KrF, at a wavelength of 248 nm. The intensity presented has been achieved, and the goal is to increase this to 10^{21} W/cm in the future.[1] The Nd laser is of the phosphate glass type, and 10^{19} W/cm^2 corresponds to a new-generation system now available.[2] Information on the CO_2 laser refers to an intensity that has been in existence for some time now. There is a presumed limit of 10^{16} W/cm^2 for this type of system.[3] Table 4 shows only the smaller of the intensities quoted.

A general conclusion that can be drawn from Table 4 is that higher frequencies favor relativistic conditions. This seems intuitively obvious, except for the reminder that, for example, the Nd laser has only about 1 eV per photon. Furthermore, if the CO_2 system is extended to 10^{16} W/cm^2, then this system also enters the relativistic domain, but with only 0.1 eV per photon.

1.5. *Limits on the Dipole Approximation in Strong Fields*

Most current strong-field experiments are being done in an environment where $z_f \ll 1$, and so (see Section 1.3.5) one expects the problem to be non-relativistic. This, in turn, leads to the expectation that a dipole approximation should be adequate since the usual condition $a_0/\lambda \ll 1$ is well satisfied in most strong-field environments, where a_0 is the atomic radius and λ is the field wavelength. This presumption will now be examined.

The most naive requirement that one might impose for validity of the dipole approximation is that a free electron, moving parallel to the field propagation direction with a velocity v, should travel only a small fraction of a wavelength during a single wave period τ. This is expressed as

$$v\tau \ll \lambda; \quad \text{or} \quad v \ll \nu\lambda = c; \quad \text{or} \quad v/c \ll 1. \tag{27}$$

[1]Information kindly supplied by T. S. Luk of the University of Illinois, Chicago Circle.
[2]Thanks are due to P. H. Bucksbaum of the University of Michigan for this information.
[3]Information kindly supplied by S. L. Chin of Université Laval, Québec.

This is the conventional non-relativistic condition in classical mechanics. However, as discussed in Section 1.3.6, an electron in a plane wave electromagnetic field is not free to move in a straight line. Instead, any straight-line motion is superimposed on a figure-eight motion with amplitude parallel to the propagation direction given by

$$|x|/\lambda = (\zeta/8)(c/\lambda\omega), \tag{28}$$

from Eqn. (19). The factor $(c/\lambda\omega)$ is just $1/2\pi$, and when $z_f \ll 1$, Eqn. (20) shows that $\zeta/8 \approx z_f/4$. Hence, the amplitude of field-induced motion given in Eqn. (28) is simply

$$|x|/\lambda \approx z_f/8\pi. \tag{29}$$

This now gives a condition in terms of field strength as

$$z_f \ll 1 \tag{30}$$

in place of the pure velocity condition of Eqn. (27).

The above considerations relate to a free electron. What if the electron is associated with a binding potential of range a_0, where a_0 is a Bohr radius? The displacement $|x|$ should then be compared with a_0 rather than λ. With $\zeta \approx 2z_f$ as before, then Eqn. (28) becomes

$$|x|/a_0 \approx (z_f/4)(c/a_0\omega). \tag{31}$$

It is easily shown that the right-hand side of Eqn. (31) is expressible in terms of the non-perturbative parameter z of Section 1.3.3, with the final result that

$$|x|/a_0 \approx \alpha z/2, \tag{32}$$

where α is the fine structure constant. To have $|x|/a_0$ small, one must then require

$$z \ll 2/\alpha \approx 300. \tag{33}$$

The condition given in Eqn. (33) is surpassed in many present-day experiments, even those with $z_f < 1$. See Table 1 for a guide to the intensity requirements.

The conclusion is that the dipole approximation is in question when the condition (33) is violated, rather than the (usually) much milder condition (30). The significance of this result has yet to be explored.

1.6. *Characteristics of a Strong-Field Theory*

From the introductory remarks to this point, certain basic features of a strong-field theory may already be inferred.

A strong-field theory must be more than non-perturbative. It is not likely even to be based on extensions of perturbative concepts. When the ponderomotive potential exceeds $\hbar\omega$ by a large factor (i.e., $z \gg 1$), the notion of an atom absorbing photons one by one on its way to a final state is no longer useful. Not only are too many stages involved, but the properties of an atomic state are no longer clear cut. States are broadened and shifted beyond recognition, and transitions may involve many thousands of photons.[4-6,50] ATI behavior, where high-order processes (often *very* high orders) are competitive with low orders are the rule, not the exception. By now, experimental evidence of the ATI phenomenon is so widespread that only a sampling of early results is referenced here.[51-53] It was not long before multiple states of ionization produced by multiphoton absorption were observed.[3,4,54] (See one of the many specific review articles on these subjects for more extensive referencing. A recent one is Ref. 55.) As with so many strong-field phenomena that have recently attracted much attention, the ATI phenomenon was explicitly remarked upon long before its observation. It was pointed out in 1970 that "at very high intensity a large number of photon

multiplicities become almost equally probable";[39] supplemented by a 1971 comment that "an extremely high-order process can be competitive with—and even dominate—the lowest order".[56]

An important adjunct of strong-field photoionization or photodetachment is that the field has major effects on the electron(s) released in the process. As discussed in Section 1.3.6, a free electron immersed in a strong laser field exhibits large-amplitude motions that can represent a considerable amount of energy. This was recognized in the earliest work on the free-electron processes of strong-field pair production, pair annihilation, and Compton scattering.[32–34,57,58] Energy conservation conditions are substantially modified by the requirement that an electron in a field can not have stationarity as its minimal energy state. The same is true when an electron is separated from an initial bound state. This is stated in the conservation conditions in the early work on the subject,[29–31,56,57] and is even described in terms of its physical meaning.[31,60] The observed effect of this field-induced motion of the electron (sometimes referred to as 'jitter motion') is to suppress the lowest order processes in multiphoton ionization.[31,61] That is, the minimum order permitted by the energy conservation conditions is higher when one considers the need to supply jitter motion to the electron than when that effect is neglected. This phenomenon was demonstrated experimentally by Kruit *et al.*[62] (see also Ref. 63).

An apparently counter-intuitive prediction from theories of extremely strong fields is that the transition amplitude can actually decline with increasing intensity beyond some extremal value.[39–42,44–49] This was also remarked upon at a very early date and then later overlooked. The words used in 1970 spoke of the "seemingly paradoxical result that high field intensities lead to smaller transition probabilities than much more modest intensities".[39] This is almost the same as the 1988 statement that "the transition rate exhibits a maximum as a function of intensity. Beyond that point an increase in intensity has the counter-intuitive effect of decreasing the transition probability".[40] The phenomenon has come to be called "stabilization". It has been found in the theories of so many different types of strong-field phenomena that one can probably view this as an expected consequence of strong fields. It must be pointed out, however, that stabilization normally is predicted from monochromatic theories. It has yet to be demonstrated that the effect is discernible experimentally in a laboratory environment where a target is subjected to a laser pulse of complex shape in three spatial dimensions and in time.

The explanation of all of the above characteristics in a single, universally applicable theoretical technique is the goal of the methods explicated here.

2. S MATRICES

2.1. *History*

The S-matrix approach to the description of transitions was introduced over fifty years ago by Wheeler,[64] and owed much of its early development to Heisenberg[65] and Stückelberg.[66] For many years, S matrices were used only in quantum field theory,[67–70] and in the theory of scattering,[71–73] both in its general form and in various applications such as elementary particle physics[74,75] and ion–atom collisions.[76] However, there is no reason to confine S matrices to continuum problems or to relativistic problems, and they offer significant advantages in many areas in atomic and molecular physics. That is, S matrix methods can be applied to every variety of problem: free–free, bound–free, free–bound, and bound–bound. S-matrix techniques in multiphoton processes date back about twenty years.[77] Although the most usual application of the S matrix in external-field electrodynamics is in the context of perturbation theory, it has been found to be especially useful as a vehicle for non-perturbative treatments.[30,31,36,40,77,78] The essential points about the S-matrix method are that it is

very simple in concept and formal statement, clear about specification of boundary conditions, and universal in application.

2.2. *Development of the General S Matrix*

An attractive feature of the S matrix is that it is directly related to the laboratory measurement process. A typical measurement is one in which a system is prepared in some known state; a physical influence is then brought to bear on this system, which causes changes away from the initial state; and then the products of the interaction are examined in order to appraise the nature and extent of the changes. These general statements will be given formal expression. Generalizations are easily developed in which the transition-causing interaction may be still active in the final state, though not in the initial state (or vice versa); and there may be latitude in deciding which of two (or more) interactions 'causes' the transition, and which is always present.

The focus of this article is S-matrix techniques as they relate to the calculation of processes occurring in very strong electromagnetic fields of frequencies such as might be provided by a laser as a source. There will thus be no consideration given here to such very formal developments as Møller wave operators or the analytic S matrix.[79–81]

The physical problems most likely to be familiar to the reader are non-relativistic, and that case is developed first. Relativistic conditions, in the present physical context, arise as a consequence of extremely strong fields in problems that are otherwise nominally non-relativistic. The relativistic S matrix is therefore also developed. It is then seen to be not only a logical extension of the non-relativistic S matrix, but is found to possess inherently covariant forms which allow one to appreciate the power and formal beauty of the method.

2.2.1. *Non-relativistic case.* The Hamiltonian is taken to consist of two parts: one which is present at all times, H_0; and an additional part which is presumed to give rise to transitions, H_I. It is not necessary that H_0 be simply a free-particle Hamiltonian. It may itself contain non-trivial interaction terms, and may be explicitly time dependent. The interaction Hamiltonian H_I may also be explicitly time dependent. The case where H_I 'turns off' at both asymptotic times is developed, although this can be generalized, as remarked. For convenience, asymptotic conditions will be designated by $t \to \infty$ and $t \to -\infty$, but in practice these asymptotic times may be separated by picoseconds or less of actual elapsed time. The Hamiltonian of the system will be stated as

$$H = H_0 + H_I; \quad \lim_{t \to \pm\infty} H = H_0. \tag{34}$$

The 'non-interacting' asymptotic states Φ of the system satisfy the Schrödinger equation

$$(i\hbar\partial_t - H_0)\Phi = 0, \tag{35}$$

whereas the complete solutions Ψ of the fully interacting system satisfy the Schrödinger equation

$$(i\hbar\partial_t - H)\Psi = 0. \tag{36}$$

The state $\Psi_i^{(+)}$ is that solution of Eqn. (36) which satisfies the boundary condition

$$\lim_{t \to -\infty} \Psi_i^{(+)}(t) = \Phi_i(t). \tag{37}$$

In other words, $\Psi_i^{(+)}$ is the state which is initially non-interacting. It is then subjected to the full Hamiltonian H, and eventually emerges from the interaction region to be analyzed for an assessment of the manner and degree to which the state has been altered by the interaction. This final analysis is generally accomplished within measuring devices where the interaction Hamiltonian H_I is no longer in effect, and so the final analysis is done by appraising the

overlap of the fully evolved state $\Psi_i^{(+)}$ at large asymptotic times onto non-interacting states Φ. Any such overlap, or transition amplitude, is termed an S matrix. That is,

$$S_{fi} = \lim_{t \to \infty} (\Phi_f(t), \Psi_i^{(+)}(t)). \tag{38}$$

The information contained in the transition amplitudes to a complete set $\{\Phi\}$ of non-interacting states serves to completely define the fully interacting state $\Psi_i^{(+)}$. The S_{fi} expressed in Eqn. (38) is in accord with the usual notion of a transition amplitude.

It bears repeating that $t \to \infty$ in Eqn. (38) simply signifies that the atom or electron being analyzed has left the interaction region and entered the final measuring device (ion counter, electron spectrometer, . . .). Actual elapsed time may be very brief.

The equations of motion of quantum mechanics are invariant under time reversal, and so Eqn. (38) may be replaced by the fully equivalent 'reversed-time S matrix'

$$S_{fi} = \lim_{t \to -\infty} (\Psi_f^{(-)}(t), \Phi_i(t)), \tag{39}$$

where $\Psi_f^{(-)}$ is that solution of Eqn. (36) which satisfies the asymptotic condition

$$\lim_{t \to +\infty} \Psi_f^{(-)}(t) = \Phi_f(t). \tag{40}$$

The $(\pm)$ superscripts on the Ψ functions are not necessary when dealing with bound states. It is useful to retain them, however, for the formal development.

It is now desired to eliminate the necessity of evaluating asymptotic limits in order to determine the S-matrix expressions. This is accomplished by using Green's operators. The retarded Green's operator $G^{(+)}(t, t_0)$ and the advanced Green's operator $G^{(-)}(t, t_0)$ both satisfy the equation

$$(i\hbar\partial_t - H_0)G^{(\pm)}(t, t_0) = \delta(t - t_0), \tag{41}$$

based on the non-interacting Hamiltonian H_0 of Eqn. (35). One operator propagates state vectors forward in time and the other backward in time in accordance with

$$G^{(+)}(t, t_0)\Phi(t_0) = -(i/\hbar)\theta(t - t_0)\Phi(t), \tag{42}$$

$$G^{(-)}(t, t_0)\Phi(t_0) = (i/\hbar)\theta(t_0 - t)\Phi(t), \tag{43}$$

where $\theta(t)$ is the standard unit step function. The two Green's operators are related by

$$G^{(-)}(t, t_0) = G^{(+)\dagger}(t_0, t). \tag{44}$$

A formal solution of Eqn. (36) is given by the integral equation

$$\Psi^{(\pm)}(t) = \Phi(t) + \int dt_1 G^{(\pm)}(t, t_1)H_I(t_1)\Psi^{(\pm)}(t_1). \tag{45}$$

When Eqn. (45) is substituted into Eqn. (38), the result is

$$S_{fi} = \lim_{t \to \infty} (\Phi_f, \Phi_i) + \lim_{t \to \infty} \int dt_1 (\Phi_f(t), G^{(+)}(t, t_1)H_I(t_1)\Psi_i^{(+)}(t_1)),$$

$$= \delta_{fi} + \lim_{t \to \infty} \int dt_1 (G^{(-)}(t_1, t)\Phi_f(t), H_I(t_1)\Psi_i^{(+)}(t_1), \tag{46}$$

when Eqn. (44) is used, or, finally,

$$(S-1)_{\mathrm{fi}} = -(i/\hbar)\int \mathrm{d}t(\Phi_{\mathrm{f}}, H_{\mathrm{I}}\Psi_{\mathrm{i}}^{(+)}), \tag{47}$$

with the help of Eqn. (43) and the fact that

$$\lim_{t\to\infty}\theta(t-t_1) = 1. \tag{48}$$

The subscript on the variable of integration has been omitted in Eqn. (47) since now only one time parameter remains. An exactly analogous procedure gives the alternative S-matrix expression

$$(S-1)_{\mathrm{fi}} = -(i/\hbar)\int \mathrm{d}t(\Psi_{\mathrm{f}}^{(-)}, H_{\mathrm{I}}\Phi_{\mathrm{i}}). \tag{49}$$

An important remark is that the functions Φ in Eqns (47) and (49) are reference states which in no way reflect the presence of the interaction causing the transition. In intense-field electrodynamics, much interest attaches to the broadening and shifting of levels that occur in the presence of the field. The most straightforward application of S-matrix techniques is carried out such that H_{I} contains the effects of the laser field, and so Φ has no field effects. These effects are confined entirely to the states Ψ. It is a convenient feature of the S matrix formalism that such field effects need not and should not be considered in the Φ states.

Equations (47) and (49) are exact. They provide a powerful tool which can be used as the foundation either of perturbative or non-perturbative calculational techniques. Specifically, Eqn. (47) is employed in Ref. 74 as the basis for development of Feynman diagram techniques in all generality. Included among the applications is the interaction with electromagnetic fields, where the full power of the Feynman diagram technique of gauge-invariant quantum electrodynamics can be based on Eqn. (47) or (49).

2.2.2. *Relativistic spinor case.* The classic textbook of Bjorken and Drell[74] provides a development of the relativistic S matrix in a physical context which is not dependent on the formal developments of quantum field theory. Yet the results are, in fact, identical to what is constructed in quantum field theory with the formalism of the Wick theorem[67–70] and all that goes with it. Yet even the development given by Bjorken and Drell[74] is not direct nor is it made manifestly covariant until the final stages. The alternative derivation given here[36,78] exactly duplicates the Bjorken and Drell S matrix, but in a succinct derivation which parallels the non-relativistic treatment in the preceding section, and yet achieves a covariant form at an early stage.

The relativistic problem comes in two varieties for our purposes. An electron possesses intrinsic spin of $\hbar/2$, and so it is properly treated by means of the Dirac equation. This is a first order differential equation, which is very simple in form. That seeming simplicity arises as a consequence of the fact that the wave function is a spinor and not a scalar quantity, and the entire problem is formulated in the four-dimensional Dirac matrix space. Basic expressions are easy to derive, but practical computations can be extremely difficult to carry through to completion. An alternative is to neglect the intrinsic spin of the electron while maintaining a relativistic theory in all other senses. This is done by treating the electron as a scalar particle whose state vector obeys the Klein–Gordon equation, which is a second order differential equation. There is the added complication that the definition of a scalar product in the Klein–Gordon space is more complicated than for the Dirac case. Yet, because there are no Dirac matrices to consider, practical computations are generally easier to accomplish than for the spinor Dirac case. The Dirac problem will be treated first because of the seeming simplicity of the formulation.

The starting point for the Dirac relativistic S matrix will again be the physically motivated Eqn. (38) or (39). In other words, one wishes to evaluate the consequences of an interaction by direct comparison of the final outcome of the interaction with a non-interacting state as reference. It is now convenient to incorporate the asymptotic 'starting' conditions (37) and (40) directly into the S-matrix expression. That is, simple orthogonality allows one to replace Eqn. (37) by the expression

$$\lim_{t \to -\infty} (\Phi_f(t), \Psi_i^{(+)}(t)) = \delta_{fi}. \tag{50}$$

This combines with Eqn. (38) to give

$$(S-1)_{fi} = \lim_{t \to +\infty} (\Phi_f, \Psi_i^{(+)}) - \lim_{t \to -\infty} (\Phi_f, \Psi_i^{(+)}), \tag{51}$$

since δ_{fi} is just the matrix element of the unit operator. In like fashion, Eqns (39) and (40) combine to give

$$(S-1)_{fi} = \lim_{t \to -\infty} (\Psi_f^{(-)}, \Phi_i) - \lim_{t \to +\infty} (\Psi_f^{(-)}, \Phi_i). \tag{52}$$

Equations (51) and (52) could also have been used in the non-relativistic case. They are entirely general, with a well-defined physical meaning. It is now desired to express these equations in terms of relativistic state vectors. As a preliminary, Eqn. (51) will have its inner product expressions rendered in the equivalent form of an integration over all space. This is done by using the Dirac metric to express the inner product in the form

$$(\Phi, \Psi) = \int d^3r \Phi^\dagger \Psi = \int d^3r \bar{\Phi} \gamma^0 \Psi, \tag{53}$$

using the standard definition of the Dirac adjoint as

$$\bar{\Phi} \equiv \Phi^\dagger \gamma^0, \tag{54}$$

when γ^0 is the Dirac matrix (see the definitions of the Dirac matrices contained in Ref. 74) which has the property $(\gamma^0)^2 = 1$. This puts Eqn. (51) in the form

$$(S-1)_{fi} = \lim_{t \to +\infty} \int d^3r \bar{\Phi}_f \gamma^0 \Psi_i^{(+)} - \lim_{t \to -\infty} \int d^3r \bar{\Phi}_f \gamma^0 \Psi_i^{(+)}, \tag{55}$$

where now Φ and Ψ are to be regarded as spinor solutions of the Dirac equation and no longer as scalar solutions of the Schrödinger equation. Clearly, Eqn. (52) can be rewritten in an analogous way.

The above expressions will now be converted to a covariant form. Consider a four-dimensional space–time Minkowski space with origin at the event corresponding to the occurrence of the quantum-mechanical transition to be described. Let τ_f be a flat, constant-time surface at a large positive time, and let τ_i be another such surface at large negative time. The surface τ_f will have its normal lying along the direction of the positive time axis, and take the normal to the surface τ_i to be in the negative direction of the time axis. If the times corresponding to τ_f and τ_i have the same absolute magnitude, then τ_f will intersect the forward light cone from the origin in a hypercircle of the same radius as that with which τ_i intersects the backward light cone from the origin. These intersections can then be connected by a hyper-circular cylindrical surface τ_s which has a spacelike normal everywhere, directed outward away from the time axis. The geometry of this configuration is shown in simplified fashion in Fig. 1, rendered in a Minkowski space with only one spatial dimension. The union

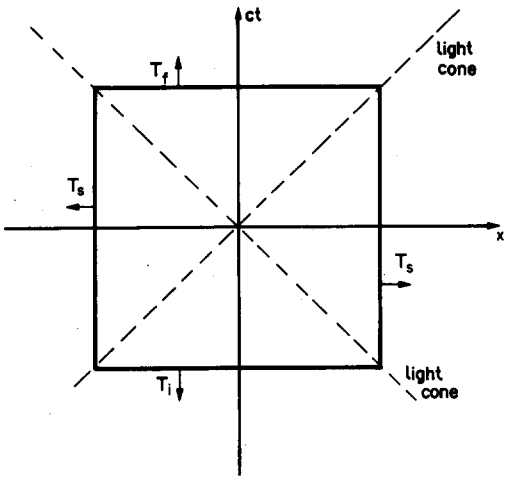

FIG. 1. Surface of integration in space–time represented in Eqn. (56) for use in the integration in Eqn. (57).

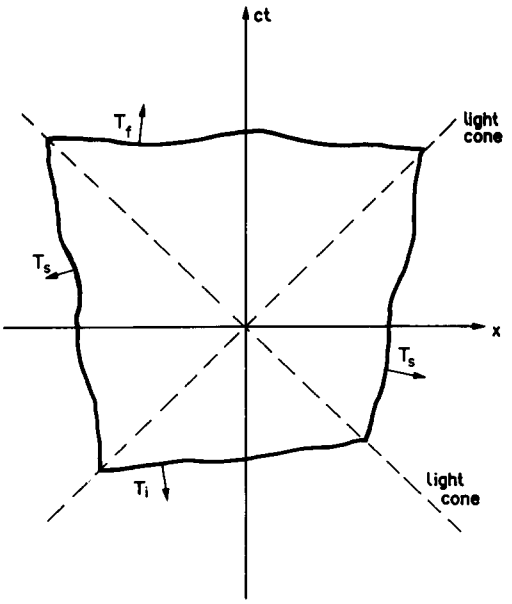

FIG. 2. Covariant generalization of the surface of integration shown in Fig. 1. This is the surface employed in Eqn. (59).

of these hypersurfaces constitutes a closed surface Σ with outwardly directed normal everywhere, i.e.

$$\Sigma = \tau_f \cup \tau_i \cup \tau_s. \tag{56}$$

If the time associated with τ_f approaches $+\infty$ (so that the time on τ_i approaches $-\infty$), then the surface τ_s will approach an infinite spacelike distance from the origin, i.e., from the quantum transition event. The state vectors can then be taken to approach zero on τ_s. Hence the right-hand side of Eqn. (55) can be rewritten as the surface integral in four-space

$$\lim_{t\to+\infty}\int d^3r\bar{\Phi}_f\gamma^0\Psi_i^{(+)} - \lim_{t\to-\infty}\int d^3r\bar{\Phi}_f\gamma^0\Psi_i^{(+)} = \oint_\Sigma d\sigma_\mu\bar{\Phi}_f\gamma^\mu\Psi_i^{(+)}. \tag{57}$$

The scalar product of two four-vectors employed in Eqn. (57) is given in general by

$$a_\mu b^\mu = a^\mu b_\mu \equiv a^0b^0 - \mathbf{a}\cdot\mathbf{b}. \tag{58}$$

That is, the conventions used in Bjorken and Drell[74] continue to be employed. The surface Σ of Eqn. (56) may now be generalized so that the surfaces τ_f, τ_i are no longer flat, although their normals must still everywhere be timelike; and the surface τ_s is now no longer perfectly a hypercircular cylinder, although its normal must still everywhere be spacelike. This generalization of Fig. 1 is rendered in Fig. 2 with one spatial dimension. With this generalized notion of Σ, the Lorentz-covariant statement of the S matrix is

$$(S-1)_{fi} = \oint_\Sigma d\sigma_\mu\bar{\Phi}_f\gamma^\mu\Psi_i^{(+)}. \tag{59}$$

The γ^μ in Eqn. (59) are the Dirac matrices $\gamma^0, \gamma^1, \gamma^2, \gamma^3$ employed with the conventions adopted by Bjorken and Drell.[74] Equation (59) is in a form in which the divergence theorem in four-space can be directly applied, leading to

$$(S-1)_{fi} = \int d^4x\,\partial_\mu(\bar{\Phi}_f\gamma^\mu\Psi_i^{(+)}). \tag{60}$$

It is now necessary to introduce the equation of motion for an electron in the simultaneous presence of an atomic binding potential and of the laser field. It is necessary to depart temporarily from the covariant expressions in Eqns (59) and (60) since the standard practice[82] of using a fixed center of force for the binding potential will be adopted here. This, of course, destroys covariance; but the group-theoretical approach[83,84] which, in principle, would allow one to retain covariance for bound states has not been implemented for the Coulomb potential. For the fully interacting state Ψ, the Dirac equation is

$$(i\gamma^\mu\partial_\mu - e\gamma^\mu A_\mu - \gamma^0 V - m)\Psi = 0, \tag{61}$$

which has the adjoint equation

$$\bar{\Psi}(i\gamma^\mu\overleftarrow{\partial}_\mu + e\gamma^\mu A_\mu + \gamma^0 V + m) = 0. \tag{62}$$

The backward-directed arrow on the ∂_μ operator in Eqn. (62) is meant to indicate that it operates to the left. That is,

$$\bar{\Psi} i\gamma^\mu\overleftarrow{\partial}_\mu = (\partial_\mu\bar{\Psi})i\gamma^\mu, \tag{63}$$

where the γ^μ must be retained to the right of $\bar{\Psi}$ to preserve the meaning of an adjoint spinor in the Dirac matrix space multiplied into the square Dirac matrices γ^μ. The transition-causing interaction is taken to be the laser field represented by the four-potential A^μ, so the non-interacting Dirac equation is

$$(i\gamma^\mu\partial_\mu - \gamma^0 V - m)\Phi = 0, \tag{64}$$

with the adjoint equation given by

$$\bar{\Phi}(i\gamma^\mu\overleftarrow{\partial}_\mu + \gamma^0 V + m) = 0. \tag{65}$$

If Eqn. (61) for $\Psi_f^{(+)}$ has $\bar{\Phi}_f$ multiplied into it from the left, and Eqn. (65) for $\bar{\Phi}_f$ is multiplied on the right by $\Psi_i^{(+)}$, the resulting pair of equations can be added, giving rise to

$$\bar{\Phi}_f(i\gamma^\mu\partial_\mu + i\gamma^\mu\overleftarrow{\partial}_\mu - e\gamma^\mu A_\mu)\Psi_i^{(+)} = 0. \tag{66}$$

This can be rewritten as

$$\partial_\mu(\bar{\Phi}_f\gamma^\mu\Psi_i^{(+)}) = -i\bar{\Phi}_f eA_\mu\gamma^\mu\Psi_i^{(+)}, \tag{67}$$

which puts Eqn. (60) into the final form

$$(S-1)_{fi} = -i\int d^4x\bar{\Phi}_f eA^\mu\gamma_\mu\Psi_i^{(+)}. \tag{68}$$

Analogous procedures can be used to convert Eqn. (52) to

$$(S-1)_{fi} = -i\int d^4x\bar{\Psi}_f^{(-)}eA^\mu\gamma_\mu\Phi_i. \tag{69}$$

Equations (68) and (69) are the final 'direct-time' and 'time-reversed' forms of the Dirac S matrix for laser-field induced transitions. Alternative terminology to be found in the literature is that the direct-time form is called the post form, and time-reversed is referred to as prior. As will be seen below, the time-reversed form has powerful advantages for the treatment of intense-field photoionization problems.

A sometimes-useful alternative form to Eqn. (68) is

$$(S-1)_{fi} = -i\int d^4x\bar{\Phi}_f(i\gamma^\mu\partial_\mu - \gamma^0 V - m)\Psi_i^{(+)}, \tag{70}$$

found with the help of the equation of motion for Ψ, Eqn. (61). For later reference, we note that the operator contained between the two states in Eqn. (70) is exactly the operator from the non-interacting equation of motion, (64).

2.2.3. *Relativistic scalar case.* The relativistic scalar-particle, or Klein–Gordon problem[78] can be treated in essentially the same way as the spinor-particle or Dirac problem.[36] The starting point again is Eqn. (51) or (52). A central distinction between the scalar and spin-1/2 cases lies in the different metric appropriate to the state space. The Dirac method in Eqn. (53) must be replaced by the (time projection of the) Klein–Gordon metric

$$(\Phi, \Psi) = \int \mathrm{d}^3 r \Phi^* (i \overleftrightarrow{\partial^0} - 2eA^0)\Psi, \tag{71}$$

where the double-arrow notation is defined to mean[74]

$$a i \overleftrightarrow{\partial^0} b \equiv a(i\,\partial^0 b) - (i\,\partial^0 a) b. \tag{72}$$

It is understood now that the Φ and Ψ states are no longer spinor states, but are scalars. The adjoint of the wave function Φ is no longer given by Eqn. (54), but is simply the complex conjugate of Φ, designated by the asterisk superscript. The next steps follow exactly as in the Dirac case, leading to the replacement of Eqn. (59) by

$$(S-1)_{\mathrm{fi}} = \oint_{\Sigma} \mathrm{d}\sigma_\mu \Phi_{\mathrm{f}}^* (i\,\partial^\mu - 2eA^\mu)\Psi_{\mathrm{i}}^{(+)}. \tag{73}$$

The Klein–Gordon metric exhibited in Eqn. (73) is the covariant extension of the time projection of that metric that appeared in Eqn. (71). Application of the four-divergence theorem gives

$$(S-1)_{\mathrm{fi}} = -i \int \mathrm{d}^4 x i\,\partial^\mu [\Phi_{\mathrm{f}}^* (i\partial^\mu - 2eA^\mu)\Psi_{\mathrm{i}}^{(+)}]. \tag{74}$$

Recourse to the Klein–Gordon equation for Ψ and the adjoint Klein–Gordon equation for Φ^* allows Eqn. (74) to be converted to the final form

$$(S-1)_{\mathrm{fi}} = -i \int \mathrm{d}^4 x \Phi_{\mathrm{f}}^* \mathscr{V}_{\mathrm{KG}} \Psi_{\mathrm{i}}^{(+)}, \tag{75}$$

for the direct-time S matrix, or

$$(S-1)_{\mathrm{fi}} = -i \int \mathrm{d}^4 x \Psi_{\mathrm{f}}^{(-)*} \mathscr{V}_{\mathrm{KG}} \Phi_{\mathrm{i}}, \tag{76}$$

for the time-reversed S matrix, with the definition

$$\mathscr{V}_{\mathrm{KG}} \equiv ie(\partial_\mu A^\mu + A^\mu \partial_\mu) - e^2 A_\mu A^\mu. \tag{77}$$

An essential step in the progression from Eqn. (74) to the final form (75) involves recourse to the Klein–Gordon equation, which has not yet been stated. For the complete state Ψ, this is

$$\{[i\,\partial_\mu - eA_\mu - g_{\mu 0} V][i\,\partial^\mu - eA^\mu - g^{\mu 0} V] - m^2\}\Psi = 0, \tag{78}$$

where $g^{\mu 0}$ is the $\mu, 0$ component of the metric tensor $g^{\mu\nu}$ of special relativity, V is the Coulomb potential of the atom (presumed, as earlier, to be represented by a fixed center of force), and A^μ is the four-potential of the laser field. With the relativistic conventions used here, we have $g^{\mu 0} = \delta_{\mu 0}$, in terms of the usual Kronecker delta. An alternative way to write Eqn. (78) is

$$\{[i\,\partial_\mu - g_{\mu 0} V][i\,\partial^\mu - g^{\mu 0} V] - \mathscr{V}_{\mathrm{KG}} - m^2\}\Psi = 0, \tag{79}$$

in terms of the $\mathscr{V}_{KG}$ of Eqn. (77). Separability of the laser interaction (as contained in $\mathscr{V}_{KG}$) and the Coulomb interaction ($g^{\mu 0}V$) in Eqn. (79) is non-trivial and not universal, and is the subject of several later comments. The Klein–Gordon equation for Φ^* is also needed, which is found simply from Eqn. (79) with $\mathscr{V}_{KG}$ removed, and the remaining equation complex conjugated.

There is an important constraint in the derivation of Eqn. (79). To be able to eliminate the cross terms between the $g^{\mu 0}V$ and eA^{μ} potentials that exist in Eqn. (78), it is necessary that the plane-wave laser field be represented in the Coulomb gauge (also called the radiation gauge) so that $eA^0 = 0$. If one uses instead the 'length gauge', where the principal contribution to the laser field potential is the scalar potential $e\mathscr{E}\cdot\mathbf{r}$, then the laser field and the Coulomb potential will be strongly coupled in Eqn. (78) and no such separable result as Eqn. (79) is possible. This is the basis of an important distinction between Keldysh-like theories to be treated later.

2.3. *Gauge Transformations in the S-Matrix Formalism*

The point of view adopted here about gauge transformations in transition amplitudes[85] is the same as that conventionally employed in other fields such as high energy physics[74] or nuclear physics.[86] This point of view is that gauge invariance of a transition amplitude is the statement that an expression such as Eqn. (47) refers to an arbitrary gauge, unspecified a priori. This is not as trivial a statement as it might seem. Suppose Eqn. (47) refers to laser-introduced transitions where there is no electromagnetic field dependence in H_0, and hence none in Φ_f. The interaction Hamiltonian H_I and hence the interacting state Ψ_i will be field dependent. Then the S matrix in gauge 'a' is

$$(S-1)_{fi} = -(i/\hbar)\int dt(\Phi_f, H_I^{(a)}\Psi_i^{(a)}), \tag{80}$$

and in gauge 'b' it is

$$(S-1)_{fi} = -(i/\hbar)\int dt(\Phi_f, H_I^{(b)}\Psi_i^{(b)}), \tag{81}$$

where superscripts ($\pm$) will be suppressed for now. The state Φ_f in both expressions is the *same* state, since in both instances it refers to a solution of Eqn. (35) for the same set of quantum numbers, and a gauge transformation is of no consequence for a state that does not depend on the electromagnetic field.

The above definition of gauge invariance of a transition amplitude is here termed 'strong gauge invariance', although it appears to be so straightforward that a special name hardly seems warranted. However, views contrary to the above are not hard to find in the literature in atomic, molecular, and optical physics. The reason is that a gauge transformation not only changes the potentials representing the field, but in quantum mechanics it also implies a phase transformation of the wave function. That is, the gauge transformation of the scalar potential ϕ and vector potential $\mathbf{A}$ generated by the scalar function $\chi(\mathbf{r}, t)$:

$$\phi \to \phi' = \phi - \partial\chi/\partial(ct) \tag{82}$$

$$\mathbf{A} \to \mathbf{A}' = \mathbf{A} + \nabla\chi, \tag{83}$$

implies also the transformation of the wave function

$$\Psi \to \Psi' = \exp(ie\chi/\hbar c)\Psi. \tag{84}$$

Some authors, therefore, regard the carrying out of a gauge transformation as requiring that each wave function in a transition amplitude must be subjected to the transformation given in Eqn. (84). Those authors would write, in gauge 'a'

$$(S-1)_{\mathrm{fi}}^{(\mathrm{a})} = -(i/\hbar)\int \mathrm{d}t(\Phi_{\mathrm{f}}, H_{\mathrm{I}}^{(\mathrm{a})}\Psi_{\mathrm{i}}^{(\mathrm{a})}), \tag{85}$$

and, in gauge 'b'

$$(S-1)_{\mathrm{fi}}^{(\mathrm{b})} = -(i/\hbar)\int \mathrm{d}t(\Phi_{\mathrm{f}}^{(\mathrm{b})}, H_{\mathrm{I}}^{(\mathrm{b})}\Psi_{\mathrm{i}}^{(\mathrm{b})}). \tag{86}$$

That is, it is presumed that there is a starting gauge in which no gauge transformation factor needs to be attached to the non-interacting wave function Φ, but that the gauge transformation to a new gauge requires that phase factor, even on Φ. Hence Φ occurs without factor identification in Eqn. (85) since there is no transformation, but then gauge 'b' must have such a factor, as in Eqn. (86). Gauges 'a' and 'b' are then, *ipso facto*, not equally fundamental, since the 'bare' non-interacting state can be employed only in one gauge. By implication, this is therefore a preferred gauge. Some extended reasoning has been presented[87–90] as to why one particular gauge should not have a phase factor attached to the non-interacting state, even though this would require that the non-interacting state must be transformed in all other gauges. The dilemma posed by the conflict between this situation and the concept of strong gauge invariance is clarified by the considerations of the following section.

2.3.1. *Gauge transformations and phase transformations.* There is a fundamental distinction between a gauge transformation and a phase transformation. A gauge transformation always implies a phase transformation of the wave function, but the converse is not true. The gauge transformation has already been defined. It is simply a change in the potentials used to represent an electromagnetic field, done in such a fashion that the electric and magnetic fields so represented are unchanged by the transformation.[91–93] This is true of Eqns (82) and (83). The gauge transformation of the potentials can be stated succinctly in relativistic notation as

$$A^{\mu} \rightarrow A^{\mu\prime} = A^{\mu} - \partial^{\mu}\chi. \tag{87}$$

In quantum mechanics, one must also transform the wave function as in Eqn. (84).[68,94] The application of the set of transformations (82), (83) [or, equivalently, (87)], accompanied by Eqn. (84), is known as a 'gauge transformation of the second kind'.[68,94] Equation (84), taken by itself, can be regarded as the definition of a phase transformation. The above remarks can be rephrased to say that when the potentials are gauge transformed, then the wave function must simultaneously be phase transformed. It is shown here that the inverse is not true. A phase transformation applied to the wave functions does not necessarily imply a gauge transformation of the potentials.

A phase transformation will now be introduced in the relativistic spinor S matrix of Eqn. (68) with ($\pm$) superscripts suppressed. This case is selected because the first-order, non-differential interaction operator associated with the relativistic spinor S matrix minimizes complication, and hence maximizes transparency of meaning. The phase transformation is introduced into the integrand in Eqn. (68) as the unit operator in the form of a product of direct and inverse phase transformations, or

$$\bar{\Phi}_{\mathrm{f}} eA^{\mu}\gamma_{\mu}\Psi_{\mathrm{i}} = \bar{\Phi}_{\mathrm{f}} eA^{\mu}\gamma_{\mu}\exp(-ie\chi)\exp(ie\chi)\Psi_{\mathrm{i}} = \overline{\exp(ie\chi)\Phi}_{\mathrm{f}} eA^{\mu}\gamma_{\mu}\exp(ie\chi)\Psi_{\mathrm{i}}, \tag{88}$$

since $\exp(-ie\chi)$ commutes with $eA^{\mu}\gamma_{\mu}$. Hence Eqn. (68) is exactly equivalent to

$$(S-1)_{\mathrm{fi}} = -i\int \mathrm{d}^4x\bar{\Phi}'_{\mathrm{f}}eA^{\mu}\gamma_{\mu}\Psi'_{\mathrm{i}}, \tag{89}$$

where the primes on the wave functions indicate functions phase transformed as in Eqn. (84). However, Eqn. (89) retains the interaction $eA^{\mu}\gamma_{\mu}$, so that no gauge transformation has taken place. By comparison with Eqn. (68), it is seen that a phase transformation has been accomplished without any gauge transformation.

Contrast the above situation with a gauge transformation, carried out in accordance with the strong gauge invariance principle expressed in Eqns (80) and (81). For ease of comparison, suppose that gauge 'a' quantities are represented with no prime, and gauge 'b' quantities are rendered with a prime. Then the relativistic gauge 'a' expression is identically the same as Eqn. (68), and the gauge 'b' expression is

$$(S-1)_{\mathrm{fi}} = -i\int \mathrm{d}^4x\bar{\Phi}_{\mathrm{f}}eA^{\mu'}\gamma_{\mu}\Psi'_{\mathrm{i}}, \tag{90}$$

in terms of the gauge-transformed $A^{\mu'}$ of Eqn. (87). The distinction between the gauge-transformed Eqn. (90) and the merely phase-transformed (89) is clear.

Apart from the obvious algebraic differences between Eqns (89) and (90), there are other important distinctions. Equation (89) patently has the same physical content as Eqn. (68), since they differ only in that a unit operator is introduced into the integrand. This is definitely not obvious for a comparison of Eqn. (90) with (68). In terms of unprimed quantities, Eqn. (90) is

$$(S-1)_{\mathrm{fi}} = -i\int \mathrm{d}^4x\bar{\Phi}_{\mathrm{f}}(eA^{\mu}-\partial^{\mu}\chi)\gamma_{\mu}\exp(ie\chi)\Psi_{\mathrm{i}}. \tag{91}$$

Equivalence between Eqn. (68) and (91) is not in the form of an identity. In fact, the demand that (68) and (91) should—by virtue of gauge invariance—give the same results can be used as a device for extracting conditions imposed by gauge invariance. In practical application, the way to demonstrate equivalence is to carry calculations to completion in both gauges and then compare the results. In a non-relativistic context, and with a very different point of view than represented here, this was done by Forney, Quattropani, and Bassani.[95,96] They find exact equivalence between the length and velocity gauges for two-photon transitions in hydrogen when all intermediate states are included in both calculations. The details of the calculations and the relative contributions of particular intermediate states are quite different in the two gauges, but the final results are the same. This agrees with the conclusions of Fried,[97] done in a spirit much closer to the present work.

A phase transformation introduced as in Eqns (88) and (89) has no effect on the transition amplitude, and has no connection with a gauge transformation, but it does have consequences. The non-interacting Dirac equation (64) gives

$$(i\gamma^{\mu}\partial_{\mu}-\gamma^0V-m)\exp(-ie\chi)\Phi' = \exp(-ie\chi)[\gamma^{\mu}(i\partial_{\mu}+e\partial_{\mu}\chi)-\gamma^0V-m]\Phi', \tag{92}$$

so the phase-transformed non-interacting spinor satisfies the equation

$$[\gamma^{\mu}(i\partial_{\mu}+e\partial_{\mu}\chi)-\gamma^0V-m]\Phi' = 0, \tag{93}$$

rather than Eqn. (64). The corresponding equation of motion for the phase-transformed fully interacting state Ψ' is

$$[\gamma^{\mu}(i\partial_{\mu}-eA_{\mu}+e\partial_{\mu}\chi)-\gamma^0V-m]\Psi' = 0, \tag{94}$$

in place of Eqn. (61).

Notice that Eqn. (94) is algebraically equivalent to

$$[\gamma^\mu(i\,\partial_\mu - eA'_\mu) - \gamma^0 V - m]\Psi' = 0, \tag{95}$$

for the gauge-transformed interacting state Ψ', when Eqn. (87) is used. This is an obvious possible source of confusion. In a phase-transformed S matrix, such as (89), it is Eqn. (94) which is appropriate. This is because the interacting state must be evaluated in terms of the phase convention established by the non-interacting state. That is, for the phase-transformed S matrix, the analog of Eqn. (70) is

$$(S-1)_{\mathrm{fi}} = -i\int \mathrm{d}^4x\bar{\Phi}'_{\mathrm{f}}[\gamma^\mu(i\,\partial_\mu + e\,\partial_\mu\chi) - \gamma^0 V - m]\Psi'_{\mathrm{i}}, \tag{96}$$

involving the operator from the equation of motion of the non-interacting state (93). By contrast, the S matrix for the gauge-transformed S matrix remains in the form (70), only with Ψ replaced by Ψ'. In other words, Eqn. (94) is the appropriate equation of motion for the merely phase transformed Ψ', and Eqn. (95) is appropriate for the gauge-transformed Ψ'.

2.3.2. *Non-Relativistic Gauge and Phase Transformations.* The relativistic treatment of gauge and phase transformations was performed first because of the simplicity provided by a first order equation of motion with a non-differential interaction term. The non-relativistic case is significantly more complicated, but it can be easily understood in light of the above work for the Dirac problem. Now the non-interacting Schrödinger equation is

$$(i\hbar\,\partial_t - V - \mathbf{p}^2/2m)\Phi = 0, \tag{97}$$

and the interacting Schrödinger equation is

$$[i\hbar\,\partial_t - e\phi - V - (\mathbf{p} - e\mathbf{A}/c)^2/2m]\Psi = 0, \tag{98}$$

where $\mathbf{p}$ is the usual $-i\hbar\boldsymbol{\nabla}$ operator, and ϕ is the scalar potential of the laser field. The difference between the operators in Eqns (97) and (98) gives the interaction Hamiltonian

$$H_{\mathrm{I}} = (1/2m)[-e\mathbf{A}\cdot\mathbf{p}/c - \mathbf{p}\cdot e\mathbf{A}/c + (e\mathbf{A}/c)^2] + e\phi. \tag{99}$$

It is clear from Eqns (98) and (99) that no particular gauge has been selected. It is entirely arbitrary.

Following the model of Eqn. (88), a phase transformation is introduced into the non-relativistic S matrix of Eqn. (47). The result is

$$(S-1)_{\mathrm{fi}} = -(i/\hbar)\int \mathrm{d}t(\Phi'_{\mathrm{f}}, H'_{\mathrm{I}}\Psi'_{\mathrm{i}}). \tag{100}$$

This differs from Eqn. (89) in that now H_{I} transforms to H'_{I} because $\exp(-ie\chi/\hbar c)$ fails to commute with H_{I}. The phase-transformed interaction Hamiltonian is

$$H'^{(\mathrm{phase})}_{\mathrm{I}} = H_{\mathrm{I}} + (e^2/mc^2)\mathbf{A}\cdot\boldsymbol{\nabla}\chi. \tag{101}$$

This is quite different from the gauge-transformed interaction Hamiltonian. From Eqns (82) and (83) employed in (98), the gauge-transformed interaction Schrödinger equation is

$$[i\hbar\,\partial_{\mathrm{t}} - e\phi + e\,\partial_{\mathrm{t}}\chi/c - V - (\mathbf{p} - e\mathbf{A}/c - e\,\boldsymbol{\nabla}\chi/c)^2/2m]\Psi = 0. \tag{102}$$

The non-interacting Schrödinger equation remains (97), and the gauge-transformed interaction Hamiltonian can be written as

$$H'^{(\mathrm{gauge})}_{\mathrm{I}} = H'^{(\mathrm{phase})}_{\mathrm{I}} + (1/2m)(e\,\boldsymbol{\nabla}\chi/c)^2 - (e\,\boldsymbol{\nabla}\chi/mc)\cdot\mathbf{p} + (i\hbar e/2mc)\,\boldsymbol{\nabla}^2\chi - e(\partial_{\mathrm{t}}\chi)/c. \tag{103}$$

Only for the trivial case χ = constant are $H'^{(\mathrm{gauge})}_{\mathrm{I}}$ and $H'^{(\mathrm{phase})}_{\mathrm{I}}$ the same.

The significant algebraic complications associated with the non-relativistic phase and gauge transformations may well be the underlying reason that the subject of gauge transformations in transition amplitudes has been for so long a source of confusion and contention in the

community of atomic, molecular, and optical physics. The Dirac case is clear and clean, and for that reason was presented first.

3. APPROXIMATIONS TO THE EXACT S MATRIX

3.1. *Perturbation Expansions*

The transition amplitude in Eqn. (47) or (49) represents the complete solution to a physical problem. Equation (47) is reproduced here for convenient reference.

$$(S-1)_{\mathrm{fi}} = -(i/\hbar)\int \mathrm{d}t(\Phi_{\mathrm{f}}, H_{\mathrm{I}}\Psi_i^{(+)}), \tag{104}$$

where the states Φ, Ψ satisfy

$$(i\hbar\,\partial_t - H_0)\Phi = 0, \tag{105}$$

$$(i\hbar\,\partial_t - H_0 - H_{\mathrm{I}})\Psi = 0. \tag{106}$$

It is often true that an exact solution for Φ is known. Were an exact solution for Ψ also known, then transitions could be predicted precisely. Generally, the equation of motion for Ψ cannot be solved exactly, and some type of approximation must be made. By far the most common approach is by perturbation theory, which will be developed here to contrast with the following non-perturbative treatments.

As shown in Eqns (41)–(45), a formal solution for Ψ can be written in terms of the Green's operators for Eqn. (105). It is, however, an integral equation, implicit in form. As given in Eqn. (45), the complete solution for Ψ is

$$\Psi^{(\pm)}(t) = \Phi(t) + \int \mathrm{d}t_1 G^{(\pm)}(t, t_1)H_{\mathrm{I}}(t_1)\Psi^{(\pm)}(t_1). \tag{107}$$

If H_{I} is a small perturbation on H_0, then a reasonable leading approximation for Ψ is simply to neglect the integral in Eqn. (107), and call this the zeroth approximation for Ψ,

$$\Psi^{(+)(0)} = \Phi. \tag{108}$$

When this is substituted in the S matrix, Eqn. (104), the first approximation is obtained,

$$(S-1)_{\mathrm{fi}}^{(1)} = -(i/\hbar)\int \mathrm{d}t(\Phi_{\mathrm{f}}, H_{\mathrm{I}}\Phi_{\mathrm{i}}). \tag{109}$$

The convention for numbering approximations as 'zeroth', 'first', ..., is determined by the number of factors of H_{I} which appear in the expression. Equation (109) is well known as a transition amplitude in first order perturbation theory. The next approximation is found by substituting Eqn. (108) in the integrand of the integral equation (107) to obtain

$$\Psi^{(+)(1)}(t) = \Phi(t) + \int \mathrm{d}t_1 G^{(+)}(t, t_1)H_{\mathrm{I}}(t_1)\Phi(t_1), \tag{110}$$

$$(S-1)_{\mathrm{fi}}^{(2)} = -(i/\hbar)\int \mathrm{d}t(\Phi_{\mathrm{f}}, H_{\mathrm{I}}\Phi_{\mathrm{i}}) - (i/\hbar)\int \mathrm{d}t \int \mathrm{d}t_1(\Phi_{\mathrm{f}}(t), H_{\mathrm{I}}(t)G^{(+)}(t, t_1)H_{\mathrm{I}}(t_1)\Phi(t_1)). \tag{111}$$

This gives the S matrix accurate to the second order in H_{I}. The next term is found by the substitution of $\Psi^{(1)}$ from Eqn. (110) into the integral in Eqn. (107) to find $\Psi^{(2)}$. That is then employed as a replacement for Ψ in the S matrix expression (104) in order to find $(S-1)_{\mathrm{fi}}^{(3)}$, and so on.

The convergence of this process is generally very difficult to assess. In principal, there will be a formal radius of convergence. If that is exceeded (which may not be manifested by easily recognizable signs), the outcome will not only be numerically unreliable, but will generally have a misleading analytical character. Furthermore, a perturbation expansion may lose practical utility even before a formal radius of convergence is reached. In Section IX of Ref. 31, a heuristic technique is presented for evaluating the radius of convergence of perturbation theory for multiphoton atomic ionization. The method may actually be fully rigorous, but that has not been proven.

In general, one judges the probable usefulness of a perturbative approach by comparing an order-of-magnitude estimate for $|H_I|$ with a similar estimate for $|H_0|$. If $|H_I| > |H_0|$, then clearly perturbation theory is not applicable. The opposite inequality, however, does not establish the utility of perturbation theory. As discussed in Section 1.3.3 on the subject of the non-perturbative intensity parameter, the problems of interest in this article fall exclusively outside the domain of perturbative solution.

3.2. *Non-Perturbative Expansions*

An important variation on the theme of perturbation expansions will be discussed here. Although it is uncommon, it occurs in the theory of strong-field ionization. Suppose that the non-interacting state Φ of Eqn. (105) has a Hamiltonian H_0 which is itself a sum of two parts,[31] i.e.,

$$H_0 = \tilde{H}_0 + V, \tag{112}$$

$$H = \tilde{H}_0 + V + H_I. \tag{113}$$

Since Ψ depends on both V and H_I, it may prove useful to expand Ψ in terms of V rather than H_I. However, the S matrix contains H_I, the interaction which "causes" the transition, as determined by the construction of the S matrix. The counting of the orders of approximation in the fully interacting state vector and in the S matrix, as described in the preceding section, is then disrupted. This procedure is neither a perturbation expansion in V nor in H_I. It is useful when H_I is a larger influence than V.

3.3. *Analytical Approximations*

A lack of precise knowledge of the fully interacting state Ψ is the underlying reason for resort to approximation methods. The most obvious procedure is to expand Ψ in powers of H_I, as in the perturbation method. An alternative, described above, is to use an expansion in V, when H has the property given in Eqn. (113). However, it may be possible to employ an analytical approximation for Ψ which is not of the form of an expansion. A method of great current interest makes use of the Kramers–Henneberger[37,38] transformation to alter the form of Ψ. This altered form can then suggest further approximations[30,98–100] which do not depend on expansions in powers of an interaction. Even if the transformed wave function is so expanded, the final form for Ψ after inverting the Kramers–Henneberger transformation will no longer be a simple expansion. In application, the methods based on the Kramers–Henneberger transformation have all required the high-frequency approximation that $\hbar\omega > E_B$, the binding energy of the system.[41,100,101]

Keldysh-like theories can be regarded as of the type employing analytical approximations for Ψ. This may take the form of an approximation on $\Psi_f^{(+)}$ in Eqn. (47), as in the Faisal approach;[30] or on $\Psi_f^{(-)}$ in Eqn. (49), as in the method of Keldysh[29] or of the author[31,36,78] This last work can alternatively be viewed as a non-perturbative expansion.

Keldysh-like theories, in their most general form, offer the prospect of a very general structure valid for all strong fields (defined by $z_I > 1$), for the entire frequency range, and directly extendible into the relativistic domain. They are most naturally expressed in an

S-matrix context. Much of the remainder of the present work is devoted to the explication of this subject.

4. KELDYSH-LIKE THEORIES

4.1. *History*

4.1.1. *Keldysh–Faisal–Reiss (KFR) theory.* Probably the most cited paper in the vigorous and mushrooming subject of the physics of bound states subjected to strong fields is the 1964 paper of L. V. Keldysh.[29] It was nearly contemporary with the early work on the free-electron strong-field problem,[32–34,57,58] and was applied in the original paper both to solid state and atomic problems. The Keldysh method is unambiguously non-perturbative, and has served as a paragon of such methods from its inception. Different, but unquestionably related, methods proposed by Faisal[30] and the present author[31,36,78] have come to be collectively referred to as the KFR method. The practice seems to have originated with Bucksbaum *et al.*,[102] and has been widely followed.

The Keldysh method is presented by its author as an *Ansatz*, but it can be understood very directly as an application of Eqn. (49). The required solution for Ψ_f for the complete final-state of the electron subjected to both laser and Coulomb fields is replaced by Ψ^{GV}, the Gordon–Volkov solution[26,27] for a free electron in a plane wave electromagnetic field. This amounts to the presumption that the laser field dominates the Coulomb field in the final state—clearly a strong-field condition. A defining feature of the Keldysh method is that H_I is taken to be the length-gauge interaction Hamiltonian

$$H_I^{(L)} = e\mathscr{E}\cdot\mathbf{r}. \tag{114}$$

Another critical element of the implementation of the technique is that the condition of high multiphoton order is imposed at an early stage to ease analytical difficulties, even though it is not inherent in the initial *Ansatz*. Thus, the method does not fare well when compared with low-order experiments.[103–106] The 1964 Keldysh paper referred both to solid state and to atomic applications. In atomic photoionization experiments, it is almost standard[2–4,52,102,107–115] to include a qualitative or numerical comparison with the predictions of Keldysh.

In 1973, Faisal[30] expressly used the S matrix of Eqn. (47) in his formulation of the photoionization problem. The core difficulty of finding a way to treat the fully interacting state $\Psi_i^{(+)}$ was treated by first carrying out a Kramers–Henneberger transformation, and then making a simple approximation for the transformed state. An additional approximation was introduced in that the final state, Φ_f, nominally a Coulomb scattering state, was replaced by a simple plane-wave free electron state. The Faisal paper contains no calculations or worked examples, and no application was made of the method for many years. In particular, there was no appreciation that there might be any connection at all between the Faisal method and the Keldysh method. They appear to be entirely different.

A method clearly related to the Keldysh approach was proposed in 1977 by Jones and Reiss[116] in application to photon-induced transitions in band-gap solids. On the basis of the same *Ansatz* used by Keldysh, but with the velocity gauge or Coulomb gauge interaction

$$H_I^{(C)} = -e\mathbf{A}\cdot\mathbf{p}/m + (e\mathbf{A})^2/2m \tag{115}$$

used in place of the length gauge interaction of Eqn. (114), it was found possible to greatly reduce the analytical complication and to obtain results without the need for *ab initio* use of a large photon number approximation.

In a 1980 paper,[31] the present author re-evaluated the atomic photoionization problem from a completely formal application of Eqn. (49) with no *Ansatzen* at all. The state $\Psi_f^{(-)}$ was given formal expansion in powers of V, the Coulomb potential, and the leading term of

the expansion was adopted. This gives the same qualitative outcome as the Keldysh method, although it displays the detailed basis for the method and exhibits the correction terms. As with the Jones and Reiss approach, the formulation is in the Coulomb gauge, the results are more tractable than the length gauge formalism, and there is no need for large photon-order assumptions.

From what has just been said, it appears that the methods of Keldysh and of the author are essentially the same, except expressed in different gauges, with some consequent advantages to the Coulomb gauge work. There was no obvious relationship between the Keldysh–Reiss derivations and the Faisal method. Two surprises were in store. One was that, although numerical fitting of the Keldysh theory and the Reiss theory to the same experiments were generally similar, the differences were nevertheless somewhat larger than one might expect. (In an exact theory, different gauges will give the same answer, but there will be distinctions in an approximate theory.) The other surprise, not realized until the first detailed agreement between theory and strong-field experiment was found in 1986–7,[117,118] was that the analytical form of the Faisal theory was identical to that of the Reiss theory, despite the very different provenances of the two methods. These two unexpected results are given further elaboration in Section 4.5 below.

4.1.2. *Tunneling theories.* The KFR theories all yield essentially the same low frequency strong-field limit that the transition probability behaves as $\exp(-2\mathscr{E}_0/3\mathscr{E})$, where $\mathscr{E}$ is the laser electric field strength and $\mathscr{E}_0$ is the Coulomb electric field at the location of the first Bohr orbit in an atom with binding energy E_B. (In the Keldysh theory, this is specifically for ground-state hydrogen. For the others it is more general.) This is precisely the form obtained in theories of the ionization of an atom by a constant field through the mechanism of tunneling through the potential barrier.[119,120] This type of tunneling behavior was found in other early theories of strong-field ionization.

Detailed results of the tunneling type, with explorations of angular distributions, polarization dependence, and so on, were found both by Nikishov and Ritus[59,121] and by Perelomov, Popov, and Terent'ev.[60,122] The first Nikishov and Ritus paper was concerned with short-range forces, and the second added Coulomb forces. Perelomov *et al.* obtain results in the form of a sum over multiphoton processes, which is a precursor of the form in which Faisal–Reiss appear naturally. Recent refinements by Ammosov *et al.*[123] extend the work of Perelomov *et al.* to the case of arbitrary initial atomic states and elliptical states of field polarization.

4.1.3. *Other related theories.* A theory due to Szöke[109,124] is based on the time-reversed S matrix of Eqn. (49), but introduces *ad hoc* corrections in the theory as a way of obtaining a fit to data in which the z_1 values are less than unity. This has good success for those data for which it is intended, but it does not do well when $z_1 > 1$.[115] The approach arises from the notion[109,124] that the initial state should be dressed by the field, which is explicitly not true when applying the time-reversed S-matrix formalism. In the spirit of strong-field S-matrix methods expounded here, Φ is well-known and independent of laser-field effects.

Another theory due to Becker *et al.*[125,126] is constructed similarly to the KFR theories, but it involves *ad hoc* 'final state' corrections involving continuum–continuum interactions, and an effective interaction Hamiltonian which enforces an I^n behavior on the transition probability, where I is the laser intensity and n is the number of photons absorbed. This, also, is outside the spirit of the formally well-defined S-matrix techniques that are the subject of this article.

4.2. *Gordon–Volkov Solutions*

The Gordon–Volkov solution is an exact solution of the quantum mechanical equation of motion for a free, charged particle in a plane-wave electromagnetic field. It has been known since the early days of quantum mechanics,[26] and has been rediscovered several

times.[27,34,127–129] The Gordon–Volkov solution is known for both scalar and spinor particles, for arbitrary polarization of the field, and for arbitrary, uni-directional wave packets. It has become familiar since the early days of strong-field physics in the 1960s, but some of its properties are still not fully appreciated. The Gordon–Volkov solution is fundamental for both Keldysh and Reiss varieties of the KFR method. It will be briefly reviewed here, with a focus on its application in the electric dipole approximation, and on its use within the length gauge.

4.2.1. *Coulomb-gauge Gordon–Volkov solution.* In principle, an electron in interaction with a plane wave electromagnetic field constitutes a relativistic system, since the electromagnetic field is fundamentally relativistic. There are circumstances under which the Gordon–Volkov solution can be employed in a non-relativistic, dipole-approximation context, and the conditions for that very important special case will be considered below. Nevertheless, the basic solution is relativistic, and is given in the radiation gauge (or Coulomb gauge) for a spinor electron as

$$\Psi^{(+)}(x) = \left(\frac{m}{EV}\right)^{1/2}\left(1 + \frac{e}{2p\cdot k} k_\mu A_\nu \gamma^\mu \gamma^\nu\right) u \times \exp\left[-ip\cdot x - i\int_{-\infty}^{k\cdot x} \mathrm{d}(k\cdot x)' \left(\frac{eA\cdot p}{p\cdot k} - \frac{e^2A^2}{2p\cdot k}\right)\right], \quad (116)$$

where units with $\hbar = 1$, $c = 1$ are used; p^μ is a constant four-vector which satisfies the mass-shell condition $p_\mu p^\mu = m^2$; k^μ is the propagation four-vector with time and space parts ω, $\mathbf{k}$, where $|\mathbf{k}| = \omega$; u is a spinor which satisfies the condition $(\gamma^\mu p_\mu - m)u = 0$; $E = |p^0|$; and $A^\mu = A^\mu(k\cdot x)$, where $k\cdot x = \omega t - \mathbf{k}\cdot\mathbf{r}$. Four-vector inner products are expressed by the rule specified in Eqn. (3). Normalization is carried out over a three-volume V to satisfy

$$(\Psi_{\mathrm{a}}^{(+)}, \Psi_{\mathrm{b}}^{(+)}) = \delta(\mathbf{p}_{\mathrm{a}} - \mathbf{p}_{\mathrm{b}})(|p_{\mathrm{a}}^0 + p_{\mathrm{b}}^0|/2E). \quad (117)$$

The spinor $\Psi^{(+)}(x)$ of Eqn. (116) satisfies the Dirac equation

$$[\gamma^\mu(i\,\partial_\mu - eA_\mu) - m]\Psi = 0. \quad (118)$$

The integral in Eqn. (116) represents a superposition over frequencies, that is, a superposition over the magnitudes of $|\mathbf{k}|$. However, all the $\mathbf{k}$ vectors must have the same direction, so the wave packet has a one-dimensional character in that sense.

The solution for $\Psi^{(-)}$ is

$$\Psi^{(-)}(x) = \left(\frac{m}{EV}\right)^{1/2}\left(1 + \frac{e}{2p\cdot k} k_\mu A_\nu \gamma^\mu \gamma^\nu\right) u \times \exp\left[-ip\cdot x + i\int_{k\cdot x}^{+\infty} \mathrm{d}(k\cdot x)' \left(\frac{eA\cdot p}{p\cdot k} - \frac{e^2A^2}{2p\cdot k}\right)\right], \quad (119)$$

where the only differences from $\Psi^{(+)}$ are in the limits on the integral and the sign in front of it.

The scalar, or Klein–Gordon, Gordon–Volkov solution shares the same exponential function as Eqn. (16), but lacks the spinor quantities that multiply it in Eqn. (116). The normalization factor in the scalar case is $(2EV)^{-1/2}$.

4.2.2. *Göppert–Mayer-gauge Gordon–Volkov solution.* The terminology 'Göppert–Mayer gauge' is here used to designate the extension of the usual length gauge to a fully four-dimensional form. It was Göppert–Mayer who introduced the length gauge,[130] which represents the electromagnetic field in the electric dipole approximation by the single component

$$\phi = -\mathscr{E}(t)\cdot\mathbf{r}. \quad (120)$$

This is necessarily an approximation, since the electromagnetic field is a vector field, not a scalar field. To express a Gordon–Volkov solution in the Göppert–Mayer gauge, it is necessary to make a relativistic extension of Eqn. (120). This can be done straightforwardly in terms of the four-vector potential[28]

$$A^{\mu} = -(k^{\mu}/\omega)\mathscr{E}(t, \mathbf{r})\cdot\mathbf{r}, \tag{121}$$

whose time component in the dipole approximation is precisely Eqn. (120). Equation (121) can also be written in a completely covariant form.[28] Although it is monochromatic as stated, it is easily extended to an arbitrary superposition of frequencies. The A^{μ} of Eqn. (121) satisfies the Lorentz condition and the transversality condition.

The relativistic Gordon–Volkov solution in the Göppert–Mayer gauge can be written in various forms,[28] but the one closest to the non-relativistic solution employed by Keldysh[29] is

$$\Psi_{\mathrm{GM}}^{(+)} = \left(\frac{1}{2EV}\right)^{1/2} \exp\Bigg[-ip\cdot x + \frac{ie\mathscr{E}_0\cdot\mathbf{r}}{\omega}\sin k\cdot x - i\int_{-\infty}^{k\cdot x} \mathrm{d}(k\cdot x)'\left(\frac{e\mathbf{p}\cdot\mathscr{E}_0}{\omega p\cdot k}\sin(k\cdot x)' - \frac{e^2\mathscr{E}_0^2}{2\omega^2 p\cdot k}\sin^2(k\cdot x)'\right)\Bigg], \tag{122}$$

which is associated with the electric field given by

$$\mathscr{E} = \mathscr{E}_0 \cos k\cdot x. \tag{123}$$

4.2.3. *Dipole approximation in the Gordon–Volkov solution.* The applicability of the dipole approximation in strong fields has already been examined in Section 1.5, and this general analysis might be expected to apply directly to the dipole approximation with respect to the Gordon–Volkov solution. This expectation is examined and it is found that the true limits are even more restrictive than the analysis of Section 1.5 would indicate.

The underlying premise in applying the dipole approximation is that the phase of a plane wave, $k\cdot x = \omega t - \mathbf{k}\cdot\mathbf{r}$, can be replaced by $k\cdot x \approx \omega t$. The usual justification for this in atomic physics is that $|\mathbf{k}\cdot\mathbf{r}| \ll 2\pi$, or $a_0/\lambda \ll 1$. In other words, the spatial extent of the atomic system, a_0, is a small part of a wavelength. In application to the Gordon–Volkov solution, quantities of the type $\sin k\cdot x$ are multiplied by field-dependent factors, and the result itself appears in the phase of an oscillatory function. Specifically, the monochromatic version of the Gordon–Volkov solutions possesses a term in the imaginary exponential which behaves as

$$(e\mathscr{E}_0 p/\hbar m\omega^2)\sin k\cdot x \approx (e\mathscr{E}_0 p/\hbar m\omega^2)[\sin\omega t - \mathbf{k}\cdot\mathbf{r}\cos\omega t], \tag{124}$$

where $\hbar$, c have been restored. It is the second term on the right that is neglected in the dipole approximation, and since this appears in the phase of an oscillatory function, one must have

$$(e\mathscr{E}_0 p/\hbar m\omega^2)|\mathbf{k}\cdot\mathbf{r}| \ll 2\pi. \tag{125}$$

If an estimate for p for an ionized electron is taken to be such that

$$p^2/2m \approx \hbar\omega, \tag{126}$$

and Eqn. (29) is used to estimate $|\mathbf{k}\cdot\mathbf{r}|$ as

$$|\mathbf{k}\cdot\mathbf{r}| \approx 2\pi|x|/\lambda \approx z_f/4, \tag{127}$$

TABLE 5. Laser intensities in W/cm^2 at which the dipole approximation fails in the Gordon–Volkov solution, based on the figure-eight motion

Wavelength	Circular polarization	Linear polarization
10 μm	7×10^{14}	10^{14}
1 μm	10^{17}	3×10^{16}

then the condition stated in Eqn. (125) can be expressed as

$$z^{1/2} z_f \ll 2\pi. \tag{128}$$

The crudest part of the estimates that enter into the result Eqn. (128) is the statement that the ionized electron described by the Gordon–Volkov solution has an energy of about $\hbar\omega$. For the strong fields under discussion here, the ATI (above-threshold ionization) phenomenon would be very well developed, and so the estimate of Eqn. (126) and hence (128) is very conservative.

In the case of linear polarization, there is a quadratic term in the phase which also makes a contribution proportional to $|\mathbf{k}\cdot\mathbf{r}|$ in the dipole approximation. This contribution is such that Eqn. (125) is replaced by

$$z|\mathbf{k}\cdot\mathbf{r}| \ll 2\pi, \tag{129}$$

and so Eqn. (128) is replaced by

$$z z_f \ll 8\pi. \tag{130}$$

Neither Eqn. (128) nor (130) has the simple form $z_f \ll 1$ that one might expect for validity of the dipole approximation. Equation (130) is more restrictive than Eqn. (128), but is associated only with linear and not with circular polarization. Table 5 is a brief listing of those laser intensities at which Eqns (128) and (130) indicate a breakdown of the dipole approximation in the Gordon–Volkov solution.

The entries in Table 5 are based solely on the projection of the figure-eight motion in the direction of propagation. All of the entries in this table are such that they violate the constraint given by Eqn. (33). The conclusion is that there is a need for relativistic forms at intensities even more modest than those listed in Table 5. The extent of the error introduced by unjustified use of the dipole approximation, however, has yet to be assessed. Preliminary indications from numerical examples in Ref. 36 for circular polarization show important effects in angular distribution, but not in total rate.

4.3. *Strong-field Approximation (SFA)*

The author's version of the KFR theory has had much attention devoted to its formal basis. Both in its original form[31] and in later evolutions[36,40,78] it exhibits fundamental differences from the other elements of the KFR trio. The connections and distinctions among the K, F, and R theories will be summarized in Section 4.5. First, the formal basis of the author's method will be reviewed. This method has been called the SFA (strong-field approximation) both to distinguish it from the Keldysh and Faisal theories, but also because its formal derivation reveals that it requires for practical application only the presumption that the ponderomotive energy of a photodetached electron should exceed the atomic binding energy of that electron. That is, the field must be 'strong'—hence the name. The method applies for both high and low field frequencies, and both relativistically and non-relativistically.

4.3.1. *Introduction to the SFA.* For many readers, this qualitative introduction to the SFA may be sufficient. It may provide more ready insight into the meaning and power of the

technique than the rigorous treatment in the following section. It is important, however, to know that there is a completely rigorous foundation for the method.

The power of the SFA arises from its formulation as a time-reversed S matrix. This makes it possible to circumvent the most difficult aspects of strong-field theories. The usual approach to strong-field photoionization requires a knowledge of Ψ_i in Eqn. (47) or (104). This presents profound difficulties since a bound state in a very strong field experiences important changes in its properties. The calculation (or approximation) of Ψ_i is the focus of most of the effort expended in research on strong fields. The 'secret' of the SFA is to use the time-reversed S matrix, which requires for the initial state only the well-known non-interacting Φ_i. The burden of approximation is shifted to the final ionized state Ψ_f, which is easily managed in a sufficiently strong field.

The SFA differs from an exact statement of the transition rate only in that the expression for a completely interacting final state is replaced by a Volkov solution—i.e., a solution for the electron in the laser field alone, with the atomic potential neglected. This becomes accurate in strong fields when the spectrum of ionized electrons becomes so hard that most of this spectrum has energies in excess of the binding potential.

One may judge the accuracy of the SFA by comparing the energy of detached photoelectrons to the atomic binding energy. It is known from elementary quantum mechanics that if the final energy of an ionized electron is sufficiently high, then the outgoing electron is well approximated by a free electron state rather than by the nominally required continuum Coulomb state. Consider an example from Section 5.2 below. The physical problem is the stabilization of ground-state hydrogen in the presence of a circularly polarized field. At a frequency $\omega = 1/8$ (in atomic units), we examine the spectrum of detached electrons at the maximum of the transition rate curve. The spectrum peaks at a detached electron energy of 64 eV, and drops to 10% of the peak value at 30 eV and at 115 eV. These energies are ample to justify the SFA. For intensities that lie beyond the peak rate in the stabilization regime, the photoelectron energies can be orders of magnitude greater than the binding energy, and justify the notion that the accuracy of the SFA improves as the field intensity increases. Limitations arise from the possibility of the opening of competing channels, such as pair production.

The SFA has no frequency limitations. Intensity limitations are in the form of a lower bound on the intensity.

4.3.2. *Formal relativistic basis.* The starting point of the SFA is the time-reversed S matrix as given in Eqn. (49). This generic expression is expressed in explicit relativistic form in Eqn. (69). One may now simply set

$$\Psi_f^{(-)} \approx \Psi_f^{(-)\mathrm{GV}}, \tag{131}$$

and obtain thereby the SFA, where $\Psi_f^{(-)\mathrm{GV}}$ is the Gordon–Volkov solution of Eqn. (119). Effectively, this is what is done by Keldysh,[29] using the non-relativistic, dipole-approximation version of the Göppert–Mayer gauge Gordon–Volkov solution of Eqn. (122). It is also the end result of the formal derivation presented in Ref. 31, in the Coulomb gauge. (Both Refs 29 and 31 use the $\Psi^{(+)}$ solution instead of the appropriate $\Psi^{(-)}$ solution. Nevertheless, when one goes to the monochromatic case, as both papers do, then the distinction between the two solutions vanishes.)

The replacement expressed in Eqn. (131) comes simply from the physical reasoning that dominance of the laser field in the final state when $z_1 > 1$ justifies the neglect of the residual Coulomb field. Furthermore, the ionized electron is likely to be found in the neighborhood of $r = 0$, the center of the Coulomb force. In the 'transition region', where $z_1 > 1$, but where one cannot yet set $z_1 \gg 1$, some loss of accuracy will occur. This can be described in terms of the spectrum of ionized electrons. For those lowest spectral peaks in the ATI spectrum where the kinetic energy of the photoelectron remains less than the binding energy of the

atom, then residual Coulomb effects will become important.[40,78,117] When $z_1 \gg 1$, these low-end spectral peaks become only a small part of the complete spectrum, and the fact that the low-end peaks are distorted by the Coulomb field becomes immaterial in describing the overall ionization process.

A comprehensive strong-field theory will now be presented, of which the SFA is the leading term. The completely interacting state Ψ depends on both the atomic potential V and the laser potential A^μ. The state Ψ can be expanded in terms of either potential.[31] but $\Psi_f^{(-)}$ is most fruitfully expanded in V when $z_1 > 1$. The required equations of motion are

$$[\gamma^\mu(i\partial_\mu - eA_\mu) - \gamma^0 V - m]\Psi = 0, \tag{132}$$

$$[\gamma^\mu(i\partial_\mu - eA_\mu) - m]\Psi^{GV} = 0, \tag{133}$$

$$[\gamma^\mu(i\partial_\mu - eA_\mu) - m]G^{GV}(x, x') = \delta^4(x - x')\mathbf{1}, \tag{134}$$

where the superscript GV on the Dirac state in (133) and the Dirac Green's function in (134) refer to 'Gordon–Volkov', δ^4 refers to a four-dimensional delta function, and $\mathbf{1}$ is the unit operator in Dirac matrix space. A complete formal solution for Ψ is given by the integral equation

$$\Psi(x) = \Psi^{GV}(x) + \int d^4x' G^{GV}(x, x')\gamma^0 V(x')\Psi(x'), \tag{135}$$

as can be confirmed by direct substitution. The Green's function $G^{GV}(x, x')$ satisfies Feynman boundary conditions, described in detail in Ref. 74 for free particles and in Ref. 35 for the Gordon–Volkov problem. The extensive exploration of the Gordon–Volkov Green's function carried out in Ref. 35 shows that there is a remarkably rich structure to the Green's function in strong fields, but the limit as the field strength approaches zero is a smooth and straighforward reduction to the ordinary free-particle Green's function.

The fully interacting spinor required for the S matrix of Eqn. (69) is the adjoint of the solution given in Eqn. (135), which involves the adjoint Green's function given by

$$\tilde{G}^{GV}(x', x) = \gamma^0 G^{GV\dagger}(x, x')\gamma^0. \tag{136}$$

$G^{GV\dagger}$ satisfies anti-Feynman boundary conditions, i.e., it propagates solutions in the opposite direction to G^{GV}, which is why the order of the arguments is reversed in $G^{GV\dagger}$ as compared to $\tilde{G}^{GV}$. (Note also the difference in notation between here and Ref. 35. In Section V of Ref. 35, $\tilde{G}$ is directly the Dirac Gordon–Volkov Green's function, whereas here $\tilde{G}^{GV}$ is the adjoint function.)

When the adjoint of Eqn. (135) is substituted into the S matrix of Eqn. (69), the result is

$$(S-1)_{fi} = -i\int d^4x \bar{\Psi}_f^{GV(-)}(x)eA^\mu(x)\gamma_\mu\Phi_i(x) - i\int d^4x \int d^4x' \bar{\Psi}_f^{(-)}(x')\gamma^0 V(x')\tilde{G}^{GV}(x', x)eA^\mu(x)\gamma_\mu\Phi_i(x). \tag{137}$$

The first term on the right-hand side of Eqn. (137) is the SFA

$$(S-1)_{fi}^{SFA} = -i\int d^4x \bar{\Psi}_f^{GV(-)}(x)eA^\mu(x)\gamma_\mu\Phi_i(x). \tag{138}$$

The second term on the right of Eqn. (137) represents all the corrections to the SFA. The $\bar{\Psi}_f^{(-)}$ contained in that expression can be expanded in powers of $\gamma^0 V$ by iterative solution of

Eqn. (135) starting with $\bar{\Psi}_f^{(-)GV}$ as the lowest order approximation in Eqn. (135). For example, the first correction term to Eqn. (138) is

$$(S-1)_{fi}^{(1)} = -i \int d^4x \int d^4x' \bar{\Psi}_f^{(-)GV}(x')\gamma^0 V(x')\tilde{G}^{GV}(x', x)eA^\mu(x)\gamma_\mu \Phi_i(x), \tag{139}$$

the second will include two factors of $\gamma^0 V$, and so on. As explained earlier, however, the resulting expansion of Eqn. (137) is not a perturbation expansion in either $\gamma^0 V$ or eA^μ. The expansion of $\bar{\Psi}_f^{(-)}$ is in powers of $\gamma^0 V$, but the S-matrix interaction is eA^μ.

The foregoing is all in terms of a true spinor theory, which is entirely appropriate in view of the spin-1/2 nature of the electron. A scalar relativistic theory can also be constructed,[78] which gives rise to the Klein–Gordon equivalent of the above Dirac theory. The entire procedure reviewed above can be followed in the Klein–Gordon case, with all the important algebraic changes that follow from using a second-order equation of motion for a scalar particle instead of a first order equation of motion for a spinor particle. Above all, the metric in the Klein–Gordon case (see Eqn. (69) or (70)) is quite different from the Dirac metric. The SFA result for a scalar particle is[78]

$$(S-1)_{fi}^{SFA} = -i \int d^4x \Psi_f^{GV(-)*}(2eA \cdot p - e^2 A \cdot A)\Phi_i. \tag{140}$$

In this expression the indicated scalar products are four-dimensional products, the wave functions Φ and Ψ are scalars rather than spinors, and p^μ is a c-number four-momentum on the mass shell, and not an operator.

4.3.3. *Limiting procedures.* The SFA expressions as stated subsume a very large amount of physics. One does not normally employ the full mechanism presented by the formal expressions. Three types of limits are commonly taken: the non-relativistic limit, the dipole limit, and the monochromatic limit. These are discussed here. Other approximations, such as the tunneling limit, or the limitation to hydrogenic 1s states, are very restrictive, and are used in the SFA only for illustrative purposes.

It is important that the SFA is derived on a relativistic basis. It is a theory intended for very strong fields; very strong fields imply a dominance of the electromagnetic field; and the electromagnetic field (in the absence of other influences) is fundamentally relativistic. In the light of Einstein's special theory of relativity, this last statement is actually a tautology. However, in practice, the atomic potential does have an important influence, and most strong-field atomic photoionization problems can be treated quite adequately by a non-relativistic approximation. The non-relativistic limit of Eqn. (140) is achievable in very general terms. In the radiation gauge the time part of the four-vector A^μ can be set to zero, so the four-vector products indicated in Eqn. (140) reduce to the three-vector products

$$A \cdot p \to -\mathbf{A} \cdot \mathbf{p}, \quad A \cdot A \to -\mathbf{A} \cdot \mathbf{A} = -\mathbf{A}^2. \tag{141}$$

The relativistic scalar Φ and Ψ functions reduce directly to the non-relativistic atomic wave function and non-relativistic Gordon–Volkov solutions, respectively. There is, however, one important remaining difference. Normalization in the Klein–Gordon metric introduces the normalization factor $(2EV)^{-1/2}$, whereas the corresponding Schrödinger solutions are normalized with $V^{-1/2}$, where V is the normalization volume in both cases. Since the non-relativistic limit of the total energy E is m, the electron mass, then the difference in normalization conventions introduces an overall factor of $(2m)^{-1}$ into Eqn. (140). The non-relativistic SFA transition amplitude is thus

$$(S-1)_{fi}^{SFA} = -i \int dt(\Psi_f^{GV(-)*}, (-e\mathbf{A} \cdot \mathbf{p}/m + e^2\mathbf{A}^2/2m)\Phi_i), \tag{142}$$

when the $\int d^4x$ is written as $\int dt \int d^3r$, and the three-dimensional spatial integration is represented by the matrix element form employed in Eqn. (142). Equation (142) is exactly the foundation of the non-relativistic SFA expounded in Ref. 31.

Reduction of the Dirac SFA result in Eqn. (138) has not been accomplished in so general a form. The difficulty lies with the Dirac matrices in the relativistic expression. Unlike many problems concerning relativistic corrections to atomic physics, one cannot use a 'large-component, small-component' analysis to find the non-relativistic limit. The SFA is a true strong-field result, and it is found that *all* components in the Dirac matrices contribute equally. Thus the non-relativistic limit of the Dirac problem has been found in the special sense that an explicit problem (ionization of 1s hydrogen) is formulated relativistically, and that explicit formulation is shown[78] to reduce in the non-relativistic limit precisely to the directly-solved non-relativistic version of the same 1s hydrogen problem.

Implicit in the reduction to the non-relativistic limit is the simultaneous introduction of the dipole approximation. The constraints governing that approximation have been treated separately in Sections 1.5 and 4.2.3 above.

An approximation employed routinely in the SFA, as in all other strong-field theories of photoionization, is the assumption in application of the formalism that the laser field is monochromatic. This is not a fundamental constraint of the underlying formalism, in which the field occurs primarily in the Gordon–Volkov solution. That solution is explicitly expressible in wave packet form, as shown in Eqns (116), (119), and (122). The integrations contained in the phase expressions of those equations are designed to accommodate uni-directional wave packets. The question of the conditions for applicability of the monochromatic approximation is considered at some length in Section VI of Ref. 31. It is concluded there that a laser pulse containing of the order of ten wave periods is adequately long for the monochromatic approximation to be valid. Recent technology makes possible pulses shorter than that limit. In principle the SFA can be applied for such ultrashort pulses, but a true wave-packet approach must then be employed. This has not been done.

If the laser pulse contains ten or more wave periods, the actual pulse shape remains important. It is then possible, however, to employ superpositions of monochromatic results to represent the actual laser pulse. This has been done by a number of investigators in comparing theory with experiment.[102,109,111,113–115,124,131] The question remains open of the degree to which such monochromatic superpositions can reproduce the results of a true *ab initio* wave packet calculation.

An alternative approach to the foundations of the SFA must be noted. Guo and Åberg,[132] starting from a second-quantized relativistic quantum electrodynamics, proceeding through the large photon-number limit to obtain the semi-classical case, and then reducing to the non-relativistic limit, obtain precisely the same final form found in Ref. 31. The work is important in that it represents an independent approach to the problem, yet arrives at the same outcome. Unfortunately, the original Dirac relativistic form is formulated so differently from that of Ref. 36 that it is not possible to establish a correspondence at that level.

4.3.4. *SFA S matrix.* The S matrix of the SFA has been stated in general form in Eqns (138), (140) and (142) for the Dirac, Klein–Gordon, and Schrödinger cases, respectively. These expressions permit a clean separation of atomic effects from laser effects. A brief sketch will be given of the Schrödinger case, using a method related to, but different in an important way from that given in Ref. 31.

The interaction Hamiltonian used in this example is the standard expression for the interaction term in radiation gauge in the dipole approximation

$$H_I(t) = -[e\mathbf{A}(t)/mc]\cdot(-i\hbar\nabla) + (1/2m)[e\mathbf{A}(t)/c]^2. \tag{143}$$

We shall define as $H_I(p, t)$ the c-number value of $H_I(t)$ when the operator $(-i\hbar\nabla)$ is replaced by an eigenvalue p. With that terminology, the Gordon–Volkov solution for the Schrödinger problem is

$$\Psi^{(-)GV} = V^{-1/2}\exp(i/\hbar)\left[\mathbf{p}\cdot\mathbf{r} - (p^2/2m)t + \int_t^\infty d\tau H_I(p,\tau)\right], \tag{144}$$

which is an eigenstate of $H_I(t)$,

$$H_I(t)\Psi^{(-)GV} = H_I(p,t)\Psi^{(-)GV}. \tag{145}$$

The property stated in Eqn. (144) is rather trivial in this non-relativistic, dipole-approximation case, but its analog remains true for the relativistic solutions. The reason is that H_I acts only on the transverse components of momentum, while the presence of the field affects only the longitudinal momentum conservation conditions.

Equations (144) and (145) lead to the SFA matrix element in the form

$$(S-1)_{fi}^{SFA} = -(i/\hbar)\int_{-\infty}^{\infty} dt H_I(p,t)(\Psi_f^{(-)GV}, \Phi_i). \tag{146}$$

The initial bound atomic state is just a stationary state, so time behavior is extracted as

$$\Phi_i(t,r) = \phi(r)\exp(-iE_i t/\hbar), \tag{147}$$

in which case space and time dependence can be separated in the S matrix expression to give

$$(S-1)_{fi}^{SFA} = -\frac{i}{\hbar V^{1/2}}\hat{\phi}_i(p)\int_{-\infty}^{\infty} dt\,\exp\left[i\left(\frac{p^2}{2m} - E_i\right)\frac{t}{\hbar}\right]H_I(p,t)\exp\left[\frac{i}{\hbar}\int_t^\infty d\tau H_I(p,\tau)\right], \tag{148}$$

where $\hat{\phi}_i(p)$ is the momentum space bound state wave function

$$\hat{\phi}_i(p) = (\exp(i\mathbf{p}\cdot\mathbf{r}/\hbar), \phi_i(\mathbf{r})). \tag{149}$$

The circular polarization case is always analytically simpler in strong-field problems than other polarizations, so that will be given here as the example. With the vector potential

$$\mathbf{A} = (a/2)(\epsilon e^{i\omega t} + \epsilon^* e^{-i\omega t}), \tag{150}$$

the interaction term is

$$H_I(p,t) = -\zeta\hbar\omega\cos(\omega t - \varphi) + z\hbar\omega, \tag{151}$$

where the phase angle φ is defined so that ζ is real and

$$\zeta = ea\mathbf{p}\cdot\epsilon e^{i\varphi}/mc\hbar\omega, \tag{152}$$

and z is the non-perturbative intensity parameter of Eqn. (6). To accomplish the integral over time in Eqn. (148), one can make use of the generating function for the Bessel functions

$$\exp[-i\zeta\sin(\omega t - \varphi)] = \sum_{n=-\infty}^{\infty} J_n(\zeta)\exp[-in(\omega t - \varphi)] \tag{153}$$

to obtain

$$\int dt \cdots = \sum J_n(\zeta)\int dt\,\exp[(i/\hbar)(p^2/2m - E_i + z\hbar\omega)]$$
$$\times\left[ze^{-in(\omega t-\varphi)} - (\zeta/2)e^{-i(n-1)(\omega t-\varphi)} - (\zeta/2)e^{-i(n+1)(\omega t-\varphi)}\right]. \tag{154}$$

Appropriate shifts in the origin of n in the summation give

$$\int \mathrm{d}t \cdots = \sum \int \mathrm{d}t \exp[(i/\hbar)(p^2/2m - E_i + z\hbar\omega) - in(\omega t - \varphi)][zJ_n - (\zeta/2)(J_{n+1} + J_{n-1})] \tag{155}$$

and then use of the recursion relations for the Bessel functions yields

$$\int \mathrm{d}t \cdots = \sum J_n(\zeta) e^{in\varphi}(z - n) 2\pi\delta(p^2/2m - E_i - n\hbar\omega + z\hbar\omega). \tag{156}$$

This gives for the SFA S-matrix element

$$(S-1)_{\mathrm{fi}}^{\mathrm{SFA}} = [(2\pi i)/V^{1/2}]\hat{\phi}_i(p)\hbar\omega \sum (n - z) J_n(\zeta) e^{in\varphi} \delta(p^2/2m - E_i - n\hbar\omega + z\hbar\omega). \tag{157}$$

Equation (157) is identical to the expression arrived at in Ref. 31, but its derivation differs in one important way. In Ref. 31, an integration by parts was performed in the integration over time, and then a surface term was discarded because it could be identified as a zero 'distribution' or 'generalized function'. As will be discussed in Section 4.6, the integration by parts accomplishes a transformation of the S matrix to a different kind of S matrix, a fact which is irrelevant to the evaluation of the physical consequences of the S matrix, but which is needlessly indirect. Furthermore, the appearance of the zero distribution has caused unease and confusion in some commentators on the procedures in Ref. 31. There is no need for any of this complication, as the present demonstration shows. The integration by parts is avoided, there is no zero distribution, but the result is identical to that obtained in Ref. 31.

Once the S matrix is established, it is then straightforward to proceed to the transition rate. The transition probability per unit time is

$$w = \lim_{t \to \infty} \frac{1}{t} |(S-1)_{\mathrm{fi}}^{\mathrm{SFA}}|^2. \tag{158}$$

The total transition rate to all possible final states is found from w by integration over the phase space of those final states available to the detached particle. This is given by

$$W = \int wV \, \mathrm{d}^3p/(2\pi\hbar)^3, \tag{159}$$

where $(2\pi\hbar)^3$ is the volume of a unit cell in the quantum-mechanical phase space. The result of Eqns (158) and (159) with the S matrix of Eqn. (157) is the transition rate per unit solid angle

$$\frac{\mathrm{d}W}{\mathrm{d}\Omega} = \frac{(2m^3\omega^5)^{1/2}c^3}{(2\pi)^2\hbar^{3/2}} \sum_{n=n_0}^{\infty} (n - z)^2 (n - z - \epsilon_B)^{1/2} |\hat{\phi}_i(p)|^2 J_n^2(z^{1/2}\gamma). \tag{160}$$

In this expression, the quantities ϵ_B, n_0, and γ are defined as

$$\epsilon_B = E_B/\hbar\omega, \quad n_0 = \{z + \epsilon_B\}, \quad \gamma = 2(n - z - \epsilon_B)^{1/2} \sin\theta, \tag{161}$$

where $E_B = |E_i|$, and the brackets on $z + \epsilon_B$ designate the smallest integer that contains the quantity within the bracket. Although Eqn. (160) contains p in its statement, it is understood that the energy conservation delta function in Eqn. (157) determines this quantity through the expression

$$p = (2m\hbar\omega)^{1/2}(n - z - \epsilon_B)^{1/2}. \tag{162}$$

The angle θ in Eqn. (161) is the angle to the direction of photoelectron emission measured from the direction of laser propagation. E_B is the binding energy.

The transition rate expressed in Eqn. (159) is a function of intensity. When employed for the description of anything other than the ionization of a single atom, it will be expressed in the form $W[I(\mathbf{r}, t)]$. That is, as a functional of the intensity distribution I, the transition

rate depends on time and space coordinates. An application of this aspect of the transition rate is described in Section 4.3.6.

Some properties of Eqn. (160) warrant special mention. The summation over n can be regarded as a sum over photon order, as the energy conservation condition implies. Many orders can contribute significantly to Eqn. (160), and this constitutes the ATI (above-threshold ionization) phenomenon. Some rather extreme possibilities can occur. In a recent computation done in connection with an exploration of the stabilization phenomenon,[133] ionization of ground state hydrogen by a circularly polarized laser of 1.46 μm wavelength at about 5×10^{17} W/cm^2 is found to require the computation of approximately 10^5 photon orders in the sum over n.

The starting point of the sum over n, as indicated in Eqn. (161), is not at $\{E_B/\hbar\omega\}$, as one normally expects. Rather, this threshold quantity is increased by z, or $U_p/\hbar\omega$ (from the definition of z in Eqn. (6)). The need to add the ponderomotive potential U_p to the binding energy E_B in finding the threshold order comes from the requirement that an electron cannot be liberated from the atom unless it is provided with enough energy to exist as a free particle with its full energy of interaction with the laser field. This was first clearly pointed out in the atomic ionization problem in Refs 31 and 61, although it was earlier well known in the free-electron problem.[32–34] Since the extra quantity z in the threshold photon order can have a significant effect in shifting the lowest possible order, the phenomenon has come to be known as 'peak suppression'. It was first observed by Kruit *et al.*[62]

Finally we note that Eqn. (160) contains atomic information entirely in the form of a momentum space wave function $\hat{\phi}_i(p)$. This convenient feature is an outcome of the use of the time-reversed S matrix. As discussed in Section 4.3.1, the time-reversed S matrix of the SFA makes possible a clean separation based on field dominance in the final state and atomic dominance in the initial state. The direct-time S matrix does not have that structure.

The circular polarization case was developed above since it is analytically simpler than linear polarization. The final result for linear polarization of the laser field, however, has an appearance identical to Eqn. (160) except that the Bessel function $J_n(z^{1/2}\gamma)$ is replaced by the generalized Bessel function $J_n(z^{1/2}\alpha, -z/2)$, where

$$\alpha = 8^{1/2}(n - z - \epsilon_B)^{1/2} \cos\theta, \tag{163}$$

and here θ is the angle between the direction of emission of the photoelectron and the polarization of the field. The generalized Bessel function can be defined by the expression

$$J_n(u, v) = \sum_{k=-\infty}^{\infty} J_{n-2k}(u) J_k(v). \tag{164}$$

An extensive listing of the properties of the generalized Bessel function is given in Appendices B–D of Ref. 31. Further generalization and study of this function has been undertaken recently.[134,135]

All of the above is for non-relativistic photoionization. It applies for any initial atomic state. Complete, fully relativistic results have been given so far[36] for only a single atomic initial state. This is a calculation of the differential transition rate for ionization from an atom with a nuclear charge of Ze in an initial hydrogenic 1s state by a circularly polarized laser. The calculation is within the Dirac theory. Everything is treated relativistically: the atomic state, the interaction term, and the Gordon–Volkov state. The solution of the Dirac equation for the hydrogen atom may be found in Bethe and Salpeter.[82] The problem calculated is one in which an average over initial electron spin states and a sum over final spin states is accomplished. That is, it is presumed that the initial state is not prepared in a particular spin state, and that no spin measurements are made in the final state. The end result for $dW/d\Omega$ is sufficiently complicated that the reader is referred to Eqn. (3.67) (supplemented by a number of supporting equations) in Ref. 36.

4.3.5. *Atomic properties.* It was emphasized in Section 4.3.1 that the SFA, by employing the time-reversed S matrix, shifts the primary dependence on atomic properties of the transition amplitude into the non-interacting atomic state Φ_i. The corollary of this argument is that Φ_i must be treated with reasonable accuracy. Little attention has been devoted to that subject. Part of the reason is that most fitting of experimental photoionization data by theory has been done with the Keldysh approximation, which is formulated exclusively for the 1s state of hydrogen. Virtually the only reported exception is the fitting[118] of circular polarization multiphoton experiments[136] by the SFA with a single-particle 5p atomic wave function to represent an outer-shell electron of the xenon used in the experiments. Agreement is quite good. Nevertheless, both experimental technique and the model used to represent the atomic wave function have been improved substantially since then.

One advance in the treatment of the atomic state within the SFA is to generalize[137] to any arbitrary hydrogenic s state, albeit still with hydrogenic binding energies, and still in a single-particle model. An important outcome of this work is the clear evidence of major quantitative and qualitative differences that are associated with different atomic states, even in the presence of extremely strong laser fields. Atomic properties retain their importance no matter how intense the laser.

A further step ahead is to incorporate actual binding energy information into the representation of the atomic state in the SFA. This is done[138] by first transforming the atomic wave function to momentum space, and then employing empirical binding energies in that state. Although that state has, so far, been restricted to ns and np hydrogenic states (for arbitrary n), at least the state has the appropriate number of nodes in configuration space as well as the correct binding. It makes a major difference in matching against experimental data.

Most attempts to match experiments with the SFA either have used 1s states (or even a state intended for negative ions[31],[115,124] or else have applied to SFA under circumstances where $z_1 < 1$,[113,124] when the SFA is not expected to be accurate. With appropriate atomic information and adequate z_1 values, agreement of the SFA with experiment is excellent.[138]

For an arbitrary (i.e., any principal quantum number n and any binding energy E_B) single-particle s state, the SFA differential transition rate of Eqn. (160) becomes

$$\left(\frac{dW}{d\Omega}\right)_s = \frac{2R_\infty \epsilon_\omega^{1/2}}{\hbar\pi}\frac{Z^2}{n^2}\sum_{j=j_0}^{\infty}\frac{(j-z)^2\sin^2 2n\chi}{(j-z-\epsilon_B)^{1/2}(j-z-\epsilon_B+\epsilon_\omega)^2}J_j^2\left(z^{1/2}\alpha, -\frac{z}{2}\right). \tag{165}$$

In this expression, the photon order is now labeled by j, rather than n as in Eqn. (160), since n is now reserved for the principal quantum number. The charge state of the atomic nucleus is Z, there are now two energy ratios,

$$\epsilon_B = E_B/\hbar\omega, \quad \epsilon_\omega = Z^2R_\infty/n^2\hbar\omega, \tag{166}$$

where R_∞ is the Rydberg energy, the lower limit on the sum over j is exactly as in Eqn. (161), i.e., $j_0 = \{z + \epsilon_B\}$, and the quantity χ in the argument of the sin function is

$$\chi = \arctan[(j - z - \epsilon_B)/\epsilon_\omega]^{1/2}. \tag{167}$$

Equation (165) is for the case of linear rather than circular polarization, and the quantity α appearing in the first argument of the generalized Bessel function is exactly the same as in Eqn. (163).

As written, Eqn. (165) is entirely in terms of dimensionless quantities except for the multiplicative factor $(2R_\infty/\hbar)$, which is just the basic frequency in atomic units, 4.134×10^{16} Hz. For arbitrary p states, Eqn. (165) becomes

$$\left(\frac{dW}{d\Omega}\right)_p = \frac{2R_\infty \epsilon_\omega^{1/2}}{\hbar\pi} \frac{Z^2}{(n^2-1)} \sum_{j=j_0}^{\infty} \frac{(j-z)^2}{(j-z-\epsilon_B)^{1/2}(j-z-\epsilon_B+\epsilon_\omega)^2}$$

$$\times \left[\cos 2n\chi + \frac{(j-z-\epsilon_B-\epsilon_\omega)}{2n\epsilon_\omega^{1/2}(j-z-\epsilon_B)^{1/2}} \sin 2n\chi\right]^2 J_j^2\left(z^{1/2}\alpha, -\frac{z}{2}\right); \quad n \geqslant 2. \quad (168)$$

The results stated above are the outcome of a single-particle treatment of the atomic wave function. Most experiments have been done with the noble gases, where such an approximation obviously has shortcomings. There is no reason, in principle, why multi-electron wave functions cannot be introduced. In practice, this entire field of investigation is still so new that such a refinement seems inappropriate in view of the many basic issues still unresolved. In due course the extension will be made.

4.3.6. *Application of the SFA to photoionization experiments.* The transition rate given in Eqn. (165) or (168) refers to an elementary process. That is, the rate stated is the transition probability per unit time exhibited by a single atom subjected to a monochromatic laser field. In an experimental environment, one must consider an assembly of atoms (albeit treated as not mutually interacting) subjected to a laser field which may exhibit a complicated intensity distribution in space and time. Furthermore, depletion effects will occur in most strong-field experiments, and this can have an important effect on a total ionization rate plotted as a function of peak laser intensity. Yet another matter to be considered is that many experiments have now been done[2-5,54,109,112,114,115,124,131,139,140] in which multiple ionization can occur, up to a final charge state of ten or so. With the presumption (not universally accepted—see Refs 141,142) that multiple ionization is sequential, it is necessary to establish the population of singly ionized atoms to calculate the number of doubly ionized atoms, and so on.

All of the above matters are treated in terms of the solution of a rate equation. Let N_m be the density of atoms of charge state m. Then, for example, the density of singly ionized atoms is found from the solution of the rate equation

$$dN_1(t, \mathbf{r})/dt = [N_0 - N_1(t, \mathbf{r})]W_1(t, \mathbf{r}), \quad (169)$$

where N_0 is the density of neutral atoms and W_1 is the total transition rate for producing single ionization of an initially neutral atom. The approximation is implicit in Eqn. (169) that depletion of the initial population N_0 to N_1 is the primary channel, and that subsequent flow into N_2, $N_3, \ldots$ is much less important. The assumption of sequential ionization gives

$$dN_m(t, \mathbf{r})/dt = [N_{m-1}(t, \mathbf{r}) - N_m(t, \mathbf{r})]W_m(t, \mathbf{r}), \quad (170)$$

where W_m is the total transition rate for production of an ion of charge $+m$ from an initial ion of charge $+(m-1)$. Again the same approximation is made that the most important depletion of the N_{m-1} population is to N_m, and not to higher ionization states. The solution of Eqn. (169) is

$$N_1(t) = N_0\left\{1 - \exp\left[-\int_{t_1}^{t} du W_1(u)\right]\right\}, \quad (171)$$

where the initial condition is $N_1(t_1) = 0$. For N_2, the solution is

$$N_2(t) = N_0 \int_{t_2}^{t} du \exp\left[-\int_{u}^{t} dv W_2(v)\right] W_2(u)\left\{1 - \exp\left[-\int_{t_1}^{u} dv W_2(v)\right]\right\}, \quad (172)$$

which satisfies the initial condition $N_2(t_2) = 0$. Integration by parts leads to a variety of possible alternative forms for Eqn. (172). The general solution of the first-order ordinary differential equation

$$dN_m/dt + W_m N_m = W_m N_{m-1} \tag{173}$$

with the boundary condition $N_m(t_1) = 0$ is

$$N_m(t) = \int_{t_1}^{t} ds W_m(s) N_{m-1}(s) \exp\left[-\int_s^t du W_m(u) \right]. \tag{174}$$

Implicit in all of the above is the assumption that an atom maintains its initial spatial location throughout the duration of the laser pulse. A simple examination of the consequences of thermal motion and recoil motion confirms that this is an acceptable approximation for picosecond pulses.

The emphasis in Eqns (169) through (174) has been the time-dependent behavior of the density of atoms and ions. In application to a realistic laboratory environment, one must include the fact that the transition rates W_m are functions of field intensity, and field intensity varies both with time and with position in the laser pulse. Specifically, the number of single ions formed in a laser pulse is found from Eqn. (171) to be

$$\mathcal{N}_1 = 2\pi N_0 \int_0^\infty r\, dr \int_{-\infty}^{\infty} dz \left(1 - \exp\left\{ -\int_{-\infty}^{\infty} du W[I(u, \mathbf{r})] \right\} \right). \tag{175}$$

The total transition rate W is found from Eqn. (165) or (168), integrated over the complete solid angle. The notation $W[I(u, \mathbf{r})]$ of Eqn. (175) is meant to convey that W depends on the intensity at a given time and location in the laser pulse. Cylindrical coordinates r, θ, z are used to integrate over the ion density N_1 to get the total number of ions $\mathcal{N}_1$. It is assumed that cylindrical symmetry exists, so the θ integration is performed to obtain the 2π factor. Initial time t_1 is nominally set to $-\infty$, and the measurement time t is set to ∞ in recognition of the summing of ion counts over the entire laser pulse. A corresponding result for $\mathcal{N}_2$, the number of doubly ionized atoms formed is, from Eqn. (172),

$$\mathcal{N}_2 = 2\pi N_0 \int_{-\infty}^{\infty} dz \int_0^\infty r\, dr \int_{-\infty}^{\infty} du \exp\left[-\int_u^\infty dv W_2(v) \right] W_2(u) \times \left\{ 1 - \exp\left[-\int_{-\infty}^{u} dv W_2(v) \right] \right\}, \tag{176}$$

where again it is understood that both W_1 and W_2 are dependent on the spatial and temporal intensity profile: $W = W[I(t, \mathbf{r})]$.

To implement Eqn. (175) or (176), it is necessary to specify an analytical form for the intensity distribution $I(t, \mathbf{r})$. As measured in the laboratory, this distribution has a spatial character resembling that of a Gaussian beam. (For example, see Section 14.5 of Ref. 143.) The temporal distribution is found empirically to be sech^2[109] or to be Lorentzian.[115] Specifically, the intensity distribution recommended by the experimentalists is of the form

$$I(t, \mathbf{r}) = I_0 F(t) \left[1 + \left(\frac{\beta \lambda z}{\pi w_0^2} \right)^2 \right]^{-1} \exp\left\{ -2 \left(\frac{r}{w_0} \right)^2 \left[1 + \left(\frac{\beta \lambda z}{\pi w_0^2} \right)^2 \right]^{-1} \right\}, \tag{177}$$

where r, z are cylindrical coordinates, λ is the laser wavelength, w_0 is the $1/e$ radius of the focal spot, and β is an empirical constant. The temporal distribution may be of the form[109]

$$F(t) = \mathrm{sech}^2(2t/T_0), \quad T_0 = T_{\mathrm{FWHM}}/\mathrm{arccosh}\, 2^{1/2}; \tag{178}$$

or it may be represented as[115]

$$F(t) = [1 + (2t/T_0)^2]^{-1}, \quad T_0 = T_{\text{FWHM}}, \tag{179}$$

where T_{FWHM} is the full width at half maximum of the temporal distribution.

It has been stated as a general condition for applicability of KFR methods to atomic photoionization that $z_1 > 1$ must be satisfied. With the notion that multiple ionization is sequential, the attention has to be focused on the first ionization event to ascertain if $z_1 > 1$ is satisfied. For example, if $z_1 < 1$ for the intensity domain where single ionization occurs, but this increases to $z_1 > 1$ for the domain where second ionization takes place, then the KFR method cannot reliably be applied, since the description of the second ionization depends upon the correct prior treatment of the first ionization event.

4.4. *Tunneling Limit*

When the laser frequency is very low, it is plausible to view the laser field as a quasistatic field which can cause ionization by depression of the Coulomb potential of the atomic nucleus, which then allows the initially bound electron to escape over the top of the depressed barrier.[114,115] A refinement of this same point of view envisions the possibility of the ionization occurring through 'barrier penetration' or 'tunneling' of the bound electron through the depressed barrier.[29,31,59,60,123,144] Unfortunately it has become commonplace in the current literature to refer to all photoionization environments in which $z_1 > 1$ (more commonly, the Keldysh factor $\gamma < 1$) as examples in which tunneling behavior occurs. This greatly oversimplifies some very sophisticated physics, much of which is incompletely explored. More will be said of this below.

At the very least, the $z_1 > 1$ condition for tunneling must be supplemented by $\omega \ll 1$. A graphic example of this need comes from investigations of stabilization (see Section 5.2), where high frequency environments exist where one nevertheless has $z_1 \gg 1$ or $\gamma \ll 1$. When high frequencies exist, where a single photon can exceed the total ionization energy, the tunneling concept is clearly inapplicable.

The barrier-suppression approximation,[114,115] represented in one dimension, is that the effective binding potential exercised by an atomic Coulomb potential due to a charge Ze, in the presence of a static electric field of amplitude $\mathscr{E}$ is

$$U(x) = -Ze^2/x - e\mathscr{E}x. \tag{180}$$

This has a maximum at $x = (Ze/\mathscr{E})^{1/2}$, at which location the potential peaks at a value

$$U_{\max} = -2(Ze^3\mathscr{E})^{1/2}. \tag{181}$$

If the electric field is strong enough so that $|U_{\max}| = E_B$, the no-field binding energy of the atom, then the electron is free to escape from the atom with no need for tunneling through a barrier. This electric field strength, from Eqn. (181) is

$$\mathscr{E}_{\text{crit}} = E_B^2/4Ze^3, \tag{182}$$

and the laser intensity which gives rise to this field strength is

$$I = (I_0/Z^2)(E_B/R_\infty)^4. \tag{183}$$

In Eqn. (183), R_∞ is the Rydberg energy, and I_0 is the laser intensity which corresponds to unity in atomic units. That is, $I_0 = 3.51 \times 10^{16}\ \text{W/cm}^2$.

An interesting sidelight of this particular model is that it gives a very simple result for the z value (the non-perturbative intensity parameter) at which the ionization threshold will occur. With the subscript 'barrier' to represent this threshold value, one finds that

$$z_{\text{barrier}} = E_B^4/[128Z^2(\hbar\omega)^3 R_\infty]. \tag{184}$$

For example, if $E_B \approx R_\infty$, the remarkably simple result is obtained that

$$z_{\text{barrier}} \approx (E_B/\hbar\omega)^3/(128Z^2). \tag{185}$$

For the set of experiments done by the Rochester group at 1053 nm with the noble gases, the simple barrier model expressed above gives reasonably good predictions for threshold intensities for ionization. When carried further, and employed on a 'go, no-go' basis throughout the spatio-temporal distribution of a laser pulse, the predictions for total ionization yield are comparable in quality to the dynamical theories tested against the experiments.[115]

The concept of quantum-mechanical tunneling through a potential barrier occurred early in the history of quantum mechanics.[145] The well-known Gamow factor for tunneling involves the negative exponential factor

$$F_G = \exp(G_G); \quad G_G = -2\pi ZZ'e^2/\hbar v \tag{186}$$

for the penetration of a nucleus of charge Ze through the Coulomb barrier of another nucleus of charge $Z'e$ with an initial relative velocity v. A related type of exponential behavior was found by Oppenheimer[119,120] for the ionization of an atom by a static electric field, with a tunneling factor of the form

$$F_0 = \exp(G_0); \quad G_0 = -(2/3)[m(2E_B)^3]^{1/2}/\hbar e\mathscr{E}. \tag{187}$$

Theories by photoionization by laser fields produce the same factor as in Eqn. (187) when one considers large field strengths and low frequencies.[29,31,59,60,123,144] Differences in the various theories arise to large extent in the so-called 'pre-factors' which multiply the F_0 of Eqn. (187).

A field frequency which is so low that $\hbar\omega \ll E_B$ will require very large field strength and very large photon orders to achieve photoionization. Theories which make some presumptions from an early stage lead directly to the type of tunneling factor given in Eqn. (187). For example, the work of Keldysh[29] is more generally formulated than a tunneling theory at the outset, but a large photon number approximation is introduced at an early stage, and so a tunneling type of result is obtained. On the other hand, although the SFA has a strong formal connection to the Keldysh theory, the use of the radiation gauge results in a theory more tractable analytically than the Keldysh theory, and it is possible to implement the theory fully in its general form. It is then found that a reduction to the tunneling limit is far from a simple matter. Explicitly exhibited multiphoton behavior remains a very pronounced feature of the SFA up to very high laser intensities and laser frequencies that are at least relatively low. The precise conditions which govern the transition to the tunneling regime have yet to be fully explicated, but it is clear that they are more subtle than simply $z_1 \gg 1$. In Ref. 31 it is found that the strong-field limit of the fully formulated theory is couched in terms of $z \gg 1$, which leads to a certain type of asymptotic form for the generalized Bessel functions that play so important a role in the theory. This introduces important simplifications, but it by no means implies the tunneling limit.

To give just one example of the subtle difficulties which can arise, consider one of the limits[31] which must be taken in the SFA to arrive at the tunneling form of Eqn. (187). An exponential factor occurs which has the form

$$G_1 = -(2z/z_1)[(z_1+2)\text{arcsinh}(z_1^{-1/2}) - (z_1+1)^{1/2}]. \tag{188}$$

The square bracket in Eqn. (188) is a function only of z_1, and it is a minor matter to show that $z_1 \gg 1$ leads directly to

$$G_1 \approx -8z/3z_1^{3/2}, \tag{189}$$

which is equivalent to Eqn. (187). However, this expression is exponentiated, and, for accuracy, one must require that the remainder term from the approximation that leads to Eqn. (189) will not be significant as an exponential factor. Equation (189) is accurate to a quantity of order $1/z_1$ in the square bracket. This is multiplied by the factor in Eqn. (189), so that one must demand a factor behaving as $\exp(z/z_1^{5/2})$ will not be important. This is now a condition that does not depend on z_1 alone. To require this to be unimportant is to require that $(E_B/\hbar\omega) \ll z_1^{3/2}$, which may be a far more stringent demand on z_1 than simply $z_1 \gg 1$. This is by no means the end of the matter, since the exponential factor containing Eqn. (188) is multiplied by other quantities which exhibit important non-tunneling behavior even when $z_1 \gg 1$.

One can introduce a qualitative, but physically motivated caution about the presumption of tunneling behavior based only on the large magnitude of z_1. For sufficiently large z_f, a parameter independent of z_1, magnetic field effects will become important irrespective of the smallness of the frequency. This is a point established in Sections 1.3.6 and 1.4. It is manifested through the figure-eight motion of the electron in a strong field, where the proportions of the figure depend only on z_f, and are a consequence of the coupling of the magnetic field into the motion. However, the concept of tunneling becomes far more complicated under these circumstances, and the simple tunneling behavior of Eqn. (187), associated with the quasistatic electric field limit, will not be valid.

The subject of 'tunneling', or, more accurately, the strong-field, low frequency limit, is presently inadequately understood. Much more work is needed.

4.5. *KFR Connections and Distinctions*

Enough has been said up to this point to now make clear how the several varieties of the KFR theory are related, and, perhaps more importantly, how they are different. A brief review of the fundamental characteristics of each serves this purpose.

The Keldysh approximation,[29] although originally presented as a physically motivated *Ansatz*, can be understood on a formal basis. It is of the nature of a time-reversed S-matrix theory, as described in Section 4.3.1, and so it has the in-principle ability to describe accurately both the atomic properties and the strong-field behavior of photoionization. It is non-relativistic, and follows, not from Eqn. (142) of the SFA, but from the closely analogous Göppert–Mayer gauge equivalent

$$(S-1)_{fi}^{Keld} = -i\int dt(\Psi_f^{GV(-)^*}, (-e\mathscr{E}\cdot\mathbf{r})\Phi_i). \tag{190}$$

Now $\Psi_f^{GV(-)}$ refers not to the non-relativistic limit of Eqn. (119) as given in Eqn. (144), but rather it refers to the significantly more complicated non-relativistic limit of the Göppert–Mayer Gordon–Volkov solution of Eqn. (122) (as rendered in the $\Psi_f^{(-)}$ form). The most important complication of Eqn. (122) is the extra exponential factor it possesses as a consequence of gauge transformation from the radiation gauge form. This significantly impedes mathematical analysis. As a consequence, Keldysh makes an early introduction of a large photon order limitation. The Keldysh approximation is thus normally employed as a tunneling method. Furthermore, it has been applied only to hydrogenic 1s states. Because of the complexity of the Göppert–Mayer Gordon–Volkov solution, it is not likely that the Keldysh approximation can be made relativistic on a practical basis.

The Faisal theory,[30] on the face of it, seems to be very different from both the Keldysh and SFA theories. It is based on a direct-time S matrix and not on a time-reversed S matrix. It would thus seem to have lost the inherent advantages of the reversed-time S matrix for strong-field problems as described in Section 4.3.1. The treatment by Faisal of the direct-time S matrix of Eqn. (47) is unusual. Normally, it is only the completely interacting state $\Psi_i^{(+)}$ in this S matrix which requires approximation. In the Faisal theory, the state Φ_f, nominally

a positive energy Coulomb state, is approximated as a simple free-particle state for the electron. The fully interacting state $\Psi_i^{(+)}$ is subjected to a Kramers–Henneberger transformation (an independent discovery of Faisal[30]), as would seem to be appropriate for a strong-field theory. His subsequent treatment of this state, however, is then more simple than that pursued, for example, by Gavrila and co-workers.[41,42,100] After application of the Kramers–Henneberger to the $\Psi_i^{(+)}$ state, Faisal replaces the space-translated state by the pure field-free atomic state as a leading approximation.

By this point in the discussion, it is no longer possible to find any formal connection between the Faisal theory and either the Keldysh approximation or the SFA. The remarkable fact is that the analytical forms written down by Faisal as his end result[30] are identical to those of the SFA.[31] Either this confluence has a very deep meaning, yet unsurmised, or it is an analytical accident.

In summary, the Keldysh approximation and the SFA are closely related. They are couched in terms of different gauges. The analytical distinctions that result from this have caused the Keldysh approximation in practice to be limited to large photon orders only (thus to the tunneling approximation), to hydrogenic 1s states, and to the non-relativistic limit. The SFA is analytically more tractable, and has none of the listed limitations. Specifically, as will be emphasized in later discussion of applications, the SFA is applicable to both very low and very high frequencies, the ability to introduce any atomic state is central to its ability to match strong-field experiments, and it connects relativistic and non-relativistic domains seamlessly. The true meaning of the Faisal version of the KFR is a mystery, but it shares the analytical form of the non-relativistic SFA, and so it shares those properties of the SFA.

4.6. *Alternative Interpretations*

An extensive development has been given here of S-matrix methods as they apply to strong-field photoionization. A consistent point of view has been adopted. The physical picture is that an atom, initially bound, is subjected to a strong laser field; this laser field causes a strong disturbance to the system, which may include ionization; the extent of this disruption is evaluated by comparison with a set of 'reference states' which do not experience interaction with the laser field. In short, the laser field is viewed as the influence which generates transitions in the system. This is not the only possible point of view.

Reference 40 contains an exhaustive examination of the possible S matrices that might be written to describe strong-field photoionization. Two basic possibilities have been treated so far, based on the direct-time and the reversed-time S matrices when the interaction Hamiltonian is due to the laser field. However, the photoelectrons from a photoionization experiment are analyzed in a region separated not only from the laser field, but also from the atomic binding potential. It is then not unreasonable to construct an S matrix in which the reference states lack the atomic binding potential but contain the laser field (albeit 'turned off' at infinity via wave packet behavior), and then regard the atomic potential as the agency which causes the photoionization. It is concluded in Ref. 40 that only the direct-time S matrix of this formulation is adapted to strong-field treatment. This S matrix is

$$(S-1)_{\mathrm{fi}} = -(i/\hbar)\int \mathrm{d}t(\Phi_{\mathrm{f}}^{(-)\mathrm{GV}}, V\Psi_i^{(+)}), \tag{191}$$

where V is the atomic potential. As before, $\Psi_i^{(+)}$ is a state containing the complete interaction due both to the laser field and to the atomic binding, and $\Phi_{\mathrm{f}}^{(-)\mathrm{GV}}$ is a state lacking the interaction causing the transition—in this case, V. Hence $\Phi_{\mathrm{f}}^{(-)\mathrm{GV}}$ is a Gordon–Volkov state, but the notation using Φ is adopted to emphasize that the S matrix of Eqn. (191) is exactly of the type of Eqn. (47), only the transition-causing interaction is different. As always, the problem is the treatment of $\Psi_i^{(+)}$, since there is no exact solution. An expansion of $\Psi_i^{(+)}$ in powers of V (which would lead to a perturbation series in V for Eqn. (191)) is not fruitful

since the initial bound state is heavily influenced by the binding and would be poorly represented by a Gordon–Volkov state or set of states. An expansion of $\Psi_i^{(+)}$ in powers of the laser interaction Hamiltonian H_I gives as the leading term

$$(S-1)_{fi} = -(i/\hbar)\int dt(\Phi_f^{(-)GV}, V\Phi_i), \tag{192}$$

where Φ_i has its earlier meaning of a bound state with no laser interaction. Equation (192) is not perturbative in either interaction since the expansion of $\Psi_i^{(+)}$ is in H_I, while the transition-causing interaction is V.

Equation (192) is really not the leading term in a strong-field theory, since successive terms in the formal expansion of $\Psi_i^{(+)}$ are in powers of H_I, which is presumed to be a large influence. Nevertheless, Eqn. (192) can be transformed to the non-relativistic form of the SFA term. In other words, the leading non-relativistic SFA term is not in itself unique. It can be arrived at from more than one kind of theory. In fact, it is easily shown that the integration by parts of the SFA terms undertaken in Ref. 31, followed by the neglect of the 'surface term' as a zero distribution, actually constituted a transformation of the SFA result to the form of Eqn. (192). As shown in Section 4.3.4, this integration by parts is unnecessary, and the SFA term can be used directly.

5. APPLICATIONS OF KELDYSH AND SFA THEORIES

5.1. *Above-Threshold Ionization (ATI)*

Above-threshold ionization has reference to the fact that strong-field photoionization can take place with the contribution of many photon orders above and including that which is the lowest allowed by conservation conditions. The lowest allowed photon order is itself altered by strong fields in that the laser field must supply the ponderomotive potential of a free electron in the laser field[31,61,62] in addition to the binding energy to separate it from the atom. In this section, as is common practice, this terminology will be applied to conventional strong-field photoionization experiments by visible or near-visible light, whether electron spectroscopy is done, or simply counting of ions.

Numerous extensive reviews of the ATI phenomenon are available, and so no attempt at completeness will be made in this section. Attention will be focused primarily on the interaction between the experiments and KFR theoretical methods.

5.1.1. *Polarization comparisons.* Multiphoton ionization is characterized by a loss of the superposition principle, so one cannot compute circular polarization amplitudes as a linear combination of linear polarization results, or vice versa. When first order perturbation theory is valid, there is no effect at all of the polarization state of the laser, and so, historically, great interest was aroused by the early two- and three-photon experiments[146,147] that showed clear dependence on the polarization state. The circular polarization rates were found to be somewhat larger than for linear polarization, as was confirmed by perturbation theory calculations.[148,149] Higher orders are very difficult to calculate, so an upper bound was found[150] for the ratio of circular to linear ionization rates, which became quite large as the photon order increased. This led to speculation that circular polarization would dominate linear at high orders. However, it was then shown[151] that an upper bound demonstrated earlier was far from being a least upper bound, and that an improved estimate of the upper bound on circular/linear rates in fact became small as high orders were approached.

This last result about circular/linear rate comparisons at high multiphoton order was refined several years later, when it was found[31,152] that the ratio was very sensitive to intensity, starting at small values (for high multiphoton order) at the lower ranges of intensity, and rising strongly toward the neighborhood of unity at very high intensity. There matters stood

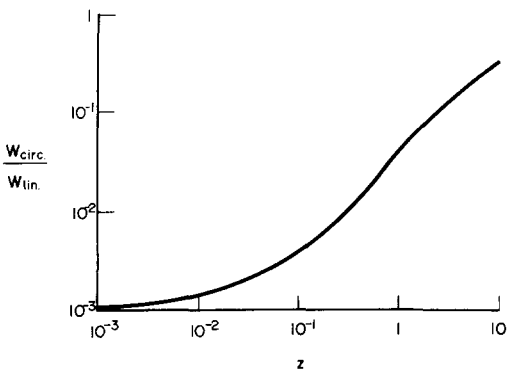

FIG. 3. Theoretical ratio of transition rates for multiphoton detachment of H^- ($\lambda = 10.6\,\mu$m) by circularly polarized light as compared to linearly polarized light, as a function of the non-perturbative intensity parameter z. The figure is a reproduction of Fig. 12 from Ref. 31.

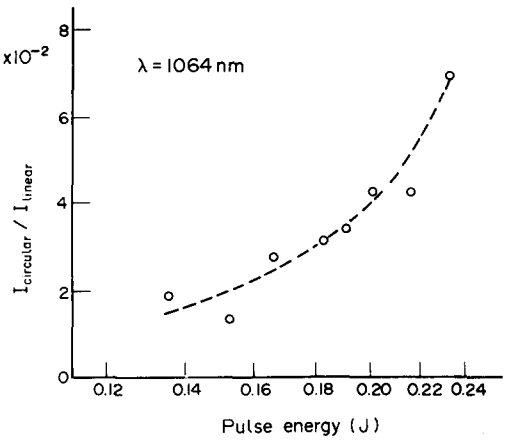

FIG. 4. Experimental circular/linear intensity ratios of photoelectrons from multiphoton ionization of xenon (λ = 1064 nm) versus laser pulse energy. These data are from Hippler *et al.*[107]

until experiments by Bucksbaum *et al.*[136] confirmed the relatively small rate for high-order photoionization by circularly polarized light. Hippler *et al.*,[107] measured circular/linear ratios and found a strong upward trend with intensity of very much the same character predicted earlier.[31,152]

Other circular/linear polarization comparisons,[6] done at large z and z_1 values, confirm many of the qualitative and quantitative predictions of both the Keldysh approximation[29] and the SFA.[31] Ionization yield ratios are not presented in this work,[6] but electron spectral distributions and angular distributions are as predicted.

In physical terms, the behavior of circular/linear rates remains incompletely explained. To some extent one can understand the domination of the linear case at high orders on the basis of one of the two qualitative explanations that have been advanced. One[31] is that a larger phase space is available in the linear case because all circularly polarized photons have their angular momenta aligned along the direction of propagation, and so the only final states available are those states in the continuum that have angular momentum at least equal to the number of absorbed photons. By contrast, all angular momentum states are available in the linearly polarized case. An alternative explanation[136] is also angular-momentum related, and refers to the higher atomic potential barrier associated with the larger angular momentum. Overlap integrals for ionization are then concentrated at larger atomic radii, which decrease the transition amplitude.

These lines of reasoning have not been sufficiently developed, and recent results indicate that the matter of polarization ratios is more complicated than previously realized. For example, the declining dominance of linear polarization over circular that is illustrated in Figs 3 and 4 may not persist as intensities continue to increase. The results of Fig. 3 were obtained in the 1970s at a time when computer capabilities were so limited that only very few intensity values were calculated. Much detail was missed thereby. Calculation of the generalized Bessel function of Eqn. (164) is especially demanding of computer time. The H^- photodetachment problem represented in Fig. 3 (and in Ref. 31) has recently been recalculated with up-to-date computational algorithms at closely spaced intensity intervals, and on a far more capable computer than previously, with the outcome presented in Fig. 5. The presentation is similar to that of Fig. 3, with a somewhat extended intensity range. Over the common intensity range in z of 10^{-3} to 10, it is seen that Fig. 3 is just a smoothed version

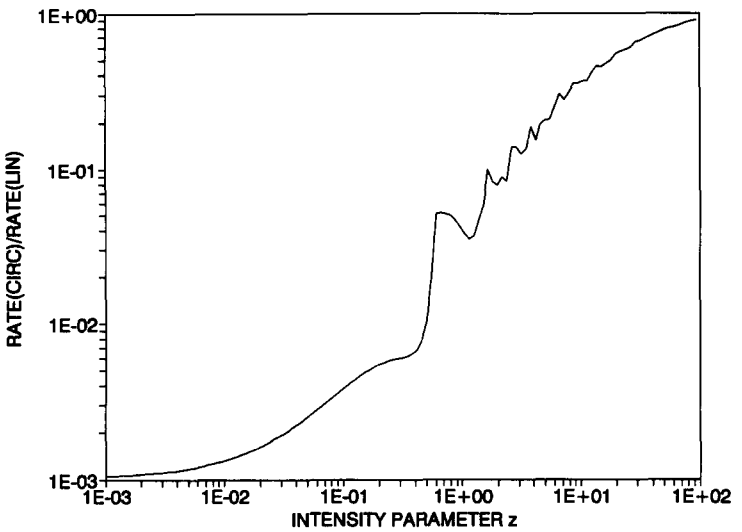

FIG. 5. Updated and extended version of Fig. 3 obtained with more sophisticated calculational algorithms, and using a closely spaced grid in intensity. Note the presence of oscillations that are smoothed over in Fig. 3. The ratio of circular to linear rates for photodetachment of H^- appears to approach unity asymptotically.

of Fig. 5. The circular-to-linear ratio approaches unity quite closely, but the ultimate asymptotic ratio remains to be established. The erratic oscillations arise from linear polarization, since circular polarization rates vary smoothly with intensity. The irregularity shown is no artifact. It occurs both with the completely-computed generalized Bessel function, and with much simplified asymptotic forms of it.

The theoretical curves given in Figs 3 and 5 are for photodetachment of a negative ion. Figure 4 gives atomic ionization experimental results. Very recently, the stabilization problem treated in Section 5.2 has given rise to computations for atomic ionization in very strong fields with both circularly and linearly polarized lasers. In those results, the ratio of circular to linear ionization rates decline steadily with increasing intensity, quite unlike all of Figs 3 to 5. Clearly, much remains to be understood about this problem.

5.1.2. *Circular polarization.* Although the first true ATI experiments were done with linear polarization, the experiments with circular polarization were largely done quite early,[107,136,153] with a later return almost exclusively to linear polarization. Notable exceptions exist.[6,113]

One of the first detailed comparisons between theory and experiment related to circular polarization. The experimental electron spectrum of Bucksbaum *et al.*[136] was matched against the SFA theory,[117,118] viewing the peak laser intensity as the lone fitting parameter. Intensity measurements could not be done very precisely, but the best fit at $z = 2.1$, $z_1 = 0.40$ corresponds to 2.3×10^{13} W/cm^2, which is within the experimental accuracy of the stated intensity of 1.5×10^{13} W/cm^2. The comparison is shown in Fig. 6.

For the relatively early era in which Fig. 6 was obtained, the agreement was considered quite good. The limitations of the SFA method when dealing with the lowest lying peaks[40,78,117] has already been discussed in Section 4.3.2. This limitation comes about because the dominance of the laser's ponderomotive potential over the atom's binding energy that is the underlying approximation in both the Keldysh and SFA methods, is questionable for a very low energy peak in the electron spectrum. The lowest energy ionized electrons will be most heavily influenced in their final states by the atomic field. Circular polarization reduces the importance of this limitation by exhibiting an inherent suppression of the low end of the

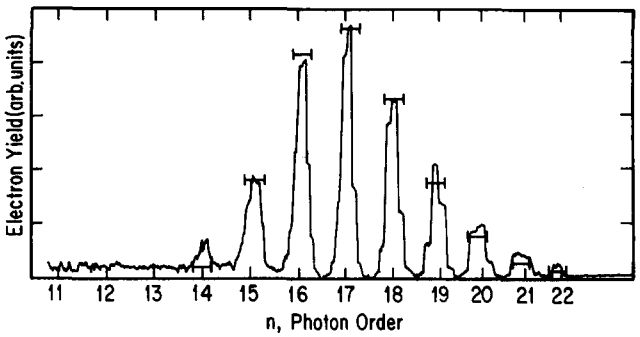

FIG. 6. Experimental spectrum of photoelectrons from the multiphoton ionization of xenon with circularly polarized light of 1064 nm, obtained by Bucksbaum *et al.*[136] Superimposed on the experimental results are the theoretical predictions of the SFA, shown by the horizontal bars. The figure is reproduced from Ref. 118.

emitted electron spectrum. This is seen in Fig. 6. The no-field lowest order of ionization arising from $n_0 \geqslant \{E_B/\hbar\omega\}$ is 11 for these experiments on the photoionization of xenon with a laser of 1064 nm wavelength. The suppression of the lowest orders associated with the ponderomotive potential, giving rise to $n_0 = \{E_B/\hbar\omega + z\}$, raises the lowest allowed order to 13. Nevertheless, Fig. 5 shows no contribution at order 13 and very little at order 14. Hence the SFA gives a reasonable prediction even though $z_1 \approx 0.4$ places the experiment rather below the region of applicability of the SFA.

Recently, Bucksbaum *et al.*[113] have refined their earlier work to take advantage of the better laboratory technique now available. They again compare the SFA theory with experiment, taking account of the spatial and temporal distribution of the laser pulse. The ionized atom again is xenon, but the wavelength is 616 nm. Their new results are shown in Fig. 7. What they find is that agreement is poor for the first spectral peak, fairly good for

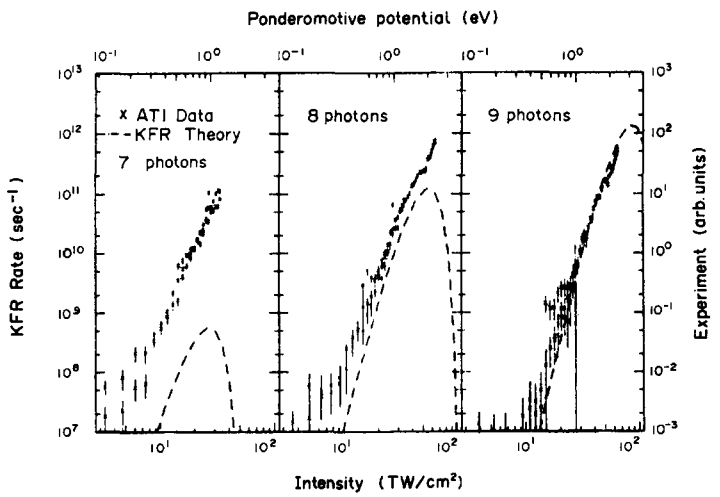

FIG. 7. Detailed comparison of experimental and theoretical rate profiles for the first three spectral peaks in the multiphoton ionization of xenon by 616 nm laser pulses. The experiment was performed at the relatively low value of the bound-state intensity parameter $z_1 \approx 0.16$. Agreement is poor for the lowest peak and improves significantly for the next two peaks. The figure is a reproduction of Fig. 3 in Ref. 113.

TABLE 6. Values of z and z_1 for some representative experiments. The table represents peak laser intensity for the first ionization of the atom listed

Reference	λ (nm)	Atom	I (W/cm^2)	z	z_1
102	532	helium	4×10^{13}	2.3	0.4
131	532	argon	2×10^{14}	2.3	0.7
124	586	argon	2×10^{14}	3.1	0.8
112	620	xenon	10^{14}	1.8	0.6
114	1053	argon	2×10^{15}	170	26
111	1064	krypton	4×10^{13}	3.6	0.6
6	10000	xenon	10^{14}	9000	170

the second peak, and excellent for the third peak. The value of z is now about 0.5, and $z_1 \approx 0.16$. These intensity parameters are substantially smaller than in the first set of experiments, and no peak suppression at all is observed, since the no-field value of $n_0 = \{E_B/\hbar\omega\}$ corresponds to the lowest measured peak. To exercise proper care in evaluation of these results, it should be noted (P. H. Bucksbaum, private communication) that there is arbitrariness along the ordinate in matching of the theory and the experiment, so that the remarkably good agreement at a photon order of nine might not be reliable. Nevertheless, only the lowest photon order shows poor agreement (as is always to be expected), the value of $z_1 \approx 0.16$ falls well below the nominal requirement of $z_1 > 1$, and no other theory has come close to satisfying such detailed scrutiny in confrontation with a relatively strong-field experiment. One might conclude that the agreement of the SFA theory with experiment is remarkably good. This commentator finds perplexing the conclusion of the authors that "[KFR] calculations do not agree with these new experimental results", and the absence of commentary by the authors on conditions of applicability of the KFR method.

5.1.3. *Linear polarization.* Most strong-field photoionization experiments have been done with linearly polarized lasers. These experiments will not be reviewed in depth. Rather the emphasis is on those experiments that have been compared or are properly comparable against theories of the KFR type. A fact of the utmost importance that receives inadequate attention is the condition $z_1 > 1$ required for KFR methods to apply. It is not always appreciated how strongly frequency-dependent this intensity parameter is. It is also necessary, when multiple ionization is observed, that the intensity domain in which the first of these ionizations occurs is the one to which the z_1 criterion applies. The other point that will be stressed below is the importance of using an applicable atomic wave function in comparing theory and experiment, and not simply using the hydrogenic 1s state universally. The SFA contains atomic information in an important way, as was stressed in Section 4.3.1.

It is found that, with adequately large z_1 values, and with appropriate atomic information employed, the SFA gives good agreement with experiments.[138] The calculation is complete and direct. There are no adjustable parameters employed at any stage, and there are no *ad hoc* elements introduced anywhere in the development of the theory.

Table 6 lists a sampling of experiments with peak laser intensities, wavelengths, and z and z_1 values. No excimer laser experiments are listed, since the short wavelength generally leads to modest z_1 values. (This limitation is no longer true for the latest technology.) The order of listing is from short wavelength to long, so that the dates of the experiments are quite randomly ordered.

The intensities selected are associated only with the first ionization state and not with higher multiplicities. This is done because of the generally accepted notion that the dominant mode of ionization is sequential, with n-fold ionization occurring as a consequence of ionization of the ion of charge $n-1$. Since z_1 values tend to be higher for more extensively stripped ions, the limiting conditions for applicability of the SFA must be sought in the first stage of ionization.

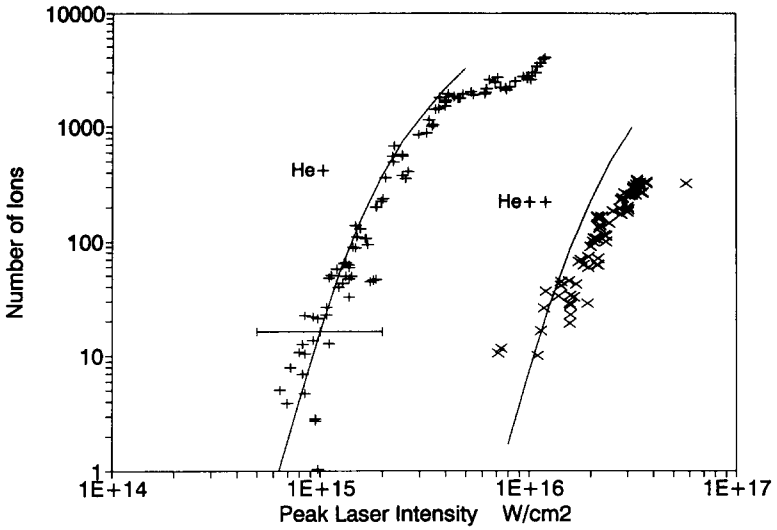

FIG. 8. Comparison of the SFA theory with experiments by Augst *et al.*[114,115] for helium photoionized by a laser of $\lambda = 1053$ nm to both He^+ and He^{2+} final states. The ion detector saturates in the neighborhood of 2000 ions.[114,115] The horizontal bar shown in the figure measures the experimental uncertainty in peak laser intensity. Data shown in Refs 114, 115 for He^{2+} for 10 ions or fewer are contaminated (D. D. Meyerhofer, private communication) and have been omitted from this figure.

In all cases, z is greater than unity, and there is no question that every experiment listed is in a non-perturbative regime. The z_1 values are the primary focus here. Most of the experiments have relatively small values of this parameter. The ones that have $z_1 \gg 1$ are either relatively recent (Ref. 114), using new technology, or represent a very long wavelength (Ref. 6).

The experimental results of Ref. 6 are compared in that source with both the Keldysh approximation and the SFA. Agreement is stated to be excellent. The other set of experiments listed in Table 6 with $z \gg 1$ is that of the Rochester group (Ref. 114). Matching of the SFA theory to those experiments has recently been done.[138] Results for two of the atoms are shown. Helium comparisons are given in Fig. 8, and argon in Fig. 9.

It is emphasized that the SFA has not previously been systematically compared with experiments under appropriate conditions. By this is meant both that one must have $z_1 > 1$, and also that a suitable wave function has been used. The He results in Fig. 8 simply use a hydrogenic 1s function, and so there is nothing novel in that. In fact, Augst *et al.* remark[115] on the excellent agreement obtained for He with the SFA method. The comparison for Ar in Fig. 9 is done with a 3p single-particle wave function constructed as described in Section 4.3.5. This makes a major difference in the fitting. Different wave functions produce quantitative results that can be orders of magnitude different, and will show 'kinks' or inflections at varying points depending on the choice. The agreement shown in Figs 8 and 9 is excellent, even without considering the various qualifications that must be stated. Experimental intensities may be off by a factor of two in either direction,[115] the ion collector saturates at about 2000–3000,[4] [115] and data relating to 10 ions or less for helium is contaminated and not considered reliable.[5] There is also an unspecified amount of uncertainty in the stipulation of the parameters which define the shape of the laser pulse. In addition,

[4]D. D. Meyerhofer, private communication.
[5]D. D. Meyerhofer, private communication.

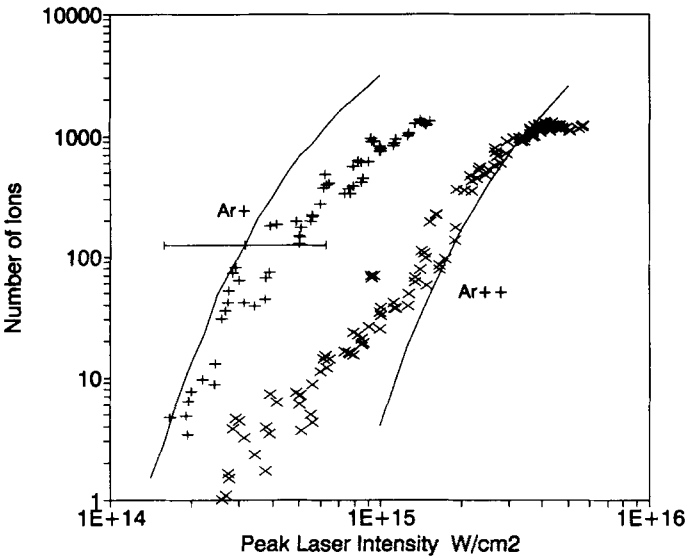

FIG. 9. Comparison of theory and the experiments of Augst *et al.*[114,115] for argon ionized to Ar^+ and Ar^{2+} states. As in Fig. 8, there is a saturation of the detector, and the horizontal bar measures the uncertainty in the measurement of the peak laser intensity. Limited computing capacity prevents calculation of higher charge states detected in the experiments.

overall efficiency of the detection system is not incorporated in the results and is not specified by the experimentalists. From the theoretical side, there is the limitation of the wave function to an uncorrelated state, established by the plausible, but nevertheless *ad hoc* procedure described in Section 4.3.5. There is also the fact that, although the peak laser intensity has $z_1 \gg 1$, that is true only at the uppermost end of the intensity curve, and even then only in the very core of the laser pulse. That is, even in the presence of the seemingly large peak value of z_1 represented in Table 6, much of the calculation actually relates to much smaller z_1 values.

Only two of the atoms represented in the Rochester experiments are reproduced here, but all have been calculated,[138] and theory and experiment are in good agreement (with the caveats already listed) in every case. This is remarkable in that previous efforts to match theory and experiment have attained reasonable agreement only when some adjustable parameter is included (for example, the adjustable multiplicative factors attached to the Keldysh approximation in Refs 109, 124, 131), or *ad hoc* corrections are introduced. More is said of this below.

5.1.4. Ad hoc *corrections*. It has been emphasized above that the SFA is formally derived from a complete relativistic theory. There are no *Ansatzen* employed. Nevertheless, the SFA depends on the dominance in the final state of the ponderomotive potential associated with the laser field over the Coulomb potential associated with the atom. Several investigators have attempted to ease the conditions of applicability by introducing *ad hoc* corrections to the Gordon–Volkov solutions to represent residual effects of the Coulomb field on the unbound electron. The first such correction was suggested by Keldysh.[29]

An ambitious effort along these lines was made by Szöke,[124] with the most detailed explication given in the Perry dissertation.[109] The basic step is to alter the momentum conservation conditions by introduction of an *ad hoc* modification intended to represent an asymptotic effect of the binding energy even after the electron has receded to large distances from the atom. One may question the formal basis for this procedure (which includes the notion—mentioned again in Section 6.3—that both initial and final states should include laser

field effects[109] in contrast to the basic Eqn. (47) and (49)), but application of the method to data-matching had good success.[109,124,131] As shown in Table 6, the peak z_1 values for the experiments were slightly less than unity. This means that most of the z_1 values in the experiment are even less than that, and so the unadorned KFR method might not be expected to be especially accurate. The Szöke method does better than KFR. However, the Coulomb correction modifies the form of the SFA. One expects that when z_1 truly is large, that this modification will be inappropriate since it is not of the type suggested by formal Coulomb corrections to the SFA. In fact, when the Szöke correction is applied to the Rochester data,[115] with $z_1 > 20$, the results are much poorer than one obtains with KFR techniques, even without proper wave function information in the SFA.

An interesting application of Coulomb corrections arises in the case of elliptical polarization. Bashkansky *et al.* extended analytically the KFR circular/linear polarization results to the more general elliptical case,[154] and then explored experimentally the angular distribution of the emitted electrons. They found rather good agreement with the predictions of the theory. However, they had presumed in the experimental arrangements that symmetry would exist about both principal polarization axes, and later discovered[111] that there was only one axis of symmetry, not two. These authors gave a qualitative explanation for the breaking of the symmetry in terms of an interaction of the emergent photoelectron with the potential of the remnant ion. This was confirmed in work by Basile *et al.*,[155] who apply an *ad hoc* Coulomb correction to the Gordon–Volkov solution, in the presence of a generalization to elliptical polarization. (This otherwise interesting paper is marred by ancillary remarks about gauge transformations which reveal self-contradictory statements on the subject, at variance with the general principles set down in Section 2.3, as well as with the accepted concept that the Keldysh and SFA formulations vary only by a simple difference in the gauge employed.)

The experiments which measured the asymmetry in the photoelectron angular distributions[154] were done at 1064 and 532 nm with the noble gases at peak laser intensities from 10^{13} to 4×10^{13} W/cm^2. Corresponding peak z_1 values are in the range of 0.01 to 0.3. These are very much pre-KFR intensities. It would be important to have experiments done at KFR values ($z_1 > 1$) to see if the *ad hoc* Coulomb correction continues to be effective, or if it exhibits the same limitation as the Szöke Coulomb correction applied to total ionization rates.

5.2. *Stabilization*

5.2.1. *Introduction.* In perturbation theory, multiphoton transition rates due to electromagnetic interactions increase with the intensity I as I^n, where n is the photon order of the interaction. In non-perturbative theories, the rate increase proceeds more slowly than I^n at high intensities. There has been no general rule found about whether the transition rate will level off asymptotically with increasing intensity, or whether there will be an eventual decline. The answer would appear to be problem-dependent. The first instance of an increase in transition rate followed by an actual decline was reported[39] over twenty years ago for the case of multiphoton induced emission from a metastable excited state. For multiphoton ionization, the early explicit demonstration of a roll-off in rate[31] has been followed in recent years by a flurry of activity showing the tendency to eventual decline in rate following a maximum. This phenomenon has come to be known as stabilization. A variety of analytical and numerical techniques have now been employed to explore the phenomenon of atomic stabilization.[40–48,133,156–167]

Diverse physical interpretations are invoked to understand the origins of the stabilization phenomenon. The interpretation depends on the analytical technique employed. For example, those methods based on the Kramers–Henneberger (KH) transformation[37,38] to an accelerated frame of reference find that critical elements in the understanding of the stabilization process revolve around the apparently dichotomous nature of the atomic potential that arises in the KH approach.[41,42,46,100,159,165] Interference effects among high-lying atomic states are at

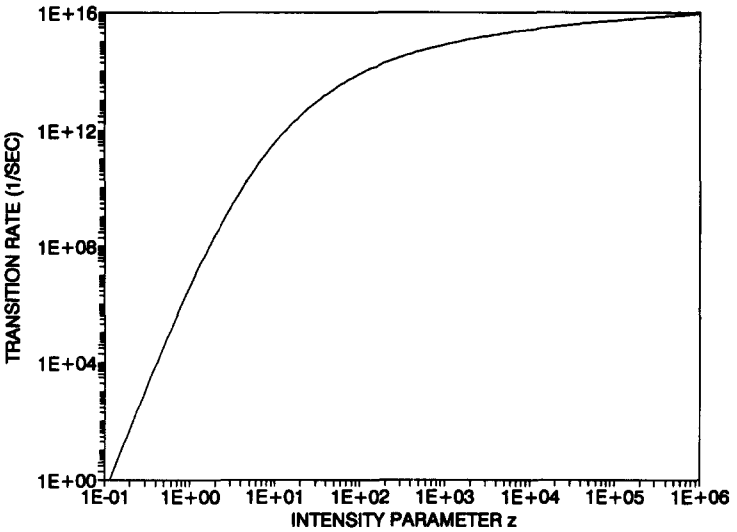

FIG. 10. Results computed by the SFA for multiphoton detachment of H^- by a circularly polarized laser of 10.6 μm. Although the highest intensity shown (10^{16} W/cm^2, $z = 10^6$, $z_1 = 3 \times 10^5$, $z_f = 0.45$) is so high as to correspond to relativistic conditions, there is no evidence of stabilization.

the heart of the stabilization phenomenon as treated by Fedorov *et al.*[44,156–158,162,164] As will be discussed below, the SFA points to a multiphoton threshold as the proximate cause of stabilization.

The exploration of the stabilization phenomenon is currently a focus of much activity. Its relevance to the present article is that it is associated with very strong fields, and that its domain of occurrence matches quite neatly the domain of applicability of the SFA. The predictions of the SFA with respect to stabilization will now be explored.

5.2.2. *Stabilization within the SFA.* It is generally recognized that stabilization is not a necessary feature of ionization in very strong fields. For example, Fig. 10 shows the transition rate for circular polarization for photodetachment of a negative hydrogen ion, plotted as a function of z, the non-perturbative intensity parameter. A value of z of about 0.1 constitutes the approximate limit of perturbation theory, so the intensity domain shown in the figure extends seven orders of magnitude beyond that limit. It is seen that the curve is leveling off, but there is no decline such as would characterize stabilization. However, stabilization investigations have focused not on negative ions, but on the hydrogen atom. Hence, the analog of Fig. 10 for the hydrogen atom will be presented.

The theory for the hydrogen atom is already present in Eqn. (165). For an initial 1s state of hydrogen, this can be simplified to the form

$$\frac{dW}{d\Omega} = \frac{4}{\pi\tau_0}\left(\frac{E_B}{\hbar\omega}\right)^{3/2} \sum_{n_0}^{\infty} \frac{(n - z - E_B/\hbar\omega)^{1/2}}{(n-z)^2} (J_n)^2, \tag{193}$$

where τ_0 is the atomic unit of time, given by $\tau_0 = \hbar/2R_\infty = 2.419 \times 10^{-17}$ s. The other quantities have been previously defined (e.g., E_B is the binding energy and z is the non-perturbative intensity parameter). For circular polarization, the quantity J_n is the ordinary Bessel function $J_n(z^{1/2}\gamma)$, where γ is given in Eqn. (161). For linear polarization, J_n is the generalized Bessel function $J_n(z^{1/2}\alpha, -z/2)$, where α is defined in Eqn. (163). The minimum photon order n_0, defined as

$$n_0 = \{E_B/\hbar\omega + z\}, \tag{194}$$

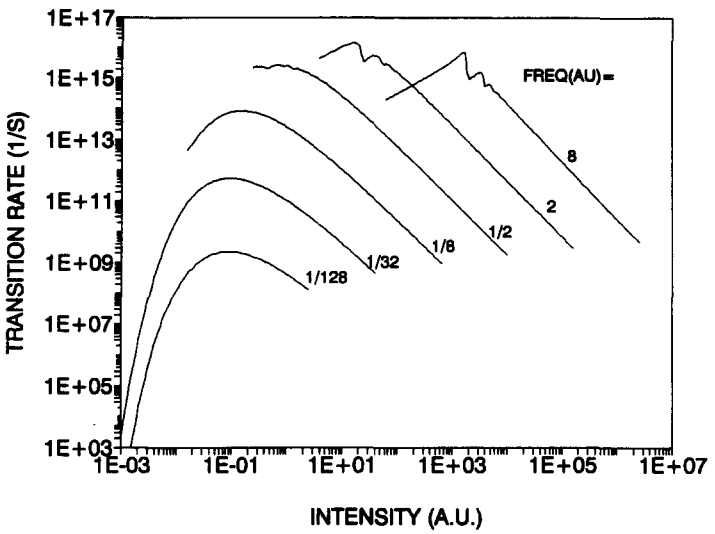

FIG. 11. Transition rates calculated by the SFA for photoionization of the ground state of hydrogen by circularly polarized radiation over a wide range of frequencies. The stabilization phenomenon is clearly exhibited for all frequencies.

was given earlier as part of Eqn. (161). It is repeated here because of its importance in the forthcoming discussion.

Total transition rates, including a sum over all orders of photons and an integration over solid angle, have been calculated for circular polarization over a range of frequencies from $\omega = 1/128$ to $\omega = 8$, in atomic units. The results are shown in Fig. 11. The stabilization phenomenon is clearly exhibited.

The low intensity cutoff of the curves in Fig. 11 is governed by the applicability of the SFA as determined by the condition $z_1 > 1$. As can be seen, this means that most of the pre-stabilization region is omitted for frequencies close to $\omega = 1$. This is a consequence of the strong-field character of the SFA method.

The termination of the curves in Fig. 11 at high intensity is governed by the desire to use the non-relativistic Eqn. (193), and not have to resort to relativistic results. The onset of relativistic effects is related to the intensity parameter z_1 of Section 1.3.5 and Eqns (14), (15). When z_f is of order unity, then the potential energy of the electron in the laser field is of the same order as the rest energy of the electron, mc^2. Relativistic effects should be expected in such a case. This is confirmed by explicit calculation in Ref. 36.

Applicability of the SFA has, so far, been couched in terms of the basic requirement $z_1 > 1$. However, more can be said. The SFA will be accurate if most of the photoelectrons emitted have energies comparable to or exceeding the binding energy of the atom, which is 13.6 eV in this case. For example, consider the case $\omega = 1/8$ in Fig. 11. The stabilization point—i.e., the intensity at which the rate is maximal—occurs at $z_1 = 10$, where the minimum photon order is 25. Ionization with a circularly polarized laser has a spectral distribution which peaks at relatively large photon orders, and the lowest photon orders do not contribute importantly for intense fields at low frequency. For this particular case, the peak of the photoelectron spectrum is at a photon order of 43, where the energy of the emitted electron is about 64 eV (or 133 eV upon recovery of the ponderomotive energy after emergence from the laser pulse). The spectrum drops to 1% of the peak value at order 31 (where the energy is 23 eV) at the

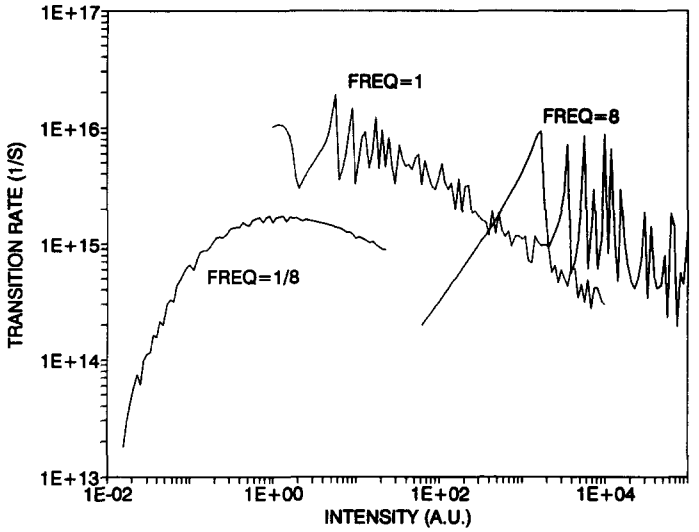

FIG. 12. Transition rates predicted by the SFA for photoionization of the ground state of hydrogen by a linearly polarized laser. Computational demands are much more stringent than for the circular polarization results in Fig. 11, and only three frequencies are shown. The stabilization phenomenon is not so well defined as in Fig. 11.

low energy end, and at order 66 (where the energy is 142 eV) at the high energy end. All of these energies are sufficiently greater than the ionization energy of 13.6 eV that the SFA should be very accurate.

At the high intensity limit of the transition rate curve for $\omega = 1/8$ (selected at $z_f = 1$), the value of z_1 is so large that the physical premises of the SFA are approaching exactness. The number of photons contributing to the process when $z_1 \approx 37{,}000$ (which is true at the end point of the $\omega = 1/8$ example) ranges from about 142,500 to about 152,200 with most of the contribution arising from $n \approx 2z \approx 147{,}300$.[36] A frequency of $\omega = 1/8$ corresponds to a photon energy of about 3.4 eV, so an electron ionized from ground state hydrogen under these circumstances has an energy of approximately the mc^2 energy of 511 keV. One should use relativistic forms here (where $z_f = 1$), but the basic point is that the photon energy absorbed by the photoelectron is about 1.5×10^5 times the binding energy of 13.6 eV, so that the effect of this binding on the emergent electron is minuscule. This is true over the entire electron spectrum.

Photoionization by linearly polarized laser light is far more difficult to compute than is the circular polarization case of Fig. 11, and the results turn out to be much more diverse as a function of frequency. Equation (193) is again the expression to be evaluated, with the sum over photon orders and the integral over solid angle accomplished. For linear polarization, however, J_n in Eqn. (193) is the generalized Bessel function of two variables[31] of Eqn. (164), which presents a profoundly more difficult computational challenge than the ordinary Bessel function. Computer-imposed limits dictate a more limited exposition of results for linear polarization than were presented for circular polarization.

The analog of Fig. 11 for circular polarization is Fig. 12 for linear polarization, but with only three frequencies shown instead of the six of Fig. 11. Furthermore, the high-intensity limit is no longer the $z_f = 1$ cutoff of Fig. 11, but is now taken to be $z_f = 0.04$. This is because of the computer time demands for the higher ranges of intensity with linear polarization. A characteristic which distinguishes the linear from the circular polarization case is the irregularity, or 'chaotic' behavior of the linear polarization results in some intensity and

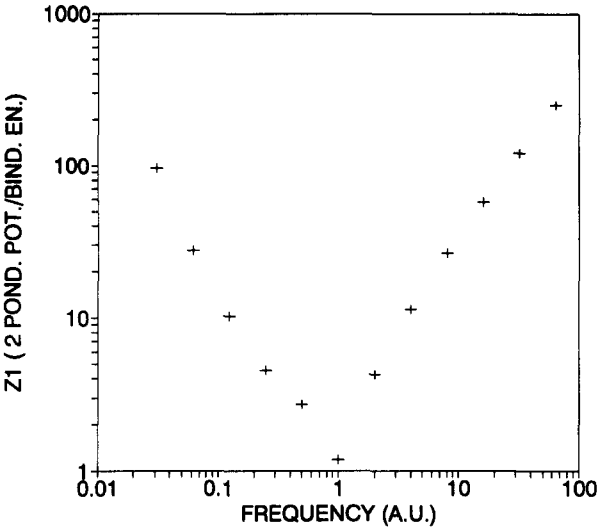

FIG. 13. The intensity as measured by z_1 at which the maximum transition rate occurs for multiphoton ionization of ground state hydrogen by a circularly polarized laser, as a function of laser frequency.

frequency domains. This has not previously been much commented upon, largely because it is not manifested unless the computations are done on a fine grid in angle and intensity. Chaotic behavior of the linear polarization results is one of many important properties which changes at $\omega = 1$. For $\omega > 1$, the transition rates behave smoothly until the critical stabilization intensity is surpassed. Then the chaotic behavior sets in, more strongly for higher frequencies than for low. On the other hand, the $\omega = 1/8$ case shows small-scale irregularities throughout the full intensity domain, present below as well as above the critical stabilization intensity.

Stabilization behavior appears in these linear polarization computations, but so weakly as to make strongly questionable their accessibility to experimental observation.

The location of the stabilization intensity as a function of frequency is an important outcome of the computations for several reasons. One is to verify the basic SFA applicability condition of $z_1 > 1$. This has actually already been accounted for in the plotting of Figs 11 and 12, since the curves commence at $z_1 = 1$. A plot of the z_1 values at the stabilization points is very revealing, as shown in Fig. 13, which gives this information for circular polarization. This figure makes manifest that, apart from the neighborhood of $\omega = 1$, the region of validity of the SFA encompasses the development of the stabilization phenomenon, from rising to decreasing rates as the intensity increases.

The most striking feature of Fig. 13 is the radical change in behavior which occurs at $\omega \approx 1$. This gives every indication that the physical nature of the stabilization process is altered at $\omega \approx 1$. That is the subject of the next section.

5.2.3. *Physical causes of stabilization from the SFA viewpoint.* High frequency stabilization is the easier case to analyze. An examination of the curves for $\omega = 2, 8$ in Fig. 11 shows a simple linear rise to a rather sharp peak, followed by a strong decline marked by some irregularities. The pattern is the same for all $\omega > 1$ curves that have been calculated. The linear rise from low intensity is a simple consequence of the single-photon character of the ionization process at lower ranges of intensity due to the fact that the ionization energy of hydrogen in a field-free region is $E_B = 1/2$ in atomic units. However, Eqn. (194) shows that the ponderomotive potential alters that single-photon threshold condition. (Recall that

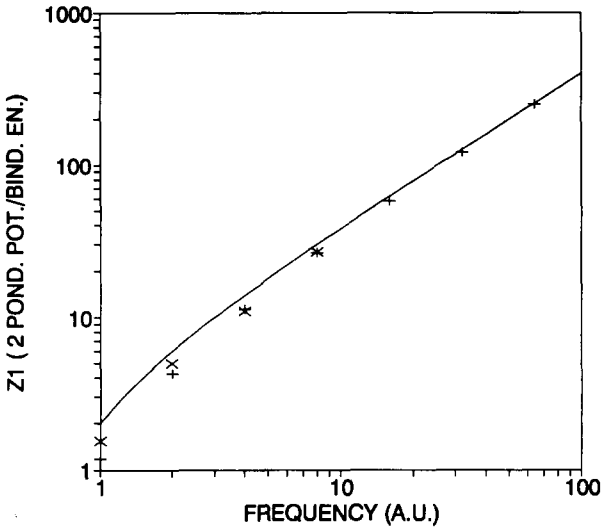

FIG. 14. Circular polarization stabilization points as in Fig. 13 for high frequencies ($\omega \geqslant 1$). Calculations with the SFA are shown by the + signs, the work of Pont and Gavrila from Ref. 42 is shown by the × marks, and the continuous curve is the prediction of Eqn. (195).

$z = U_p/\hbar\omega$.) The peak in each of the $\omega > 1$ curves correspond closely to the intensity where the minimum photon order indexes upwards from $n_0 = 1$ to $n_0 = 2$. From Eqn. (194), this first step upward from a one-photon minimum to a two-photon minimum occurs where $E_B/\hbar\omega + z = 1$. When this is expressed as a condition on z_1, where $z_1 = 2z\hbar\omega/E_B$, the prediction for the location of the critical intensity is

$$z_1 = 2(\hbar\omega/E_B - 1) \tag{195}$$

when ω is greater than unity (in atomic units).

Figure 14 shows the SFA results which correspond to $\omega > 1$ (given by the + marks), along with the smooth curve representing Eqn. (195). Also shown are the critical intensities found by Pont and Gavrila[42] (shown by the × marks), all of which correspond to $\omega > 1$. The agreement with Eqn. (195) in all cases is excellent for both types of theories, especially for the larger values of ω. The agreement is impressive in view of the contrast between the Kramers-Henneberger technique of Pont and Gavrila and the SFA.

The Kramers-Henneberger (KH) transformation underlies much of the work done on the stabilization problem. This transformation leads to approximations which are valid only at high frequencies. The SFA method has the ability to encompass both the Keldysh and KH domains of validity.

For $\omega < 1$, the situation is different, as seen in Fig. 13. Equation (195) has no relevance to $\omega < 1$, where the critical z_1 for stabilization falls with increasing frequency rather than rising as in Eqn. (195). This difference between $\omega > 1$ and $\omega < 1$ is reinforced by Fig. 11, which shows no direct evidence for a photon threshold associated with the stabilization point. Thresholds occur, of course, for $\omega < 1$; but they represent a progress from some $n_0 > 1$ to the next larger n_0, they are not connected with any alteration of the smoothness of the curve, and they are not associated with the maximum in the transition rate.

To understand this difference in behavior with frequency domain, the following simple calculation is instructive. The number of photons contained in the laser beam within the volume occupied by the undisturbed atom is

$$n_a = (4\pi/3)a_0^3\rho, \tag{196}$$

where a_0 is the Bohr radius, ρ is the photon density, and n_a is the number of photons present in the atomic volume. However, according to the condition of Eqn. (194) on the minimum number of photons required for ionization, one must have

$$n_0 > z = U_p/\hbar\omega. \tag{197}$$

The requirement that the photons available within the atomic volume should equal or exceed the number required for ionization gives, from a combination of Eqns (196) and (197), the condition in atomic units that $\omega > 1$. Hence one may regard ionization under conditions where $\omega < 1$ as one in which there is a shortage of nearby photons. The ionization process requires photons from a larger (possibly much larger) volume of the laser beam than is available within the immediate vicinity of the atom to be ionized. This 'photon availability' concept would lead one to expect photoionization to be progressively more difficult as the frequency declines below $\omega = 1$, which is the general character of the actual behavior as shown in Fig. 13.

In the introductory remarks on stabilization in Section 5.2.1, it was noted that the physical interpretation of the stabilization phenomenon depends on the analytical technique employed. It has just been observed in Fig. 14 that the KH method and the SFA predict the same stabilization points while relying on very different physical insights. This can be carried a step further by noting the strong-field level-interference interpretation of stabilization. That point of view allows for stabilization in the hydrogen atom, but not in a system bound by a short-range potential, where only one or a few bound levels may exist. One may ask how such a situation appears in the framework of the SFA. The reader is referred to the qualitative introduction to the SFA in Section 4.3.1, where it was pointed out that the beauty of the method is that the time-reversed S matrix places all of the essential strong-field ionization information into the unperturbed initial atomic wave function Φ_i. Thus it is the analytical structure of Φ_i which determines whether stabilization will or will not occur. The wave function used in the calculation of the negative-ion photodetachment results of Fig. 10 is of the form of $e^{-\alpha r}/r$, which is associated with a delta-function-like potential, and has only one bound state. Figure 10 shows no stabilization. Figure 11 comes from a hydrogenic 1s wave function, which is one of an infinite family of bound-state functions representing the Coulomb bound states. Figure 11 shows stabilization. The SFA method gives the same qualitative outcome as the level-interference scheme, but by very different means.

5.3. *Relativistic Effects*

5.3.1. *Introduction.* This section is, of necessity, incomplete and preliminary. Whereas experiments have already been done in which relativistic effects should be present (see Sections 1.3.5, 1.3.7, 1.4, and especially Tables 3 and 4), no laboratory study has focused on this matter. The theoretical situation is not much farther advanced than the experimental side. There have been few theoretical relativistic treatments of photoionization. Two of these theoretical papers[78,132] have been concerned with formal developments, whereas only one[36] presents a calculational algorithm with practical numerical applications thereof. That work will be reviewed in the next section.

The algorithm developed in Ref. 36 is only for the case of a circularly polarized laser, since that is analytically simpler than other polarization states. Nevertheless, the analytic complexity of the result is considerable. One may appraise it to be an order of magnitude more involved than the corresponding non-relativistic expression.

5.3.2. *Circular polarization results.* The differential transition rate has been explicitly found for a circularly polarized laser field as given by the four-vector potential

$$A^\mu(x) = (a/2)(\epsilon^\mu e^{-ik\cdot x} + \epsilon^{\mu *} e^{ik\cdot x}), \tag{198}$$

where k^μ is the propagation four-vector, and the polarization vector ϵ^μ is

$$\epsilon^\mu = 2^{-1/2}(0, \hat{x}^1 \pm i\hat{x}^2). \tag{199}$$

As is usual in relativistic work, the 'natural units' with $\hbar = c = 1$ are used, and the x, y, z spatial coordinates are renamed x^1, x^2, x^3. Equation (199) implies that the direction of propogation of the laser field is taken to be along the $\hat{x}^3$ direction. The Dirac relativistic formalism of Eqn. (138) is applied to the photoionization of ground state hydrogen by substituting for the initial state Φ_i the known 1s solution of the Dirac equation[74,82] for the Coulomb potential of nuclear charge Ze. The result so obtained is then entirely of Dirac form, and is stated in closed analytical form. The expression is averaged over initial spin states of the atomic electron, and summed over final spin states of the photoelectron.

The result thus arrived at is

$$\frac{dW}{d\Omega} = \frac{2m^2(ea)^2}{\pi(Z/a_0)^3} \sum_n \frac{p}{m} \frac{(u_A + u_B + u_C)}{[1 + (\rho a_0/Z)^2]^4}, \tag{200}$$

where, from the energy conservation condition, the momentum parameter p is

$$p = (n\omega - \eta\omega - E_B)^{1/2}(2m + n\omega - \eta\omega - E_B)^{1/2}. \tag{201}$$

Numerous special symbols remain to be defined. The factor $(ea)^2$ in Eqn. (200) can be replaced by $(ea)^2 = 2m^2 z_f$, where z_f is exactly the free-electron intensity parameter of Section 1.3.5, expressed now in terms of the amplitude a of the vector potential of Eqn. (198). The quantity a_0 is the customary Bohr radius, ρ is

$$\boldsymbol{\rho} = \mathbf{p} - (n - \eta)\mathbf{k}, \tag{202}$$

and η is

$$\eta = \frac{e^2 a^2}{4p \cdot k}, \tag{203}$$

where n is the photon order and k^μ is the propagation four-vector of the laser field. The dimensionless quantities u_A, u_B, u_C in Eqn. (200) are

$$\begin{aligned} u_A = \tfrac{1}{4}\mathscr{P}\Bigg\{\Bigg[\Bigg(J_{n+1}(\zeta)\Bigg)^2 + \Bigg(J_{n-1}(\zeta)\Bigg)^2\Bigg]\Bigg[\Bigg(\frac{E}{m} - 1\Bigg)\gamma^2\Bigg(\frac{\rho a_0}{Z}\Bigg)^4 \mathscr{U}^2 \\ + \Bigg(\frac{E}{m} + 1\Bigg)\beta^2\Bigg(\frac{\rho a_0}{Z}\Bigg)^2 \mathscr{V}^2 + 2\gamma(\beta m a_0)\Bigg(\frac{\rho a_0}{Z}\Bigg)^2 \\ \times \frac{p}{m}\cos\theta\Bigg(\frac{p}{m}\cos\theta - (n - \eta)\frac{\omega}{m}\Bigg)\mathscr{U}\mathscr{V}\Bigg] \\ - 4J_{n+1}(\zeta)J_{n-1}(\zeta)\gamma(\beta m a_0)\Bigg(\frac{\rho a_0}{Z}\Bigg)^2\Bigg(\frac{p}{m}\Bigg)^2 \sin^2\Theta\,\mathscr{U}\mathscr{V}\Bigg\}, \end{aligned} \tag{204}$$

$$\begin{aligned} u_B = -(\omega/2m)n\mathscr{P}(\rho a_0/Z)^2[J_n(\zeta)]^2 \times \{(\gamma\rho a_0/Z)^2\mathscr{U}^2 - 2\beta\gamma(m a_0/Z) \\ \times [(E/m) + (n - \eta)(\omega/m) - 2(p/m)\cos\Theta]\mathscr{U}\mathscr{V} + \beta^2\mathscr{V}^2\}, \end{aligned} \tag{205}$$

$$u_C = \frac{\omega}{m}\frac{z}{\left(\frac{E}{m} - \frac{p}{m}\cos\Theta\right)}\mathscr{P}[J_n(\zeta)]^2\left[\gamma^2\left(\frac{\rho a_0}{Z}\right)^4 \mathscr{U}^2\right.$$

$$\left. + 2\gamma(\beta m a_0)\left(\frac{\rho a_0}{Z}\right)^2\left(\frac{p}{m}\cos\Theta - (n-\eta)\frac{w}{m}\right)\mathscr{U}\mathscr{V} + \beta^2\left(\frac{\rho a_0}{Z}\right)^2 \mathscr{V}^2\right]. \quad (206)$$

Further definitions now required are

$$\mathscr{P} = \frac{(1+\gamma)[\Gamma(\gamma)]^2 2^{2(\gamma-1)}}{\Gamma(1+2\gamma)}\frac{[1+(\rho a_0/Z)^2]^{2-\gamma}}{(\rho a_0/Z)^6}, \quad (207)$$

$$\mathscr{U} = \sin\mathscr{X} + (\rho a_0/Z)\cos\mathscr{X}, \quad (208)$$

$$\mathscr{V} = \gamma(\rho a_0/Z)\cos\mathscr{X} - [1+(1+\gamma)(\rho a_0/Z)^2]\sin\mathscr{X}, \quad (209)$$

$$\mathscr{X} = \gamma \arctan(\rho a_0/Z), \quad (210)$$

$$\gamma = (1 - Z^2\alpha^2)^{1/2}, \quad (211)$$

$$\zeta = \frac{eap}{2^{1/2}p\cdot k}\sin\Theta. \quad (212)$$

In Eqn. (211), α is the usual fine structure constant, and the angle Θ in Eqns (204), (205), (206) and (212) is the angle of spherical polar coordinates as measured to the direction of photoelectron emission from the direction of laser propagation as the polar axis. The energy E which appears is the relativistic energy, related to the momentum by

$$E^2 = p^2 + m^2. \quad (213)$$

The set of Eqns (200)–(212) reduces[36] in the non-relativistic limit exactly to the circular polarization version of Eqn. (193).

There is an energy conservation condition associated with the set of Eqns (200)–(212), which is

$$E = 1 + \omega[n - E_B - z/(E - p\cos\Theta)], \quad (214)$$

when the further notational simplification is introduced that E, E_B, p, and ω are all expressed in units of m, the electron mass. It is seen that this equation is implicit, since E and p both appear on the right-hand side of the equation, and E, p are related as in Eqn. (213). An explicit analytical statement of the energy conservation condition requires the solution of a difficult quartic equation. It is easier to solve Eqn. (214) numerically as a function of n and Θ. The solution of Eqn. (214) is quite straightforward until very large values of the intensity parameter z are reached. Then, for example, for a particular n value, energy conservation can be satisfied for some values of Θ, but not for others. There is a threshold value of n for which $E \geqslant 1$, and that threshold may acquire a dependence on Θ when z is very large.

A number of calculated examples of the above relativistic solution are given in Refs 36 and 40. One is reproduced here as Fig. 15. This shows the angular distribution in both relativistic and non-relativistic cases of photoelectrons ionized from ground state hydrogen by a laser of wavelength 1.06 μm at an intensity $z = 10^4$ (1.1×10^{17} W/cm^2). There is a substantial shift of the angular distribution forward from the waist direction.

5.4. *Qualitative Features of Strong Fields with Circular Polarization*

5.4.1. *Non-relativistic case.* Some important qualitative insights can be obtained very simply because of the relative analytical simplicity of circular polarization results. Consider the general result for circular polarization in Eqn. (160), or its hydrogenic 1s counterpart in

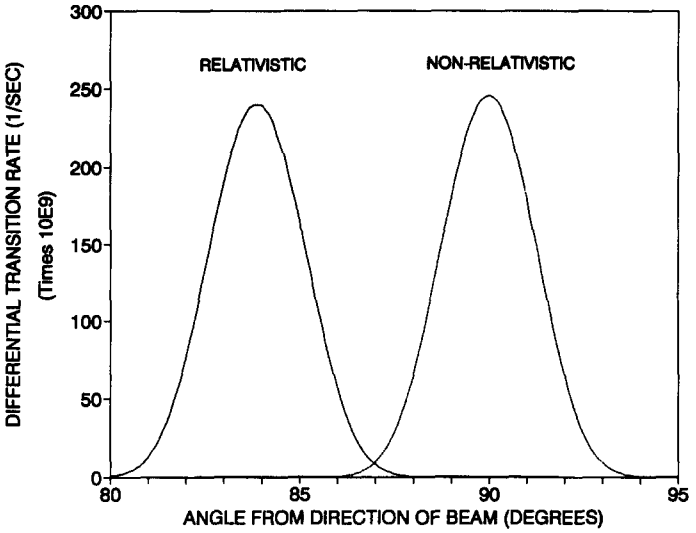

FIG. 15. Relativistic and non-relativistic angular distributions of photoelectrons ionized from the ground state of hydrogen by a circularly polarized laser with $\lambda = 1.06\,\mu m$ at $z = 10^4$ (1.2×10^{17} W/cm^2). The angle is measured from the direction of propagation of the beam. The non-relativistic distribution is symmetric about 90°, and the relativistic distribution is displaced forward by an amount given approximately by Eqn. (220) or (221).

Eqn. (193). Angular dependence is entirely within the argument of the Bessel function, which may be written as $J_n(\zeta)$, where n is the photon order, and $\zeta = z^{1/2}\gamma$, with γ given in Eqn. (161) as

$$\gamma = 2(n - z - \epsilon_B)^{1/2} \sin\theta. \tag{215}$$

For high intensity, $z \gg 1$, the threshold photon order constraint in Eqn. (161) of $n_0 \geqslant z + E_B$ means that n will always be large. It is elementary to show that $\zeta < n$ always, and so one may use the elementary qualitative asymptotic form

$$J_n(\zeta) \sim (\zeta/2)!/n!. \tag{216}$$

This means that the magnitude of J_n will be greatest for the largest possible value of ζ, and will decline rapidly as ζ departs from that value. Hence non-relativistic, circular polarization photoionization peaks at $\theta = \pi/2$ and falls off symmetrically to both sides of that value. For any such peak, i.e., for $\theta = \pi/2$ and for fixed n, Eqn. (193) achieves a maximum value as a function of z when $z = (n - \epsilon_B)/2$. For sufficiently large z, then $z \gg \epsilon_B$ and hence also $n \gg \epsilon_B$. Hence the result is obtained that spectra peak at

$$n = 2z + \epsilon_B \approx 2z. \tag{217}$$

Equation (217) is well verified by experiments.[6]

5.4.2. *Relativistic case.* Relativistic and non-relativistic angular distributions are of almost identical shapes. They differ in that the relativistic distribution is shifted forward. The reason for the forward displacement is that photon orders are so large that the absorbed photon momentum becomes important. This effect can be quantitatively estimated by noting that energy conservation conditions reflect the fact that an energy $n\hbar\omega$ is absorbed from the photon field, of which an energy $z\hbar\omega$ is required to provide the classical oscillatory motion of the particle in the field, as discussed in Sections 1.3.3 and 1.3.6. This leaves $(n - z)\hbar\omega$ for the directed kinetic energy of the photoelectron. The non-relativistic result $\theta = \pi/2$ can be

used to say that, to first approximation, all of the photoelectron momentum is transverse and given by

$$p_\perp \approx [2m(n - z - \epsilon_B)\omega]^{1/2} \approx [2m(n - z)\omega]^{1/2}, \tag{218}$$

where we revert to the relativistic practice of setting $\hbar = c = 1$. There is, however, a relativistic forward momentum coming from the fact that $(n - z)$ forward-directed photons contribute to the directed momentum of the photoelectron, or

$$p_\parallel \approx (n - z)\omega. \tag{219}$$

The forward angular displacement of the peak is then

$$\theta_d = \arctan(p_\parallel / p_\perp) \approx \arctan[(n - z)\omega/2m]^{1/2} \approx \arctan(z\omega/2m)^{1/2}, \tag{220}$$

where the last result comes from using Eqn. (217). An alternative expression for Eqn. (220) comes from the connection $z\omega/2m = z_f/4$, where z_f is the free-electron intensity parameter of Section 1.3.5. Equation (220) then takes the extremely simple form

$$\theta_d \approx \arctan(z_f^{1/2}/2). \tag{221}$$

This prediction agrees accurately with all detailed calculations done to date, including the results of Fig. 15.

5.5. *Very-High-Order and Very-Strong-Field Applications*

Equation (217) obtained above makes possible very direct appraisals of the dominant photon orders which contribute strong-field, circular-polarization photoionization. The three state-of-the-art laser systems listed in Table 4 have peak z values of about 10^4, 10^5, and 10^4, respectively. Hence the dominant photon orders which will contribute are about twice those numbers. No such simple result as Eqn. (217) is known for linear polarization, but a rough estimate remains possible. Because of the threshold condition

$$n_0 = \{z + E_B/\hbar\omega\} > z, \tag{222}$$

the simple inequality $n > z$ always hold. In practical calculations at very high intensities, the most prominent peaks in a spectrum of photoelectrons produced by a strong laser field of linear polarization are those at the lowest end, followed by a very extended spectrum that declines only gradually until a rather abrupt final roll-off that generally occurs as $n \to 2z$. (This is thus quite unlike the shape of the circular polarization spectrum where the maximum is at $n \approx 2z$, with a rather symmetrical distribution about that value.) For either polarization, $n \approx 2z$ gives the correct order of magnitude for the strong-field photon order to be expected, and that number is seen from Table 4 to be impressively large.

Still essentially unexamined is the matter of ionization from Rydberg states by very low frequency radiation. Numbers as large as those mentioned above can occur in this case as well, as some preliminary calculations along these lines indicate.[137] In this connection, it is appropriate to mention experiments reported by Gallagher,[50] who employs two low-intensity lasers to excite an atom to a Rydberg state, from which it is ionized by microwaves. The energy of the emergent photoelectrons is so far above threshold that about 3×10^5 microwave photons must be absorbed.

In anticipation of the examination of ionization from Rydberg states by the SFA, one complicating feature immediately comes to the fore. It is customary in dealing with Rydberg states to use a scaled frequency defined by $\omega_0 \equiv n_0^3\omega(au)$, and a scaled electric field given by $\epsilon_0 \equiv n_0^4\epsilon(au)$, where n_0 is the principal quantum number. However, the non-relativistic SFA

depends on two intensity parameters, z and z_1, whose expressions in terms of these scaled quantities are

$$z = \frac{n_0 \epsilon_0^2}{4\omega_0^3}, \tag{223}$$

$$z_1 = (\epsilon_0/\omega_0)^2. \tag{224}$$

The SFA 'scaling' is more complicated than simple Rydberg scaling, and incompatible with it. In other words, the prediction of the SFA method is that the customary Rydberg scaling will not hold for very strong fields.

6. CRITICAL COMMENTARY ON THE KFR METHOD

6.1. *Internal Consistency*

The Keldysh theory and its KFR successors have caused some puzzlement in the atomic, molecular, and optical (AMO) physics community. They are non-perturbative techniques, designed from the outset to accommodate strong fields. In no sense do they constitute a continuous evolution of techniques long familiar in AMO physics. Practitioners in the field have manifested their discomfort with this situation by attempting to test the KFR theory against more conventional concepts, or seeking to find comparative tests against either experiments or against theories that have evolved continuously from standard techniques. Some of these efforts will be reviewed.

A well-known formal challenge to the validity of the Keldysh approximation comes from Autunes-Neto and Davidovich.[168] After various manipulations, they conclude that the Keldysh approximation is internally inconsistent. This line of thought was taken up by Milonni,[169,170] who arrives at the result that the Keldysh approximation is a weak-field theory, not a strong-field theory. Mittleman returns to the theme that the Keldysh approximation is internally inconsistent.[171]

These criticisms were examined by the present author, with the conclusion[78] that the putative shortcomings of the KFR work did not have their origins in the KFR method, but rather in the improper application of a technique employed in common by all the above-mentioned critics. That technique is to apply a contact transformation to remove from a matrix element an exponentiated purely time-dependent function. It is a procedure common in AMO physics. It is shown here that the structure of the Keldysh approximation and the SFA make it plain why a contact transformation in the spirit of Autunes-Neto *et al.* cannot be applied to those strong-field formulations.

The basic premise of the KFR critics can be understood from an expression like Eqn. (49) for a transition matrix element. Consider the non-relativistic case when $\Psi_f^{(-)}$ in Eqn. (4a) is approximated by a Gordon–Volkov solution, that is,

$$M_{fi}^{SFA,NR} = (\Psi_f^{(-)GV}, H_I \Phi_i). \tag{225}$$

The $\Psi_f^{(-)GV}$ solution is shown in Eqn. (144). The entire factor

$$F(t) = \exp(i/\hbar) \int_t^\infty d\tau H_I(p, \tau) \tag{226}$$

is a function of time alone, where $H_I(p, \tau)$ is defined by Eqns (145) and (147). That is,

$$F(t) = \exp[if(t)], \tag{227}$$

and when the absolute square of Eqn. (225) is taken for substitution into the Fermi golden rule for the transition probability, then all contribution from $F(t)$ vanishes. This is the basic reasoning behind the conclusion that a contact transformation, as given by Eqn. (226), will not alter transition probabilities.

Some warning signs are already in clear evidence that this procedure has problems. First is the fact that Eqn. (226) contains the entirety of field dependence from the Gordon–Volkov solution, and not only the effect of the $\mathbf{A}^2$ term, which is the term the KFR critics have seized upon. The same reasoning applies to the entire field-dependent phase of the non-relativistic Gordon–Volkov solution. Carrying their logic one step further reduces Eqn. (225) to a quantity which has nothing at all to do with the laser field. The next warning sign is the comparison with the relativistic case, and the physical expectation that relativistic and non-relativistic calculations should interface smoothly. When the relativistic Gordon–Volkov solution is employed for $\Psi_f^{(-)GV}$, then Eqn. (226) is unambiguously a function of both t and $\mathbf{r}$, and there can be no thought of a contact transformation. This is true of $\mathbf{A}^2$, so one may examine that. The magnitude of the $\mathbf{A}^2$ contribution to the energy is given directly by the ponderomotive potential. A practical case in point is a laser field of 1 μm at 10^{16} W/cm^2, which is currently to be found in the laboratory, and is not relativistic ($z_f \approx 4 \times 10^{-3}$). The ponderomotive potential is about 10^3 eV. The $\mathbf{A}^2$ term, present relativistically in excess of a keV, suddenly appears to vanish non-relativistically when a contact transformation is applied. Something is wrong.

To all these danger signs, one can add other fundamental difficulties that confront the conclusions of the critics. These include the correct tunneling limit that emerges from the KFR method (Milonni finds the KFR method to be weak-field in nature), the prediction of stabilization (unambiguously a strong-field effect), and the unmatched numerical accuracy of KFR predictions of very strong-field experiments (Mittleman speaks of errors of factors of 10^9.[172]

The resolution of the problem is straightforward. It can be approached in several ways. One is to note that the familiar form of the Fermi golden rule is not valid for strong fields. The golden rule was derived originally[173] with perturbation theory in mind. The S-matrix theory developed in Section 2.3 expressly does not use the Fermi golden rule. Transition rates are found *ab initio*. Most particularly, the S matrix contains not only the matrix element of Eqn. (225), it always contains as well an integration over time, as shown in Eqn. (47) or (49). If one extracts an $\mathbf{A}^2$ term from either $\Psi_i^{(+)}$ in Eqn. (47) or from $\Psi_f^{(-)}$ in Eqn. (49), the energy-conserving delta function is correspondingly altered. The extraction of $\mathbf{A}^2$ is then clearly impermissible.

An alternative, but equivalent, viewpoint is that the removal of a purely time-dependent exponential factor from Ψ by a contact transformation shifts the zero from which energies are measured in that state. On the other hand, Φ contains no $\mathbf{A}^2$ term, is not subjected to a contact transformation, and so its energy continues to be measured from the pre-transformation zero of energy. Transition amplitudes are measured by comparison of Ψ and Φ. The inconsistency introduced by the contact transformation is clear. The error is major because of the large possible magnitude of the ponderomotive potential.

Yet another, but still equivalent, view of the inconsistency is suggested by an argument that Mittleman advances[171] in support of his introduction of a contact transformation. He remarks that one can shift a Lagrangian by a total-time-derivative term without altering the dynamics of the system. One can use this argument to alter by removal of $\mathbf{A}^2$ the Lagrangian (and Hamiltonian) $H_0 + H_I$ which describes Ψ. However, Ψ is directly confronted with Φ in the basic S matrix

$$S_{fi} = \lim_{t \to \infty} (\Phi_f, \Psi_i).$$

The state Φ is governed by H_0, which does not contain $\mathbf{A}^2$. The situation is as described above. The total-time-derivative shift changes the zero of energy related to Ψ, while not doing so for Φ. The inconsistency is evident.

An interesting footnote to the above is reviewed here. The problems described above can be seen from a new perspective by a fresh look at the Fermi golden rule. Such a rule can be

generalized[78] to the Floquet problem,[174] in a non-relativistic, dipole-approximation, monochromatic application. Floquet behavior[175–177] is such that a state in interaction with a field possesses sidebands spaced at integer multiples of $\hbar\omega$ about the unperturbed energy. For comparison with the generalization, the simple Fermi golden rule is stated first. For stationary states such that both Φ and Ψ have the form

$$\Phi_f(\mathbf{r}, t) = \phi_f(\mathbf{r})\exp(-iE_f t/\hbar),\ \Psi_i(\mathbf{r}, t) = \psi_i(\mathbf{r})\exp(-iE_i t/\hbar), \tag{228}$$

then the S matrix

$$(S-1)_{fi} = -(i/h)\int dt(\Phi_f, V\Psi_i^{(+)}) \tag{229}$$

gives rise to the transition rate

$$w = (2\pi/\hbar)\delta(E_f - E_i)|T_{fi}|^2, \tag{230}$$

where the T matrix T_{fi} is simply

$$T_{fi} = (\phi_f, V\psi_i). \tag{231}$$

Equation (230) is a statement of the golden rule. However, when $\Psi_i^{(+)}$ exhibits Floquet behavior, then (see Appendix B of Ref. 78) the S matrix can be written

$$(S-1)_{fi} = -2\pi i \sum \delta(E_f - E_i - n\hbar\omega + z\hbar\omega)T_{fi}^{(n)}, \tag{232}$$

and the golden rule generalizes to

$$w = (2\pi/\hbar)\sum_n \delta(E_f - E_i - n\hbar\omega + z\hbar\omega)|T_{fi}^{(n)}|^2. \tag{233}$$

The $n\hbar\omega$ term in the delta function refers to transitions between Floquet sideband states in this time-dependent problem, but the term $z\hbar\omega$ is just the ponderomotive potential, since z is defined by Eqn. (6). The $\mathbf{A}^2$ term is no longer in the separate $T_{fi}^{(n)}$, it is now in the overall energy conservation condition.

6.2. *One-Dimensional Behavior*

When a problem presents great difficulties in a fully formulated theory, a common practice in physics is to simplify the premises. One traditional example of such reductionism is to employ a one dimensional model as a way of gaining insight into a problem which is forbidding in three dimensions. This has been done with strong-field photoionization. See Ref. 55 for an extensive review of one-dimensional numerical methods.

The reduction to one dimension has been imposed also upon the KFR method, with unexpected results.[178–180] When the energy spectrum of emitted electrons in an ATI process is examined with a one-dimensional KFR method, the spectrum acquires a ragged, almost random appearance which is quite unlike observed spectra, and also unlike spectra calculated by direct integration of the one-dimensional Schrödinger equation. Various conclusions have been drawn from this failure of reasonable behavior in the one-dimensional KFR, but none of the authors take note of the fact that the one-dimensional KFR spectra are also totally unlike the three-dimensional KFR spectra, and the three-dimensional KFR results do, in fact, resemble both experiments and direct numerical integration of the Schrödinger equation. The resolution of this conundrum is direct.[181] When one calculates the angular distribution of emitted photoelectrons in a three-dimensional KFR theory, the emission in the exact forward direction changes significantly from one spectral peak to another, even though the total emission of electrons when integrated over all angles varies in the expected smooth fashion. The one-dimensional KFR theory retains only information from the forward direction. It is shown[181] that emission in the forward direction has no correspondence with the total emission probability. This explains the anomaly. Three-dimensional KFR is predictive, while one-dimensional KFR makes no sense. The KFR method is inherently three-dimensional.

6.3. *Insights from Critical Commentary*

The remarks of the critics of the KFR method can be understood in the fashion shown above, but constructive lessons can be found in the criticisms. For example, the conviction that one can carry out a contact transformation without further inspection of the premises behind such a move is reinforced by several features commonly accepted in the AMO community. One derives from the long dependence on perturbation theory. When the problem of an atom in a laser field is treated directly by perturbation theory, at no finite order does the $\mathbf{A}^2$ term appear in exponentiated form. Yet that is a characteristic overtly displayed by the non-perturbative Gordon–Volkov solution. Already mentioned is the common acceptance of the Fermi golden rule in its familiar form.

Another difference between standard AMO practices and the strong-field S-matrix approach exemplified here is the emphasis placed upon application of boundary conditions in the S-matrix method. As shown in Eqn. (38), the S matrix is based on a comparison of a fully interacting state with the non-interacting state that normally characterizes the system in the spatio-temporal domain where measurements are made. This leads to an expression like Eqn. (47), where the transition amplitude confronts one state of type Ψ with another of type Φ. However, it is common practice in AMO physics to write a transition matrix element with both initial and final states of the same type. In lowest order perturbation theory, both states are of the non-interacting Φ type, but it is common for authors to simply make both states of Ψ type when formulating a theory intended to go beyond perturbation theory. Matrix elements expressed as $(\Psi_f, H_I\Psi_i)$ are commonly to be found in the literature. Thus the presumption follows that if an $\mathbf{A}^2$ term is removed from Ψ_i by a contact transformation, this will be balanced by a removal of a corresponding $\mathbf{A}^2$ term from Ψ_f, and so the inconsistent energy assignments described in Section 6.1 will not happen. The resolution of this problem is simply to explore from first principles how one arrives at a transition amplitude, as has been done in this article. For boundary conditions to be found in all current multiphoton ionization experiments, the applicable S matrices are those mixing Φ and Ψ states as in Eqns (47) and (49).

In connection with the last point just made, an interesting object lesson comes from the numerical methods of Kulander.[48,182–184] His technique is to solve the Schrödinger equation numerically for the atom in the presence of the laser field, and to follow an electron to the outer boundaries of his numerical experiment. When the electron crosses that boundary, and so departs from both the atom and the laser field, it is counted as ionized. This qualitative description matches exactly the content of Eqn. (47). A fully interacting state $\Psi_i^{(+)}$ is followed until it finally ends up as some particular non-interacting state Φ_f. Effectively, Kulander's matrix element is of the type $(\Phi_f, H_I\Psi_i)$.

A further interesting point comes from the contrast between the one-dimensional and three-dimensional treatment of the KFR method. The transparent conclusion is that the three-dimensional treatment makes sense and the one-dimensional does not. Certainly this is expected from a relativistic treatment, where the figure-eight behavior of the electron in a strong field is fundamental, but it persists in the non-relativistic, dipole-approximation limit. This contrast does not exist in direct numerical solution of the equations of motion, as the work of Eberly and collaborators[55] has shown. This needs to be understood more fully, but the interim conclusion is that the SFA is a fundementally relativistic formalism which retains some of those inherent characteristics even when applied non-relativistically.

Finally, there is the phenomenon noted in Section 5.2.3 on the physical interpretation of the stabilization phenomenon. The physical insight one gains from an analysis of a problem will be couched in terms strongly influenced by the character of the analytical technique. Thus, when an investigator speaks of what 'really happens physically', his perceptions depend on the analytical context of his method. This will be very different for Keldysh and SFA

methods than for other techniques. Stabilization appears to have one 'cause' in the SFA, and a different 'cause' in (for example) KH approaches. This is all part of the frequently painful adjustments involved in a change of paradigm, as so cogently described by Kuhn.[1]

7. APPRAISAL AND OUTLOOK

In Section 1.2 of this article, reference was made to some of the qualitative changes to conventional quantum optics that are associated with the very strong field environment. This can now be taken to be the closing theme as well.

As is evident from the formal structure of the SFA which has been the principal focus of the developments reported here, it may seem that there are more formal similarities between the SFA and the standard techniques of high energy physics (as explicated, for example, in Ref. 74) than there are to the usual methods of quantum optics. There is one very good reason for this, related to the importance attached to the use of relativistic methods to underlie the theory. The SFA is a formalism which treats atomic ionization in a context where the interaction energy of the ionized electron with the laser field exceeds the binding interaction of the atom. That is, the laser field dominates the atomic potential. A laser-dominated interaction, however, may be expected to be fundamentally relativistic just as Maxwell's equations are fundamentally relativistic. (An interesting historical sidelight is that Einstein claimed that he was not aware of the Michelson–Morley experiment at the time he formulated his special theory of relativity. Einstein's motivation for the special theory came from the desire to reformulate Newtonian mechanics to share the same Lorentz symmetry exhibited by the Maxwell equations.) By contrast to this situation, the structure of quantum optics (and all of atomic physics) is governed by the dominance of the binding potential of the atom. It not only underlies perturbation theory, but it explains the pervasiveness of the electric dipole approximation. A plane-wave electromagnetic field has equal magnitudes of electric and magnetic components, but their consequences are, of course, vastly unequal throughout the field of quantum optics. This is easily understood both on the basis of the long wavelength of the typical laser as compared to the atomic size, and also on the basis of the smallness of the v/c ratio causing the electric Lorentz force on an electron to greatly exceed the magnetic Lorentz force. This comfortable situation breaks down in very strong fields, as has been seen in Sections 1.5 and 4.2.3.

Despite the emphasis above on the 'dominance' of the laser field over the atomic field for a sufficiently strong laser, it still remains true that the singularity at the origin of the Coulomb potential can never be overcome. This is a theoretician's way of saying that the identity of the atom persists no matter how strong the field. The recent work on stabilization just reinforces this view.

A brief list will now be given of some broadly defined areas in strong-laser physics where much interesting work remains to be done. In some instances, our present knowledge is scant almost to the vanishing point. There is no pretence to completeness in this list. The selection of items is motivated by the relevance to applicability of the techniques reviewed in this paper, and by those topics associated with major changes in the mode of thinking customary in quantum optics.

The emphasis in the preceding paragraphs suggests relativistic effects as a start. Experimentally, this area is essentially a blank, although one can predict that this deficit will be overcome more quickly than that on the theoretical side of the ledger. The list here is open-ended. It is not known whether there are important spin effects, whether polarized-electron experiments are worth doing, and so on. Ignorance also shrouds the influence of relativity on the stabilization phenomenon as well as on spectral or angular distribution characteristics. Yet

little of this can be done until the development of a linear polarization theory in parallel to the circular polarization results summarized in Section 5.3.2.

Relativistic effects reflect as well on the opening up of potentially important pair production channels in competition with photoionization.[6]

The stabilization phenomenon *per se*, now the subject of so much theoretical activity, is far from fully understood. Is there stabilization for low frequencies, as the above-reported results suggest for circular polarization, or is it present at high frequencies only, as some investigators conclude? Why does linear polarization appear so different from circular, as is indicated in Section 5.2? Another question refers to the need for wave-packet behavior to have stabilization occur at all. Some commentators are convinced it is necessary; in the S-matrix approach it appears not to be. This may be settled earlier than some other questions. What are the SFA predictions for stabilization of higher-lying levels in hydrogen, and what are the consequences of exploring other than initial S states?

A theoretical activity not yet attempted, but certainly possible, is the treatment of harmonic production by SFA methods.[7] It is not known whether such techniques would possess advantages. They very well might, especially in view of the transparently available relativistic extensions.

The entire subject of quantum manifestations of chaos is very active. Some of the results shown in this article suggest such behavior in regions not previously examined. Many other suggestive-looking results have also been obtained, but their interpretation and possible implications have not been pursued.

A long-standing problem that has received inadequate theoretical attention is to explain in detail the complicated photoelectron spectra obtained from very strong few-femtosecond laser pulses. Again, the SFA should be a suitable technique, especially if developed from a true a priori wave packet theory instead of the theory expounded above, in which monochromatic results are later superposed to represent space–time distributions. The true wave-packet theory is available because the Gordon–Volkov solution is known in such form.

The entire subject of very-strong-field laser-assisted and microwave-assisted processes is very large and very promising. It is also difficult for the theoretician. A few theoreticians and experimentalists have been laboring in this area for some time. It is due for considerable expansion.

REFERENCES

1. T. S. KUHN, *The Structure of Scientific Revolutions*, University of Chicago, Chicago (1970).
2. U. JOHANN, T. S. LUK, H. EGGER, and C. K. RHODES, *Phys. Rev. A* **34,** 1084 (1986).
3. T. S. LUK, U. JOHANN, H. EGGER, H. PUMMER and C. K. RHODES, *Phys. Rev. A* **32,** 214 (1985).
4. S. L. CHIN, F. YERGEAU and P. LAVIGNE, *J. Phys. B* **18,** L213 (1985).
5. F. YERGEAU, S. L. CHIN and P. LAVIGNE, *J. Phys. B* **20,** 723 (1987).
6. P. B. CORKUM, N. H. BURNETT and F. BRUNEL, *Phys. Rev. Lett.* **62,** 1259 (1989).
7. C. Y. TANG, P. G. HARRIS, A. H. MOHAGHEGHI, H. C. BRYANT, C. R. QUICK, J. B. DONAHUE, R. A. REEDER, S. COHEN, W. W. SMITH and J. E. STEWART, *Phys. Rev. A* **39,** 6068 (1989).
8. P. G. HARRIS, H. C. BRYANT, A. H. MOHAGHEGHI, C. Y. TANG, J. B. DONAHUE, C. R. QUICK, R. A. REEDER, S. COHEN, W. W. SMITH, J. E. STEWART and C. JOHNSON, *Phys. Rev. A* **41,** 5968 (1990).
9. S. MANDELSTAM, *Ann. Phys. (N.Y.)* **19,** 1 (1962).
10 B. S. DEWITT, *Phys. Rev.* **125,** 2189 (1962).
11. F. J. BELINFANTE, *Phys. Rev.* **128,** 2832 (1962).
12. M. LÉVY, *Nucl. Phys.* **57,** 152 (1964).
13. F. ROHRLICH and F. STROCCHI, *Phys. Rev.* **139,** B476 (1965).
14. M. PRIOU, *Nucl. Phys.* **81,** 641 (1966).
15. E. J. KONOPINSKI, *Electromagnetic Fields and Relativistic Particles*, McGraw-Hill, New York (1981).
16. Y. AHARONOV and D. BOHM, *Phys. Rev.* **115,** 485 (1959).
17. T. T. WU and C. N. YANG, *Phys. Rev. D* **12,** 3843 (1975).

[6]My thanks to S. L. Chin for emphasizing this possibility to me.
[7]This was urged some time ago by A. L'Huillier.

18. T. T. Wu and C. N. Yang, *Phys. Rev. D* **12,** 3845 (1975).
19. R. G. Chambers, *Phys. Rev. Lett.* **5,** 3 (1960).
20. H. A. Fowler, L. Marton, J. A. Simpson and J. A. Suddeth, *J. Appl. Phys.* **32,** 1153 (1961).
21. H. Boersch, H. Hamisch, K. Grohmann and D. Wohlleben, *Z. Phys.* **165,** 79 (1961).
22. A. Tonomura, N. Osakabe, T. Matsuda, T. Kawasaki, J. Endo, S. Yano and H. Yamada, *Phys. Rev. Lett.* **56** 792 (1986).
23. R. A. Webb, S. Washburn, C. P. Umbach and R. B. Laibowitz, *Phys. Rev. Lett.* **54,** 2696 (1985).
24. L. D. Landau and E. M. Lifschitz, *The Classical Theory of Fields*, Pergamon, Oxford (1975).
25. E. S. Sarachik and G. T. Schappert, *Phys. Rev. D* **1,** 2738 (1970).
26. W. Gordon, *Z. Phys.* **40,** 117 (1926).
27. D. M. Volkov, *Z. Phys.* **94,** 250 (1935).
28. H. R. Reiss, *Phys. Rev. A* **19,** 1140 (1979).
29. L. V. Keldysh, *Zh. Eskp. Teor. Fiz.* **47,** 1945 (1964) [*Sov. Phys. JETP* **20,** 1307 (1965)].
30. F. H. M. Faisal, *J. Phys. B* **6,** L312 (1973).
31. H. R. Reiss, *Phys. Rev. A* **22,** 1786 (1980).
32. H. R. Reiss, *J. Math. Phys.* **3,** 59 (1962).
33. A. I. Nikishov and V. I. Ritus, *Zh. Eksp. Teor. Fiz.* **46,** 776 (1964) [*Sov. Phys. JETP* **19,** 529 (1964)].
34. L. S. Brown and T. W. B. Kibble, *Phys. Rev.* **133,** A705 (1964).
35. H. R. Reiss and J. H. Eberly, *Phys. Rev.* **151,** 1058 (1966).
36. H. R. Reiss, *J. Opt. Soc. Am. B* **7,** 574 (1990).
37. H. A. Kramers, *Collected Scientific Papers*, North-Holland, Amsterdam (1956).
38. W. C. Henneberger, *Phys. Rev. Lett.* **21,** 838 (1964).
39. H. R. Reiss, *Phys. Rev. Lett.* **25,** 1149 (1970).
40. H. R. Reiss, In *Atoms in Strong Fields*, C. A. Nicolaides, C. W. Clark and M. H. Nayfeh (eds), Plenum, New York (1990).
41. M. Pont, N. R. Walet, M. Gavrila and C. W. McCurdy, *Phys. Rev. Lett.* **61,** 939 (1988).
42. M. Pont and M. Gavrila, *Phys. Rev. Lett.* **65,** 2362 (1990).
43. J. Parker and C. R. Stroud, *Phys. Rev. A* **40,** 5651 (1989).
44. M. V. Fedorov and A. M. Movsesian, *J. Opt. Soc. Am. B* **6,** 928 (1989).
45. Q. Su, J. H. Eberly and J. Javanainen, *Phys. Rev. Lett.* **64,** 862 (1990).
46. K. Burnett, P. L. Knight, B. R. M. Piraux and V. C. Reed, *Phys. Rev. Lett.* **66,** 301 (1991).
47. J. Grochmalicki, M. Lewenstein and K. Rzążewski, *Phys. Rev. Lett.* **66,** 1038 (1991).
48. K. C. Kulander, K. J. Schafer and J. L. Krause, *Phys. Rev. Lett.* **66,** 2601 (1991).
49. J. Mostowski and J. H. Eberly, *J. Opt. Soc. Am. B* **8,** 1212 (1991).
50. T. F. Gallagher, *Phys. Rev. Lett.* **61,** 2304 (1988).
51. P. Agostini, M. Fabre, G. Mainfray, G. Petite and N. K. Rahman, *Phys. Rev. Lett.* **42,** 1127 (1979).
52. B. W. Boreham and B. Luther-Davies, *J. Appl. Phys.* **50,** 2533 (1979).
53. P. Kruit, J. Kimman and M. J. van der Wiel, *J. Phys. B* **14,** L597 (1981).
54. A. L'Huillier, L. A. Lompré, G. Mainfray and C. Manus, *J. Phys. B* **16,** 1363 (1983).
55. J. H. Eberly, J. Javanainen and K. Rzążewski, *Phys. Rep.* **205 (5)** (1991).
56. H. R. Reiss, *Phys. Rev. Lett.* **26,** 1072 (1971).
57. I. I. Gol'dman, *Zh. Eksp. Teor. Fiz.* **46,** 1412 (1964) [*Sov. Phys. JETP* **19,** 954 (1964)].
58. I. I. Gol'dman, *Phys. Lett.* **8,** 103 (1964).
59. A. I. Nikishov and V. I. Ritus, *Zh. Eksp. Teor. Fiz.* **50,** 255 (1966) [*Sov. Phys. JETP* **23,** 168 (1966)].
60. A. M. Perelomov, V. S. Popov, M. V. Terent'ev, *Zh. Exp. Teor. Fiz.* **50,** 1393 (1966) [*Sov. Phys. JETP* **23,** 924 (1966)].
61. H. G. Muller, A. Tip, and M. J. van der Wiel, *J. Phys. B* **16,** L679 (1983).
62. P. Kruit, J. Kimman, H. G. Muller and M. J. van der Wiel, *Phys. Rev. A* **28,** 248 (1983).
63. K. G. H. Baldwin, *Thesis*, Australian National University, Canberra, Sept. (1979).
64. J. A. Wheeler, *Phys. Rev.* **52,** 1107 (1937).
65. W. Heisenberg, *Z. Phys.* **120,** 513, 673 (1943).
66. E. C. G. Stückelberg, *Helv. Phys. Acta* **17,** 3 (1943); **18,** 21, 195 (1945).
67. S. S. Schweber, *Relativistic Quantum Field Theory*, Row, Peterson, Evanston, IL (1961).
68. J. M. Jauch and F. Rohrlich, *The Theory of Photons and Electrons*, Springer-Verlag, Berlin (1976).
69. J. D. Bjorken and S. D. Drell, *Relativistic Quantum Fields*, McGraw-Hill, New York (1965).
70. C. Itzykson and J. B. Zuber, *Quantum Field Theory*, McGraw-Hill, New York (1980).
71. M. L. Goldberger and K. M. Watson, *Collision Theory*, Wiley, New York (1964).
72. P. Roman, *Advanced Quantum Theory*, Addison-Wesley, Reading, MA (1965).
73. R. G. Newton, *Scattering Theory of Waves and Particles*, Springer-Verlag, Berlin (1982).
74. J. D. Bjorken and S. D. Drell, *Relativistic Quantum Mechanics*, McGraw-Hill, New York (1964).
75. A. O. Barut, *The Theory of the Scattering Matrix*, Macmillan, New York (1967).
76. M. R. C. McDowell and J. P. Coleman, *Ion–Atom Collisions*, North-Holland, Amsterdam (1970).
77. H. R. Reiss, *Phys. Rev. A* **1,** 803 (1970).
78. H. R. Reiss, *Phys. Rev. A* **42,** 1476 (1990).
79. G. F. Chew, *S-Matrix Theory of Strong Interactions*, Benjamin, New York (1961).
80. S. C. Frautschi, *Regge Poles and S-Matrix Theory*, Benjamin, New York (1963).
81. R. J. Eden, P. Landshoff, D. I. Olive, and J. Polkinghorne, *Analytic S-Matrix Theory*, Cambridge University Press, Cambridge (1966).

82. H. A. BETHE and E. E. SALPETER, *Quantum Mechanics of One- and Two-Electron Atoms*, Springer-Verlag, Berlin (1957).
83. P. A. M. DIRAC, *Rev. Mod. Phys.* **21,** 392 (1949).
84. Y. S. KIM and M. E. NOZ, *Phase Space Picture of Quantum Mechanics*, World Scientific, Singapore (1991).
85. H. R. REISS, to be published.
86. J. L. FRIAR and S. FALLIEROS, *Phys. Rev. C* **34,** 2029 (1986).
87. K. H. YANG, *Ann. Phys. (N.Y.)* **101,** 62 (1976).
88. D. H. KOBE and A. L. SMIRL, *Am. J. Phys.* **46,** 624 (1978).
89. D. H. KOBE and K. H. YANG, *J. Phys. A* **13,** 3171 (1980).
90. W. E. LAMB, R. R. SCHLICHER, and M. O. SCULLY, *Phys. Rev. A* **36,** 2763 (1987).
91. W. K. H. PANOFSKY and M. PHILLIPS, *Classical Electricity and Magnetism*, Addison-Wesley, Reading, MA (1955).
92. J. D. JACKSON, *Classical Electrodynamics*, Wiley, New York (1975).
93. A. O. BARUT, *Electrodynamics and Classical Theory of Fields and Particles*, Macmillan, New York (1964).
94. J. J. SAKURAI, *Advanced Quantum Mechanics*, Addison-Wesley, Reading, MA (1967).
95. J. J. FORNEY, A. QUATTROPANI and F. BASSANI, *Nuovo Cimento B* **37,** 78 (1977).
96. F. BASSANI, J. J. FORNEY and A. QUATTROPANI, *Phys. Rev. Lett.* **39,** 1070 (1977).
97. Z. FRIED, *Phys. Rev. A* **8,** 2835 (1973).
98. C. K. CHOI, W. C. HENNEBERGER and F. C. SANDERS, *Phys. Rev. A* **9,** 1895 (1974).
99. C. K. CHOI, W. C. HENNEBERGER, S. N. MIAN and F. C. SANDERS, *Phys. Rev. A* **12,** 715 (1975).
100. M. GAVRILA and J. Z. KAMIŃSKI, *Phys. Rev. Lett.* **52,** 613 (1984).
101. G. W. FORD and R. F. O'CONNELL, *Phys. Rev. A* **13,** 1281 (1976).
102. P. H. BUCKSBAUM, M. BASHKANSKY and D. W. SCHUMACHER, *Phys. Rev. A* **37,** 3615 (1988).
103. J. H. YEE, *Phys. Rev. B* **3,** 355 (1971).
104. F. ADDUCI, I. M. CATALANO, A. CINGOLANI and A. MINAFRA, *Phys. Rev. B* **15,** 926 (1977).
105. N. G. BASOV, A. Z. GRASYUK, I. G. ZUBAREV, V. A. KATULIN, and O. N. KROKHIN, *Zh. Eksp. Teor. Fiz.* **50,** 551 (1966) [*Sov. Phys. JETP* **23,** 366 (1966)].
106. V. NATHAN, A. H. GUENTHER and S. S. MITRA, *J. Opt. Soc. Am. B* **2,** 294 (1985).
107. R. HIPPLER, H. SCHWIER, H. J. HUMPERT and H. O. LUTZ, *Z. Phys. D* **5,** 21 (1987).
108. T. J. MCILRATH, P. H. BUCKSBAUM, R. R. FREEMAN, and M. BASHKANSKY, *Phys. Rev. A* **35,** 4611 (1987).
109. M. D. PERRY, *Ph. D. Dissertation*, Lawrence Livermore National Laboratory, UCRL-53852, Nov. (1987).
110. W. XIONG, F. YERGEAU, S. L. CHIN and P. LAVIGNE, *J. Phys. B.* **20,** 723 (1987).
111. M. BASHKANSKY, P. H. BUCKSBAUM and D. W. SCHUMACHER, *Phys. Rev. Lett.* **60,** 2458 (1988).
112. S. L. CHIN, C. ROLLAND, R. B. CORKUM and P. KELLY, *Phys. Rev. Lett.* **61,** 153 (1988).
113. P. H. BUCKSBAUM, L. D. VAN WOERKOM, R. R. FREEMAN, and D. W. SCHUMACHER, *Phys. Rev. A* **41,** 4119 (1990).
114. S. AUGST, D. STRICKLAND, D. D. MEYERHOFER, S. L. CHIN and J. H. EBERLY, *Phys. Rev. Lett.* **63,** 2212 (1989).
115. S. AUGST, D. D. MEYERHOFER, D. STRICKLAND and S. L. CHIN, *J. Opt. Soc. Am. B* **8,** 858 (1991).
116. H. D. JONES and H. R. REISS, *Phys. Rev. B* **16,** 2466 (1977).
117. H. R. REISS, In *Photons and Continuum States of Atoms and Molecules*, N. K. RAHMAN, C. GUIDOTTI and M. ALLEGRINI (eds), Springer-Verlag, Berlin (1987).
118. H. R. REISS, *J. Phys. B* **20,** L79 (1987).
119. J. R. OPPENHEIMER, *Phys. Rev.* **31,** 66 (1928).
120. L. D. LANDAU and E. M. LIFSCHITZ, *Quantum Mechanics*, Pergamon, Oxford (1958).
121. A. I. NIKISHOV and V. I. RITUS, *Zh. Eksp. Teor. Fiz.* **52,** 223 (1967) [*Sov. Phys. JETP* **25,** 145 (1967)].
122. A. M. PERELOMOV, V. S. POPOV, and M. V. TERENT'EV, *Zh. Eksp. Teor. Fiz.* **51,** 309 (1966) [*Sov. Phys. JETP* **24,** 207 (1967)].
123. M. V. AMMOSOV, N. B. DELONE and V. P. KRAINOV, *Zh. Eksp. Teor. Fiz.* **91,** 2008 (1986) [*Sov. Phys. JETP* **64,** 1191 (1986)].
124. M. D. PERRY, A. SZÖKE, O. L. LANDEN, and E. M. CAMPBELL, *Phys. Rev. Lett.* **60,** 1270 (1988).
125. W. BECKER, R. R. SCHLICHER and M. O. SCULLY, *J. Phys. B* **19,** L785 (1986).
126. W. BECKER, R. R. SCHLICHER, M. O. SCULLY and K. WÓDKIEWICZ, *J. Opt. Soc. Am. B* **4,** 743 (1987).
127. N. D. SENGUPTA, *Bull. Calcutta Math. Soc.* **39,** 147 (1947).
128. A. H., TAUB, *Rev. Mod. Phys.* **21,** 388 (1949).
129. I. I. GOL'DMAN, *Izv. Akad. Nauk Armenii* **17,** 129 (1964).
130. M. GÖPPERT-MAYER, *Ann. Phys. (Leipzig)* **9,** 273 (1931).
131. M. D. PERRY, O. L. LANDEN, A. SZÖKE and E. M. CAMPBELL, *Phys. Rev. A* **37,** 747 (1988).
132. D. S. GUO and T. ÅBERG, *J. Phys. A* **21,** 4577 (1988).
133. H. R. REISS, *Invited Paper at Big Sky Workshop on Super-Intense Laser-Atom Physics*, Big Sky, MT, June (1991) (to be published).
134. G. DATTOLI, L. GIANNESSI, L. MEZI and A. TORRE, *Nuovo Cimento B* **104,** 327 (1990).
135. G. DATTOLI, A. TORRE, S. LORENZUTTA, G. MAINO, and C. CHICCOLI, *Nuovo Cimento B* **106,** 21 (1991).
136. P. H. BUCKSBAUM, M. BASHKANSKY, R. R. FREEMAN, T. J. MCILRATH and L. F. DIMAURO, *Phys. Rev. Lett.* **56,** 2590 (1986).
137. H. R. REISS, *Acta Phys. Polon.* **A78,** 199 (1991).
138. R. S. BARDFIELD and H. R. REISS, *Bull. Am. Phys. Soc.* **36,** 1249 (to be published).
139. A. L'HUILLIER, L. A. LOMPRÉ, G. MAINFRAY and C. MANUS, *Phys. Rev. A* **27,** 2503 (1983).
140. L. A. LOMPRÉ, A. L'HUILLIER, G. MAINFRAY and C. MANUS, *Phys. Lett.* **112A,** 319 (1985).

141. K. Boyer and C. K. Rhodes, *Phys. Rev. Lett.* **54,** 1490 (1985).
142. A. Szöke, *Phys. Rev. Lett.* **56,** 720 (1986).
143. P. W. Milonni and J. H. Eberly, *Lasers*, Wiley, New York (1988).
144. N. B. Delone and V. P. Krainov, *Atoms in Strong Light Fields*, Springer-Verlag, Berlin (1985).
145. G. Gamow, *Z. Phys.* **51,** 204 (1928).
146. R. A. Fox, R. M. Kogan and E. J. Robinson, *Phys. Rev. Lett.* **26,** 1416 (1971).
147. R. M. Kogan, R. A. Fox, G. T. Burnham and E. J. Robinson, *Bull. Am. Phys. Soc.* **16,** 1411 (1971).
148. J. P. Hernandez and A. Gold, *Phys. Rev.* **156,** 26 (1967).
149. P. Lambropoulos, *Phys. Rev. Lett.* **28,** 585 (1972).
150. S. Klarsfeld and A. Maquet, *Phys. Rev. Lett.* **29,** 79 (1972).
151. H. R. Reiss, *Phys. Rev. Lett.* **29,** 1129 (1972).
152. H. R. Reiss, In *Coherence and Quantum Optics V*, L. Mandel and E. Wolf (eds), Plenum, New York, pp. 853–859 (1984).
153. F. Yergeau, G. Petite and P. Agostini, *J. Phys. B* **19,** L663 (1986).
154. M. Bashkansky, P. H. Bucksbaum, and D. W. Schumacher, *Phys. Rev. Lett.* **59,** 274 (1987).
155. S. Basile, F. Trombetta and G. Ferrante, *Phys. Rev. Lett.* **61,** 2435 (1988).
156. M. V. Fedorov and A. M. Movsesian, *J. Opt. Soc. Am. B* **5,** 850 (1988).
157. A. M. Movsesyan and M. V. Fedorov, *Zh. Eksp. Teor. Fiz.* **95,** 47 (1989) [*Sov. Phys. JETP* **68,** 27 (1989)].
158. M. V. Fedorov and A. M. Movsesian, *J. Opt. Soc. Am. B* **6,** 1504 (1989).
159. M. Pont, N. R. Walet and M. Gavrila, *Phys. Rev. A* **41,** 477 (1990).
160. J. Parker and C. R. Stroud, *Phys. Rev. A* **41,** 1602 (1990).
161. M. Dörr, R. M. Potvliege and R. Shakeshaft, *Phys. Rev. Lett.* **64,** 2003 (1990).
162. M. V. Fedorov, M. Yu. Ivanov, and A. M. Movsesian, *J. Phys. B* **23,** 2245 (1990).
163. M. Dörr, R. M. Potvliege, D. Proulx and R. Shakeshaft, *Phys. Rev. A* **43,** 3729 (1991).
164. Yu. V. Dubrovskiĭ, M. Yu. Ivanov and M. V. Fedorov, *Zh. Eksp. Teor. Fiz.* **99,** 228 (1991) [*Sov. Phys. JETP* **72,** 228 (1991)].
165. V. C. Reed, P. L. Knight and K. Burnett, *Phys. Rev. Lett.* **67,** 1415 (1991).
166. R. Grobe and C. K. Law, *Phys. Rev.* **A44,** R4114 (1991).
167. M. Pont and R. Shakeshaft, *Phys. Rev. A* **44,** R4110 (1991).
168. H. S. Antunes-Neto and L. Davidovich, *Phys. Rev. Lett.* **53,** 2238 (1984).
169. P. W. Milonni, *Phys. Rev. A* **38,** 2682 (1988).
170. P. W. Milonni and J. R. Ackerhalt, *Phys. Rev. A* **39,** 1139 (1989).
171. M. H. Mittleman, *Phys. Rev. A* **40,** 463 (1989).
172. Y. Abranyos and M. H. Mittleman, *Phys. Rev. A* **42,** 4284 (1990).
173. E. Fermi, *Nuclear Physics*, University of Chicago Press, Chicago (1950).
174. G. Floquet, *Ann. Ecole Norm. Sup.* **12,** 47 (1883).
175. J. H. Shirley, *Phys. Rev.* **138,** B979 (1965).
176. S. I. Chu and W. P. Reinhardt, *Phys. Rev. Lett.* **39,** 1195 (1977).
177. S. I. Chu and J. Cooper, *Phys. Rev. A* **32,** 2769 (1985).
178. L. A. Collins and A. L. Merts, *Phys. Rev. A* **37,** 2415 (1988).
179. J. Javanainen and J. H. Eberly, *Phys. Rev. A* **39,** 458 (1989).
180. K. LaGattuta, *Phys. Rev. A* **40,** 683 (1989).
181. H. R. Reiss, *Phys. Rev. A* **41,** 6530 (1990).
182. K. C. Kulander, *Phys. Rev. A* **35,** 445 (1987).
183. K. C. Kulander, *Phys. Rev. A* **36,** 2726 (1987).
184. K. C. Kulander, *Phys. Rev. A* **38,** 778 (1988).